

Electronic Thesis and Dissertation Repository

9-24-2014 12:00 AM

The Role Of The RNA-Binding Protein Rho Guanine Nucleotide Exchange Factor In The Cellular Stress Response

Kevin WH Cheung
The University of Western Ontario

Supervisor
Dr. Michael J. Strong
The University of Western Ontario

Graduate Program in Pathology
A thesis submitted in partial fulfillment of the requirements for the degree in Master of Science
© Kevin WH Cheung 2014

Follow this and additional works at: <https://ir.lib.uwo.ca/etd>



Part of the [Molecular and Cellular Neuroscience Commons](#)

Recommended Citation

Cheung, Kevin WH, "The Role Of The RNA-Binding Protein Rho Guanine Nucleotide Exchange Factor In The Cellular Stress Response" (2014). *Electronic Thesis and Dissertation Repository*. 2440.
<https://ir.lib.uwo.ca/etd/2440>

This Dissertation/Thesis is brought to you for free and open access by Scholarship@Western. It has been accepted for inclusion in Electronic Thesis and Dissertation Repository by an authorized administrator of Scholarship@Western. For more information, please contact wlsadmin@uwo.ca.

The Role Of The RNA-Binding Protein Rho Guanine Nucleotide Exchange Factor In
The Cellular Stress Response

(Thesis format: Monograph)

by

Kevin Wing-Hong Cheung

Graduate Program in Pathology

A thesis submitted in partial fulfillment
of the requirements for the degree of
Master of Science

The School of Graduate and Postdoctoral Studies
The University of Western Ontario
London, Ontario, Canada

© Kevin Wing-Hong Cheung 2014

Abstract

Amyotrophic lateral sclerosis (ALS) is a progressive neurodegenerative disease for which the pathological mechanism is heterogeneous and a cure has been elusive. Recent developments have linked specific proteins found in pathological neuronal cytoplasmic inclusions (NCIs) of ALS motor neurons to familial variants of the disease. These proteins, including TAR DNA-binding protein of 43 kDa (TDP-43), fused in sarcoma/translocated in liposarcoma (FUS), and Rho guanine nucleotide exchange factor (RGNEF) share the common characteristic of being RNA-binding proteins that colocalize within NCIs. RGNEF is unique however in also possessing RhoA activation capacity, suggesting a role in the cell stress response. My thesis confirms this role, and I also observed that the domain responsible for RhoA activation is not critical for RGNEF's protective effects. Altogether, my work further supports the hypothesis of a pathological mechanism of dysfunctional stress response in ALS motor neurons where cytoprotective proteins are sequestered in NCIs, leading to neurodegeneration.

Keywords

Amyotrophic Lateral Sclerosis, *NEFL* mRNA, RGNEF, TDP-43, FUS, MTT assay, confocal microscopy, stress granules, transport granules

Dedication

I dedicate my work to my parents; their support has meant everything.

I also dedicate this thesis to the individuals who suffer from amyotrophic lateral sclerosis. Their indomitable spirit is truly awe inspiring and is truly the reason that ALS research is so meaningful. May we move ever closer to solving this terrible disease.

Acknowledgments

There are many who have helped me throughout my Master's thesis. Whether through experimental design, thesis editing, or something else, these people played a vital role in the completion of my Master's thesis.

I would like to thank and acknowledge the help of my committee members: Dr. Frank Beier, Dr. Martin Duennwald, and Dr. Subrata Chakrabarti. Their help in committee meetings, with experimental suggestions and interpretation of results, has undoubtedly changed my thesis for the better. As well, their help in editing my thesis was greatly appreciated.

I thank Dr. Kathryn Volkening for her critical input and helpful oversight of my experimental data and writing of both abstracts and presentations. Her leadership within the lab was irreplaceable and she provided support whenever it was needed.

I thank Dr. Cristian Droppelmann for his help in generating the various RGNEF constructs and the stable RGNEF cell line. Also, I thank Dr. Droppelmann for his critical input for the experiments performed, and his invaluable mentorship with lab techniques, statistical analysis, and scientific thinking. Our discussions in and out of the lab were enlightening and enjoyable, and I could not have learned as much as I did without him.

I thank Dr. Danae Campos-Melo and Dr. Muhammad Ishtiaq for their aid and friendliness throughout the lab. Dr. Campos-Melo especially; in protocol execution and troubleshooting and in helping prepare for my thesis defense she helped improve my thesis significantly. I also thank Wendy Strong and Cheryl Leystra-Lantz for their work throughout the lab. The excellent state of Strong Lab is maintained and bettered through their efforts.

I thank Dr. Chandan Chakraborty for overseeing the Pathology graduate program. His help, from the time of application to his role as chief examiner, has been vital during my Master's career. Furthermore, his journal club course was engaging and useful in practicing and improving my presentation style.

I thank Alex Moszczynski for his friendship and support throughout my Master's in the Strong Lab. The time I spent these past two years, whether in the lab or at a conference in San Diego, was more fun and more enjoyable thanks to his brimming positivity. I also thank

Michael Tavolieri, Sali Farhan and Karen Dunkerly. Their input during presentations has improved my presenting style and their participation in lab meetings has been energizing.

I thank the administrative staff of the Dean's office, including Nicole Farrell, Jessica Jamieson, and Lyndsay Caslick. Their kindness and help in organizing meetings with Dr. Strong were essential both throughout my Master's and in completing my thesis.

I thank the Department of Pathology administrative staff, including Tracey Koning, Cheryl Campbell, Susan Stewart, and Susan Underhill. Their kindness, patience and efforts helped immensely for the entirety of my Master's.

Finally, I greatly thank Dr. Michael Strong for his supervision. His immense wisdom and apt guidance throughout my Master's thesis were admirable and invaluable. Though there were times when I faltered during my thesis, I could always rely on him to point me in the right direction. In addition, I thank Dr. Strong for his tireless efforts to work with me to improve and complete my thesis. His knowledge and input have influenced and improved my experimental design immeasurably.

Thank you, Dr. Strong and everyone, for seeing my work to the end.

Table of Contents

Abstract.....	ii
Dedication.....	iii
Acknowledgments.....	iv
Table of Contents.....	vi
List of Tables.....	ix
List of Figures.....	x
List of Abbreviations.....	xii
Chapter 1.....	1
1 Thesis rationale.....	1
1.1 Background of amyotrophic lateral sclerosis.....	5
1.2 Neuropathology and the disease process of ALS.....	6
1.2.1 Neuronal cytoplasmic & nuclear inclusions in ALS.....	7
1.2.2 Microglial pathology and the role of oxidative injury in ALS.....	8
1.2.3 The role of astrocytes and excitotoxicity in ALS.....	10
1.3 The three known variants of ALS.....	11
1.4 Gene mutations associated with ALS.....	12
1.4.1 Intermediate filaments.....	12
1.4.2 Copper/zinc superoxide dismutase.....	16
1.4.3 Chromosome 9 open reading frame 72.....	16
1.4.4 Ataxin-2.....	17
1.4.5 TAR DNA-binding protein of 43 kDa.....	18
1.4.6 Fused in sarcoma/translocated in liposarcoma.....	19
1.4.7 Ewing's sarcoma protein and TATA-binding protein associated factor 2N.....	19

1.4.8	Angiogenin.....	20
1.4.9	Heterogeneous nuclear ribonucleoprotein A1	20
1.4.10	Senataxin.....	20
1.5	RNA granules.....	21
1.5.1	Stress granules	23
1.5.2	Transport granules	24
1.5.3	Processing bodies.....	24
1.5.4	Nuclear paraspeckles	25
1.6	Rho guanine nucleotide exchange factor	26
1.7	RGNEF's potential role in stress response	30
1.8	Hypothesis.....	31
Chapter 2	32
2	Specific aims	32
2.1	Cell lines and transfections	32
2.2	Western blot	34
2.3	RGNEF constructs	38
2.4	Stress conditions	42
2.5	Immunofluorescence and confocal microscopy.....	42
2.6	Cell survival assays.....	43
2.7	siRNA experiments.....	45
2.8	Statistical analysis.....	46
Chapter 3	48
3	Experimental results.....	48
3.1	Survival experiments in stably transfected cells.....	48
3.2	Survival experiments in transiently transfected cells.....	51
3.3	Trypan blue assay	53

3.4 RNA silencing experiments	53
3.5 Survival experiments examining different constructs of RGNEF	57
3.6 RNA granules and RGNEF localization under stress	62
Chapter 4.....	66
4 Discussion	66
4.1 RGNEF protects against stress.....	66
4.2 N-terminal portion of RGNEF is important for its stress protection	67
4.3 RGNEF localizes to transport granules under stress.....	73
4.4 Conclusion and future directions	74
Bibliography	77
Curriculum Vitae	105

List of Tables

Table 1: Functional groupings of genetic mutations associated with ALS	2
Table 2: Types of RNA granules found in neurons	22
Table 3: Antibodies used for western blotting	37
Table 4: Primers used in PCR to generate different RGNEF constructs.	39
Table 5: Antibodies used in immunocytochemistry for confocal microscopy	44

List of Figures

Figure 1: Comparing different intermediate filament proteins found in neurons.....	14
Figure 2: Comparing the protein structures of RGNEF and p190RhoGEF.....	27
Figure 3: Flowchart describing process of transfecting and seeding cells for use in experiments.....	35
Figure 4: Comparison of the different deletion constructs of RGNEF.....	41
Figure 5: Survival over time of cells exposed to different oxidative and osmotic stress concentrations.....	49
Figure 6: Survival over time of cells exposed to sustained or recovery heat shock protocols.....	50
Figure 7: Survival over time of transiently transfected cells exposed to arsenite or sorbitol stress.....	52
Figure 8: Survival of transiently transfected cells exposed to 0.5 mM arsenite or 400 mM sorbitol stress measured using the trypan blue exclusion assay.....	54
Figure 9: Survival of stably transfected RGNEF-myc cells transfected with siRNA against RGNEF and exposed to arsenite or sorbitol stress.....	55
Figure 10: Survival over time of cells transiently transfected with different constructs of RGNEF and exposed to arsenite or sorbitol stress.....	59
Figure 11: Confirming efficiencies of transfections of different RGNEF constructs by western blot and immunofluorescence microscopy.....	61
Figure 12: Localization of RGNEF-myc and TIA-1 stress granules formed when stably transfected RGNEF-myc cells are exposed to arsenite or sorbitol stress.....	63
Figure 13: Localization of RGNEF-myc and staufen transport granules formed when stably transfected RGNEF-myc cells are exposed to arsenite or sorbitol stress.....	64

Figure 14: Comparison of stress granules and transport granules 65

Figure 15: Review of deletion constructs of RGNEF used in experiments 69

Figure 16: A proposed model for the folding of RGNEF 72

List of Abbreviations

3' UTR	3' untranslated region
ALS	Amyotrophic lateral sclerosis
<i>ANG</i>	Gene encoding angiogenin
ANOVA	Analysis of variance
<i>ARHGEF28</i>	Gene encoding Rho guanine nucleotide exchange factor
Bcl-2	B-cell lymphoma 2
BMAA	Beta-methylamino L-alanine
BSA	Bovine serum albumin
<i>C9ORF72</i>	Chromosome 9 open reading frame 72
cDNA	Complementary deoxyribonucleic acid
CFTR	Cystic fibrosis transmembrane conductance regulator
DAG	Diacylglycerol
DCP1A	Decapping enzyme 1A
DH	Dbl-homology domain
DMEM	Dulbecco's modified eagle's medium
DMSO	Dimethyl sulfoxide
DNA	Deoxyribonucleic acid
DNEN	Differentially Expressed in Normal and Neoplasia
EAAT	Excitatory amino acid transporter

ECL	Enhanced chemiluminescence (reagent)
<i>E. Coli</i>	<i>Escherichia Coli</i>
EWS	Ewing's sarcoma protein
<i>EWSR1</i>	Gene encoding Ewing's sarcoma protein
FAK	Focal adhesion kinase
fALS	Familial amyotrophic lateral sclerosis
FBS	Fetal bovine serum
Fisher LSD	Fisher least significant difference
FUS	Fused in sarcoma/translocated in liposarcoma
<i>FUS</i>	Gene encoding fused in sarcoma/translocated in liposarcoma
G3BP	Ras GAP SH3 binding protein
GDP	Guanosine diphosphate
GLT-1	Glutamate transporter-1
GSK3 β	Glycogen synthase kinase 3 beta
GTP	Guanosine triphosphate
HCl	Hydrochloric acid
HEK 293T	Human embryonic kidney 293 cell line containing large T antigen
HIV	Human immunodeficiency virus
hnRNP A1	Heterogeneous nuclear ribonucleoprotein A1
<i>HNRNPA1</i>	Gene encoding heterogeneous nuclear ribonucleoprotein A1

JIP-1	c-Jun N-terminal kinase interacting protein 1
LB	Lysogeny broth
LC3	Microtubule-associated protein 1 light chain 3
lncRNA	Long non-coding ribonucleic acid
LRRK2	Leucine-rich repeat kinase 2
mRNA	Messenger ribonucleic acid
miRNA	Micro ribonucleic acid
mtSOD1	Mutant copper/zinc superoxide dismutase protein
MTT	Thiazol blue tetrazolium bromide
NaCl	Sodium chloride
NCI	Neuronal cytoplasmic inclusion
NEAT1	Nuclear-enriched abundant transcript 1
<i>NEFH</i>	Gene encoding high molecular weight neurofilament
<i>NEFL</i>	Gene encoding low molecular weight neurofilament
NF	Neurofilament
NFH	High molecular weight neurofilament
NFL	Low molecular weight neurofilament
NFM	Medium molecular weight neurofilament
NIH	National Institutes of Health
NNI	Neuronal nuclear inclusion

NP-40	Nonidet P-40
<i>OPTN</i>	Gene encoding optineurin
PABP1	Poly(A)-binding protein 1
PB	Processing body
PBS	Phosphate buffered saline
PCR	Polymerase chain reaction
PH	Pleckstrin homology domain
PKC	Protein Kinase C
PMSF	Phenylmethylsulfonyl fluoride
<i>PRPH</i>	Gene encoding peripherin
RAN	Repeat-associated non-ATG (translation)
RBM-45	RNA-binding motif 45 protein
RGNEF	Rho guanine nucleotide exchange factor
RGNEF+	Cells stably transfected, overexpressing RGNEF
RNA	Ribonucleic acid
RNAi	Ribonucleic acid interference
rRNA	Ribosomal ribonucleic acid
ROS	Reactive oxygen species
sALS	Sporadic amyotrophic lateral sclerosis
SDS	Sodium dodecyl sulfate

<i>SETX</i>	Gene encoding senataxin
SG	Stress granule
siRNA	Small interfering ribonucleic acid
SOD1	Copper/Zinc superoxide dismutase
<i>SQSTM1</i>	Gene encoding sequestome 1 (or p62)
TAF15	TATA-binding protein associated factor 2N
<i>TAF15</i>	Gene encoding TATA-binding protein associated factor 2N
TARDBP	Gene encoding TAR DNA-binding protein of 43 kDa
TDP-43	TAR DNA-binding protein of 43 kDa
TIA-1	T-cell intracellular antigen 1
TNF α	Tumor necrosis factor alpha
VEGF	Vascular endothelial growth factor
XRN1	5'-3' exoribonuclease 1

Chapter 1

1 Thesis rationale

Amyotrophic lateral sclerosis (ALS) is a progressive, incurable neurodegenerative disease affecting primarily motor neurons with a relatively uniform world-wide incidence rate of approximately 2.2 of 100,000 people (Chio et al., 2013). Typically, the patient develops progressive muscle paralysis with death within 3 – 5 years from a loss of respiratory function (Rowland & Shneider, 2001). The risk of developing ALS increases with age, with a peak age at onset within the 6th decade of life. This means that as the baby-boomer population reaches this peak in onset an increasing number of cases can be anticipated (Strong, Kesavapany, & Pant, 2005; Chio et al., 2013).

The neuropathological hallmark of ALS has been traditionally described as being two-fold: the presence of degeneration of descending supraspinal motor tracts such as the corticospinal tract, and the loss of specific populations of cortical, brainstem and spinal motor neurons. The latter has traditionally been associated with the presence of neuronal cytoplasmic inclusions (NCIs) that are composed of neuronal intermediate filaments, most typically neurofilaments. The contemporary view however also includes both NCIs and neuronal nuclear inclusions (NNIs) that are composed of a variety of proteins, the most common of which are either RNA binding proteins or proteins whose function impacts on RNA metabolism (Strong, 2010). Intraneuronal inclusions are pathological aggregations of misfolded protein that are not specific to ALS pathology, but have been observed in a diverse number of neurodegenerative disorders (for example, Alzheimer's disease, Huntington's disease, and Parkinson's disease) (Roussel et al., 2013). Their presence can be seen as an indicator of pathology as inclusions are not often observed in individuals without disease phenotype.

An important advance in our understanding of ALS has been the increasing awareness of a common link between these inclusions and the various forms of ALS that are familial in nature (fALS).

Table 1: Functional groupings of genetic mutations associated with ALS

Gene	Locus	Inheritance	Alternative phenotype
Enzymes			
FIG4	6q21	Unknown	PLS
SOD1	21q22.11	Dominant	FTLD, PMA
Expanded repeats			
ATXN2	12q24.1	Dominant	PMA
C9ORF72	9p21.2	Dominant	FTLD
RNA metabolism-related proteins			
ANG	14q11.1-q11.2	Dominant	FTLD
ARHGEF28	5q13.2	Unknown	None
EWSR1	22q12.2	Unknown	None
FUS	16q12	Both dominant and recessive	FTLD
HNRNPA1	12q13.1	Dominant	None
SETX	9q34.13	Dominant	CMT or dHMN
TAF15	17q11.1-q11.2	Unknown	None
TARDBP	1p36.22	Dominant	FTLD
Cytoskeleton proteins			
NEFH	22q12.2	Uncertain	None
PRPH	12q12-q13	Sporadic	None
PFN1	17p13.3	Dominant	None
Intracellular transport proteins			
CHMP2B	3p11.2	Dominant	FTLD
DCTN1	2p13	Dominant	None
VAPB	20q13.33	Dominant	PMA, PLS
VCP	9p13.3	Dominant	FTLD
Ubiquitin-related proteins			
SQSTM1	5q35	Dominant	FTLD
UBQLN2	Xp11.21	Dominant	FTLD
Multifunctional proteins			
OPTN	10p13	Dominant	FTLD
Others			
ALS2	2q33.1	Recessive	PLS
DAO	12q24	Dominant	None
EPHA4	2q36.1	Unknown	None
SPG11	15q21.1	Recessive	None
Unknown	18q21	Dominant	None
Unknown	15q15.1-21.1	Recessive	None
Unknown	20p13	Dominant	None

Gene abbreviations: ANG: Angiogenin; ARHGEF28: Rho Guanine Nucleotide Exchange Factor; ATXN2: Ataxin 2; C9orf72: Chromosome 9 Open Reading Frame 72; CHMP2B: Charged Multivesicular Body Protein 2b; DAO: D-Amino-Acid Oxidase; DCTN1: Dynactin 1; EPHA4: Ephrin Type-A Receptor 4; EWSR1: Ewing Sarcoma Breakpoint Region 1; FIG4: Phosphatidylinositol 3,5-bisphosphate 5-phosphatase; FUS: Fused in Sarcoma/Translocated in Liposarcoma; HNRNPA1: Heterogeneous Nuclear Ribonucleoprotein A1; NEFH: High Molecular Weight Neurofilament; OPTN: Optineurin; p62/SQSTM1: Sequestosome-1; PFN1: Profilin 1; PRPH: Peripherin; SETX: Senataxin; SOD1: Superoxide Dismutase 1; SPG11: Spatacsin; TAF15: TATA-Binding Protein Associated Factor 2N; TARDBP: TAR DNA-Binding Protein of 43 kDa; UBQLN2: Ubiquilin 2; VAPB: Vesicle-Associated Membrane Protein-Associated Protein B and C; VCP: Valosin-Containing Protein.

Phenotype abbreviations: CMT: Charcot-Marie-Tooth Disease; dHMN: Distal Hereditary Motor Neuropathy; FTLD: Frontotemporal Lobar Degeneration; PLS: Primary Lateral Sclerosis; PMA: Progressive Muscular Atrophy.

*Table adapted from: (Droppelmann, Campos-Melo, Ishtiaq, Volkening, & Strong, 2014)

As will be described, and as seen in Table 1, examples of such proteins for which genetic linkages have been found with fALS and for which neuronal inclusions have been observed include: mutant copper/zinc superoxide dismutase (mtSOD1) (Rosen et al., 1993), TAR DNA-binding protein of 43 kDa (TDP-43) (Neumann et al., 2006), fused in sarcoma/translocated in liposarcoma (FUS) (Kwiatkowski, Jr. et al., 2009), and TATA-binding protein-associated factor 2N (Couthouis et al., 2011). The aggregation and mutation of RNA-binding proteins and their genes in ALS is an emerging field which points towards disrupted RNA homeostasis as a pathogenic mechanism for motor neuron death in ALS. Following this RNA hypothesis of ALS pathogenesis, my thesis involves the study of a novel dual-function protein that our laboratory has discovered: Rho guanine nucleotide exchange factor (RGNEF; the human homologue of p190RhoGEF). RGNEF is both a signal transduction protein that can activate the RhoA signaling pathway and an RNA-binding protein that can affect the stability of target mRNA (Volkening, Leystra-Lantz, & Strong, 2010; Droppelmann, Keller, Campos-Melo, Volkening, & Strong, 2013). While similar to the previously mentioned RNA-binding proteins in that it forms pathological NCIs in ALS spinal motor neurons, RGNEF NCIs also colocalize with other RNA-binding protein inclusions such as TDP-43 and FUS (Keller et al., 2012).

As previous studies have shown that ALS-related RNA-binding proteins, such as TDP-43 and FUS, protect cells against cellular stress (Higashi et al., 2013; Sama et al., 2013), this thesis will examine **the hypothesis that RGNEF participates in the cellular stress response**. As I will describe, this hypothetical role in the stress response could be readily attributed to: (a) the participation of RGNEF in the formation of RNA stress granules as a component of the physiological response of the neuron to injury, or (b) the the signal transduction pathways mediated through RhoA activation as a result of RGNEF's guanine exchange factor activity. In this chapter, I will describe the disease process of ALS, the proteins involved in ALS pathology, and how RGNEF may be contributing to ALS, including previous studies performed on the protein.

1.1 Background of amyotrophic lateral sclerosis

The classical description of amyotrophic lateral sclerosis (ALS) is as a neurodegenerative disorder characterized by the progressive loss of both upper and lower motor neurons (Rowland & Shneider, 2001; Strong, 2010). Upper motor neurons synapse with other motor neurons while lower motor neurons synapse directly with muscle cells. Upper motor neurons, also termed descending supraspinal neurons, originate either from within the cortex (predominantly in the precentral motor cortex, but also in the supplementary motor cortex and the postcentral parietal cortex) or from within more primitive motor nuclei of the brainstem. The vast majority of these neurons cross at the level of the medulla to course through the ventral and lateral corticospinal tracts to innervate the contralateral spinal motor neurons. A separate population of upper motor neurons innervates select motor nuclei of the brainstem to control the oropharyngeal muscles through the bulbar motor neurons. Because both the upper and lower motor neurons are involved to varying degrees in ALS, the symptoms of ALS can differ from one individual to the next depending on which motor neurons are affected and to what degree (Purves et al., 2001). In general, the symptoms of ALS present first as wasting or weakness of the hands or legs (in which case it is termed limb onset), or as slurred speech and dysphagia (in which case it is termed bulbar onset). This difference is driven by the primary site of neuronal loss: spinal motor neurons or bulbar motor neurons, respectively (Rowland & Shneider, 2001).

Death from ALS usually occurs within 3 to 5 years of symptom onset and generally from respiratory failure (Al-Chalabi & Hardiman, 2013). The disease course is however extremely heterogeneous and can be affected by the initial site of symptom onset, the time to diagnosis, or the age at symptom onset. For example, patients with limb onset ALS have a higher median survival than patients with bulbar onset ALS. Also, older patients have a lower median survival than younger patients (Scotton et al., 2012; Cui et al., 2014).

Though ALS has been recognized as a discrete clinical and neuropathological entity since the time of its description by Jean-Martin Charcot in 1869, there is no cure and the underlying pathogenesis is only now becoming clearer (Charcot & Joffroy, 1869). It has

been suggested that the failure of many pharmacotherapeutic agents to meaningfully alter the course of ALS can in part be attributed to a significant delay in diagnosis from the time of symptom onset with affected patients thus being significantly advanced by the time of treatment intervention. However there remains no definitive diagnostic test or biomarker for ALS (Kiernan et al., 2011). Clinical neurologists utilize the El Escorial diagnostic criteria, created in 1994 and updated in 2007 to include the Awaji-Shima criteria, to diagnose ALS based on clinical, electrophysiological and genetic criteria (Brooks, 1994; Nodera, Izumi, & Kaji, 2007). When applied, these criteria are both sensitive and specific and have allowed for earlier diagnoses to be made for ALS patients (Chaudhuri et al., 1995; Costa, Swash, & de Carvalho, 2012). Whilst there have thus been advances in the early diagnosis of ALS, there remains only a single approved pharmacotherapy for the disease process of ALS (although there are many successful symptomatic therapies). As such, an anti-glutamate compound called Riluzole remains the only approved treatment, and even this only extends survival of patients by 2 to 3 months (Miller, Mitchell, & Moore, 2012). Currently, research is being performed to better characterize the molecular mechanisms of the disease in hopes of finding a targetable cause of the disease so that it can be arrested.

1.2 Neuropathology and the disease process of ALS

The neuropathological characterization of ALS can be considered in terms of both the conventional pathology and the more rapidly evolving contemporary pathology. Typically, there is a significant loss of muscle, thinning of the ventral spinal roots and atrophy of the spinal cord that is grossly observable (Strong et al., 2005). The loss of the descending supraspinal motor neurons gives rise to prominent pallor and gliosis of the ventral and lateral corticospinal tracts, while the loss of the cortical motor neurons gives rise to marked precentral cortical atrophy (Rowland & Shneider, 2001). In individuals where there is an associated frontotemporal dementia, there is significant frontal lobar atrophy often extending into the temporal and parietal lobes (Strong, 2001).

At the light microscopic level, affected motor neurons exhibit a range of pathologies, including NCIs, NNIs and axonal swelling (neuroaxonal spheroids). Gliosis, evidenced by microglia and astrocyte proliferation also occurs and may negatively affect the

neuronal milieu in an inflammatory or excitotoxic manner, respectively (Strong et al., 2005).

1.2.1 Neuronal cytoplasmic & nuclear inclusions in ALS

Neuronal inclusions are one of the hallmarks observed in degenerating motor neurons of ALS. There have been several different types of inclusions noted in ALS: Bunina bodies, hyaline conglomerate inclusions, and ubiquitinated inclusions (Xiao, McLean, & Robertson, 2006). Bunina bodies are granular, eosinophilic inclusions found in both dendrites and soma of ALS motor neurons that immunostain positive for proteinase inhibitor cystatin C, suggesting that they are of lysosomal origin (Okamoto, Hirai, Amari, Watanabe, & Sakurai, 1993). Hyaline conglomerate inclusions are argyrophilic, or silver-stained, structures found in the perikarya, or soma, of ALS motor neurons. They are immunoreactive for neurofilaments and peripherin, implying that the disorganization of neuronal cytoskeleton is important in the pathology of ALS (Strong et al., 2005).

Ubiquitinated inclusions can be dense and circular or fibrillar skeins and they are observed in the perikarya of ALS motor neurons (Leigh et al., 1991). These structures colocalize with other protein inclusions, as shown by immunoreactivity to such proteins as TAR DNA-binding protein of 43 kDa (TDP-43) (Neumann et al., 2006), RGNEF (Keller et al., 2012), fused in sarcoma (FUS) (Deng et al., 2010), RNA-binding motif 45 protein (RBM-45) (Collins et al., 2012), and optineurin (OPTN) (Maruyama et al., 2010).

Ubiquitinated inclusions are the most prevalent form of inclusion observed in ALS motor neurons (Piao et al., 2003). The function of ubiquitin is to bind and mark short-lived proteins for elimination primarily through the proteasome-degradation pathway. The accumulation of ubiquitinated proteins within ALS motor neurons suggests that the proteasome pathway is adversely affected and that a buildup of proteins marked for degradation eventually may lead to cellular damage and death (Bruijn, Miller, & Cleveland, 2004). In support of this, *UBQLN2*, a gene coding for the ubiquitin-like protein ubiquilin 2, is observed to be mutated in cases of familial ALS (Deng et al., 2011). The ALS-associated mutation has been shown to impair the proteasome pathway.

The presence of ubiquitinated inclusions in ALS has also provided a valuable insight into mechanisms that may be disrupted through understanding the nature of the proteins that are integrated into the ubiquitinated inclusions. To date, the vast majority of these proteins have been associated with RNA metabolism, including TDP-43, RGNEF, FUS, RBM-45, and OPTN (Droppelmann et al., 2014).

Related to the hypothesis of aberrant RNA metabolism is the altered mRNA levels of intermediate filament proteins in ALS and the observation that intermediate filament proteins are disorganized in ALS. Specifically, ALS motor neurons often show ubiquitinated inclusions of neurofilament and peripherin proteins (Wong, He, & Strong, 2000). Moreover, mutations in the genes encoding high-molecular weight neurofilament (*NEFH*) and peripherin (*PRPH*) have been linked to cases of ALS (Figlewicz et al., 1994; Gros-Louis et al., 2004). It is hypothesized that when these intermediate filament proteins are mislocalized to intraneuronal inclusions in ALS, their function in maintaining the neuron's structural integrity is compromised and processes such as axonal transport can be greatly affected. Indeed, a mouse model of ALS where high molecular weight neurofilament (NFH) protein was overexpressed showed defects in axonal transport (Collard, Cote, & Julien, 1995). In addition, deficits in axonal transport are described as an early sign of disease in transgenic mouse models of ALS involving mutations in the gene encoding superoxide dismutase 1 (*SOD1*; model is often referenced as mtSOD1 mouse model) (Williamson & Cleveland, 1999). However, it should be noted that neurofilament inclusions themselves may not necessarily be pathogenic. It was observed that by increasing the expression of either NFH or low molecular weight neurofilament (NFL) in a mtSOD1 transgenic mouse model of ALS, mice survived longer (Nguyen, Lariviere, & Julien, 2001). Although we are still unsure whether inclusions observed in ALS are a pathological cause or consequence of the disease, it is clear that their presence plays a significant role in the ongoing degeneration of motor neurons (Strong et al., 2005; Sanelli, Sopper, & Strong, 2004; Sanelli & Strong, 2007).

1.2.2 Microglial pathology and the role of oxidative injury in ALS

Microglia are a type of macrophage-like glial cell found throughout the nervous system. They are highly mobile cells that function to detect and remove pathogens and large

cellular debris from the nervous system (Raivich, 2005). However, microglia may also initiate neuroinflammation and cause profound neuronal damage. These two functions must be delicately balanced to preserve a healthy neuronal environment (Moisse & Strong, 2006). Microglia exist in two forms: a passive state where they monitor the neuronal environment for cellular insults through the extension of long cellular processes and an active state where they enlarge and gain their macrophage-like phagocytic function to capture the source of the cellular insult as well as release pro-inflammatory factors to recruit other immune cells to the area (Kreutzberg, 1996; Kalla et al., 2001).

In ALS, microglia have proliferated and appear to be more active than in controls (Troost, van den Oord, & Vianney de Jong, 1990). In addition, mouse models of ALS have shown that diseased motor neurons are more susceptible to death upon microglia activation (Raoul et al., 2002). A similar observation has been made *in vitro* using immortalized motor neuron (NSC-34) and microglial (BV-2) cells (He, Wen, & Strong, 2002). This increase microglial activity in ALS may contribute to an adverse inflammatory response causing increased neuronal apoptosis and oxidative damage in the area. Apoptosis may be caused by factors secreted from microglial cells, including tumor necrosis factor alpha, Fas ligand or nitric oxide (Moisse & Strong, 2006). Microglia can induce oxidative damage through a number of pathways, including the release of reactive oxygen species (ROS) such as superoxide and hydrogen peroxide, and the generation of reactive nitrating species (Banati, Gehrmann, Schubert, & Kreutzberg, 1993).

Key to our underlying hypothesis, ALS motor neurons show signs of increased oxidative stress such as lipid peroxidation and protein glycoxidation (Shibata et al., 2001; Ferrante et al., 1997). Oxidative damage may also be caused through mitochondrial dysfunction or excitotoxicity. Mitochondrial dysfunction has been inferred to have a pathological role in ALS because of the observation of abnormal mitochondrial morphology and because of the effects of mtSOD1 protein in disrupting mitochondrial function (Strong et al., 2005). The pathogenic role of mtSOD1 in inducing motor neuron degeneration has been confirmed through studies of transgenic mice harbouring a variety of different SOD1 mutations (Bruijn et al., 2004). Specifically for mitochondria, mtSOD1 has been shown to bind to a protein of the Bcl-2 family which interacts with the mitochondrial membrane

(Pasinelli et al., 2004). This interaction appears to cause cell death, likely through destabilization of the mitochondrial membrane leading to the release of pro-apoptotic factors and ROS (Brunelle & Letai, 2009).

1.2.3 **The role of astrocytes and excitotoxicity in ALS**

Astrocytes, similar to microglia, are another type of glial cell that have been implicated in ALS pathology. Astrocytes are not only critical to the formation of the blood brain barrier, but they play a role in regulating the extracellular milieu of neurons, including ion and neurotransmitter homeostasis (Tacconi, 1998). In ALS, astrocytes not only proliferate and appear to replace degenerating motor neurons with a glial scar, they may also contribute directly to motor neuron death – a hypothesis substantiated by observations from mtSOD1 mouse models (Levine, Kong, Nadler, & Xu, 1999). Moreover, the physiological role of astrocytes in regulating glutamate homeostasis, and thus intraneuronal calcium levels, is altered in ALS in a manner that has been suggested to either enhance or directly lead to motor neuron death through excitotoxic mechanisms (van Damme et al., 2007; Bruijn et al., 1997).

The process of glutamate excitotoxicity involves the excitatory neurotransmitter glutamate and its cognate receptors. Excessive calcium influx has been shown to be associated with the induction of oxidative injury through the formation of reactive oxygen species (Heath & Shaw, 2002). Excitotoxicity may be caused by either the abundance of glutamate release from presynaptic neurons or the inability of glutamate transporters (called excitatory amino acid transporters or EAAT) to clear glutamate from the synapse; both cases lead to the build-up of glutamate in the synapse. Astrocytes in ALS have been observed to have a significant depletion of the EAAT2 (or GLT-1) protein and a decrease in glutamate transport efficiency (Rothstein, Martin, & Kuncl, 1992; Rothstein, van Kammen, Levey, Martin, & Kuncl, 1995).

There is increasing evidence to suggest that motor neuron degeneration in ALS is associated with alterations in autophagy in addition to significant alterations in the proteasome-degradative pathway (Kabashi & Durham, 2006). Autophagy is similar to the proteasome-degradative pathway in that they both act as a mechanism of quality control

in the cell. The process of autophagy involves the breakdown of proteins and organelles that are no longer necessary within cytoplasmic vesicles called autophagosomes. Support for the hypothesis that autophagy is disturbed in ALS has been provided by the finding in ALS of mutations in the gene *SQSTM1* which encodes p62, or sequestosome 1. p62 is an adapter protein that can facilitate the localization of ubiquitinated proteins and organelles to autophagosomes through an interaction with microtubule-associated protein 1 light chain 3 (LC3) protein that is bound to autophagosome membranes (Kim, Hailey, Mullen, & Lippincott-Schwartz, 2008; Pankiv et al., 2007). Protein aggregates and dysfunctional mitochondria observed within ALS motor neurons often colocalize with p62 and may be indicative of the disruption of autophagy resulting in non-clearance of these pathological structures (Chen, Zhang, Song, & Le, 2012).

1.3 The three known variants of ALS

Three variants of ALS are recognized: the classical sporadic variant (sALS), the familial variant (fALS) and the Western Pacific variant. The latter variant occurs in a hyperendemic focus amongst the Chamorro peoples of Guam and the Japanese inhabitants of the Kii Peninsula (Garruto, 2006). Since its description in 1945, the incidence of Guamanian ALS has decreased dramatically (Garruto, Yanagihara, & Gajdusek, 1985). This has led to the proposal that ALS in the Western Pacific is an example of an environmental trigger for the disease, perhaps in association with enhanced genetic susceptibility, for which two hypotheses have been advanced. The first involves *Cycas circinalis* toxicity and in particular the biomagnification of the neurotoxin beta-methylamino L-alanine (BMAA) through either the consumption of flying foxes that eat the seeds or through the use of cycad flour in traditional foodstuffs (Cox & Sacks, 2002). However, this seemed unlikely since animals would exhibit no findings of ALS after accumulating large amounts of BMAA and the fact that free BMAA could not be detected in Chamorros with or without disease symptoms (Steele & McGeer, 2008). A second hypothesis cites the modernization and westernization of Guamanian society for the decline in Guamanian ALS as traditional foods and lifestyle have been changed as a result of the western influence from the United States. Currently, the etiology of

Guamanian ALS remains unresolved and research continues as cases are still observed, albeit at a lower incidence (Plato et al., 2003).

Although the remaining cases of ALS (accounting for over 95% of those observed worldwide) can be considered either sALS or fALS, this dichotomization is increasingly being challenged as our understanding of the pathogenesis of ALS increases exponentially. Much of our current understanding of ALS can be attributed to the genetic discoveries made in fALS. In fact, there may be a genetic component to all forms of ALS (Al-Chalabi et al., 2012), a hypothesis strengthened by the observation of increased ALS risk to relatives of patients with apparent sALS (Hanby et al., 2011).

The importance of this increasing overlap between sALS and fALS lies in the commonality of the NCIs and NNIs between all of the variants. Indeed, in a blinded study of both fALS and sALS, our laboratory was unable to differentiate amongst these two variants of ALS using immunohistochemical markers of both the traditional (intermediate filament inclusions) and contemporary (RNA binding proteins) pathologies of ALS (Keller et al., 2012). Given this, it is germane to our hypothesis to briefly examine the various genetic mutations associated with ALS (Table 1). The common thread underlying the mechanism of action of many of the pathogenic mutations associated with ALS is firstly a fundamental alteration in RNA metabolism, and secondly for many of the gene products, an alteration specifically in the low molecular weight neurofilament RNA mRNA (*NEFL* mRNA) stability. As will be also discussed, *RGNEF* lies at the intersection of both *NEFL* mRNA stability regulation and the cellular response to oxidative stress.

1.4 Gene mutations associated with ALS

1.4.1 Intermediate filaments

The neuronal intermediate filaments are a family of cytoskeletal proteins that include neurofilaments, peripherin, vimentin, nestin, and α -internexin (Szaro & Strong, 2010). As shown in figure 1, they share common features of an N-terminus head domain which regulates filament assembly, a central coiled-coil (α -helical coil) domain that facilitates

protein-protein interactions, and a C-terminus tail domain that contains phosphorylation sites of varying length which are key to modulating neuronal structure.

Neurofilaments (NFs) are found abundantly within neurons and serve to provide structural stability within the cell, determine the axonal thickness (or calibre) and improve axonal outgrowth (Szaro & Strong, 2010). There are three different isoforms of neurofilament: low molecular weight neurofilament (NFL; 66 kDa), medium molecular weight neurofilament (NFM; approx. 160 kDa), and high molecular weight neurofilament (NFH; approx. 220 kDa). The intact NF protein is a heteropolymer of the individual NF subunit proteins in which NFL must first dimerize either as a homopolymer or as a heteropolymer with either α -internexin, peripherin or vimentin. NFM and NFH then polymerize with this core unit through interactions in their N-terminus domains, while their highly phosphorylated C-terminus domains project from this core assembly. Any disruption of this assembly, as for instance will occur with a loss of NFL protein thus altering the NF protein stoichiometry, will lead to NF inclusions and motor neuron loss (Lee & Cleveland, 1996; Lee, Xu, Wong, & Cleveland, 1993; Gama Sosa et al., 2003; Cote, Collard, & Julien, 1993).

As described earlier, the accumulation of neurofilament within NCIs is a common pathological hallmark in ALS (Al-Chalabi et al., 2012; Hirano, Donnenfeld, Sasaki, & Nakano, 1984; Sasaki & Maruyama, 1992). Key to our understanding of the pathogenesis of ALS and to the role of RGNEF in the disease process, there is convincing evidence across multiple labs, including ours, that the levels of *NEFL* mRNA are selectively suppressed within ALS spinal motor neurons, within transgenic mouse models of ALS, and within induced pluripotent stem cell models of ALS (Bergeron et al., 1994; Wong et al., 2000; Menzies et al., 2002; Chen et al., 2014). This has been postulated to contribute directly to pathological NCI formation.

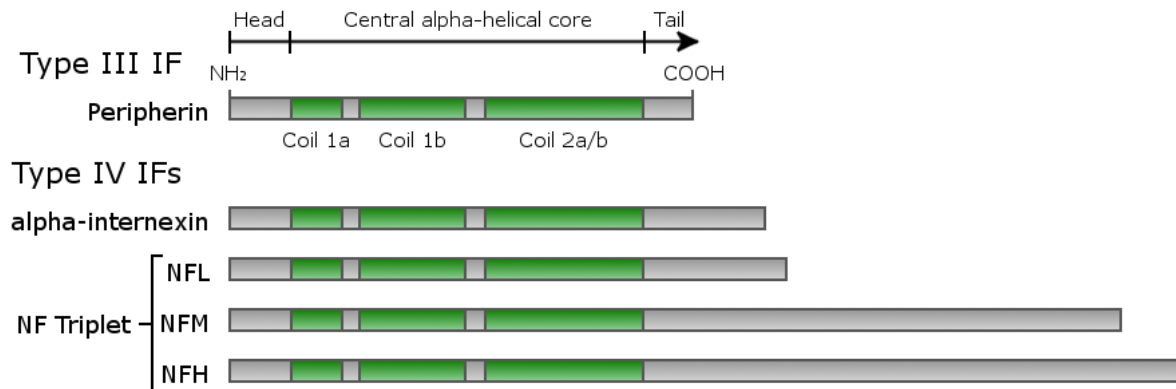


Figure 1: Comparing different intermediate filament proteins found in neurons. All the neuronal intermediate filament proteins share a similar structure consisting of an N-terminal head domain, a central α -helical core, and a C-terminal tail domain. The α -helical cores are required for polymerization, while the C-terminal tails and N-terminal heads regulate filament assembly and neuronal structure respectively. Longer tail domains indicate a greater opportunity for post-translational protein modifications such as phosphorylation which affect the spatial interactions between the intermediate filament proteins and consequently the neuronal structure as well. Interestingly, peripherin and α -internexin share a similarity in size as NFL. This similarity may explain the replacement of peripherin and α -internexin by NFL in mature neurons.

IF = intermediate filament; NFL = low weight neurofilament; NFM = medium weight neurofilament; NFH = high weight neurofilament.

*Figure adapted from: (Szaro & Strong, 2010)

In addition to this selective suppression of *NEFL* mRNA in ALS, mutations in *NEFH* have been observed in ALS (Al-Chalabi et al., 2012). Although this occurs in less than 1% of the sALS population, this is further evidence of the role of alterations in NF metabolism as key to the pathogenesis of ALS even if only as potential risk factors (Gros-Louis, Gaspar, & Rouleau, 2006).

Peripherin is an intermediate filament protein found within peripheral neurons of the nervous system. While sharing a number of characteristics of NFs, peripherin appears earlier than neurofilament proteins during development and is required for axonal elongation, an observation recapitulated in regenerating axons after neuronal injury. With maturation, peripherin is largely replaced by NFs (Szaro & Strong, 2010). Similar to *NEFH*, the gene encoding peripherin, *PRPH*, has rarely been found to be mutated in sALS, suggesting a potential role in disease susceptibility (Gros-Louis et al., 2004). This postulate is supported by the observation that mice overexpressing peripherin exhibit progressive, age-dependent motor neuron degeneration (Millecamps, Robertson, Lariviere, Mallet, & Julien, 2006). Moreover, peripherin has been found within ubiquitinated inclusions of ALS motor neurons and transgenic mtSOD1 mouse models of ALS show peripherin inclusions as an early sign of disease (Corbo & Hays, 1992). Interestingly, the levels of peripherin protein are altered in ALS and this alteration may be a result of the increased levels of *PRPH* mRNA seen in ALS cases. Consequently, the disturbance in peripherin levels may be a result of aberrant RNA homeostasis, similarly described for NFs, and lending support to the hypothesis that RNA metabolism is altered in ALS.

Although α -*internexin* is very similar in molecular weight and structure to NFL (Lee & Cleveland, 1996), it differs in being expressed earlier in neuronal development and in being restricted in expression to the central nervous system (Szaro & Strong, 2010). As neurons mature, NFL protein gradually replaces α -internexin, though α -internexin is not completely replaced and has been shown to be able to co-assemble with NFs (Yuan et al., 2006). Thus, similar to peripherin, problems in α -internexin assembly could lead to problems in NF assembly. In contrast to both NFs and peripherin, there have been to date no reports of mutations in the gene encoding α -internexin or of α -internexin

immunoreactive NCIs in ALS. However, α -internexin has been seen to aggregate and form neuronal spheroids in transgenic mtSOD1 mouse models suggesting that it can indeed play a role in the induction of motor neuron degeneration (Wong et al., 2000; King, Blizzard, Southam, Vickers, & Dickson, 2012).

1.4.2 **Copper/zinc superoxide dismutase**

Superoxide Dismutase 1 (*SOD1*), the gene that encodes for the copper/zinc superoxide dismutase (SOD1), was the first gene to be linked to fALS and accounts for about 12% of all fALS cases (Rosen et al., 1993; Chio et al., 2008). Although transgenic mouse models of mtSOD1 have proven to be useful in understanding the pathogenic mechanisms of mtSOD1 toxicity (Pasinelli et al., 2004), there remains controversy regarding the extent to which this model of ALS truly recapitulates the disease process of ALS (Ludolph et al., 2007). This is especially due to its failure to predict responsiveness to experimental therapies for the treatment fALS.

SOD1 is responsible for removing reactive oxygen species in the cell, specifically converting the highly-reactive superoxide radical into hydrogen peroxide (Gurney et al., 1994). Though most mutations in the *SOD1* gene inhibit the SOD1 protein's dismutase ability, some mutations do not affect it at all, though still maintaining a disease phenotype. This suggests that the protein may be gaining toxic function (Al-Chalabi et al., 2012). Although a number of potential mechanisms of mtSOD1-mediated neurotoxicity have been postulated, our lab has demonstrated that one such gain of function is the ability for mtSOD1 to interact directly with the *NEFL* mRNA 3' untranslated region (3' UTR) and destabilize it, leading to a marked alteration in NF protein stoichiometry (Ge, Wen, Strong, Leystra-Lantz, & Strong, 2005). In patients harbouring mtSOD1, NCIs immunoreactive with antibodies to SOD1 are rarely observed and have been postulated to impair axonal transport (Bruijn et al., 1998).

1.4.3 **Chromosome 9 open reading frame 72**

C9ORF72 is a newly discovered gene involved in both sALS and fALS, now accounting for the majority of genetically originating cases. The mutation of the gene is observed as a massive intronic hexanucleotide (GGGCC) repeat expansion (DeJesus-Hernandez et al.,

2011; Renton et al., 2011). The number of repeat expansions found within ALS patients ranges between 600 to 2,000 repeats, while normal individuals appear to have about 23 repeats (Al-Chalabi et al., 2012; DeJesus-Hernandez et al., 2011). However, the exact threshold of repeats necessary for disease induction by *C9ORF72* is unknown due to difficulties in sequencing GC rich DNA (Stepito, Gallo, Shaw, & Hirth, 2014). Currently, *C9ORF72* mutations account for about 40% of all fALS cases (Renton, Chio, & Traynor, 2014).

The protein product of *C9ORF72* is not known, though bioinformatics studies suggest that the protein is related to Differentially Expressed in Normal and Neoplasia (DNEN) - a GDP/GTP exchange factor that can activate Rab GTPases (Levine, Daniels, Gatta, Wong, & Hayes, 2013). Rab GTPases may be important in neurodegeneration because of their effects on membrane vesicle trafficking (Stenmark, 2009).

There are currently three somewhat overlapping hypothesis regarding the mechanism of toxicity of *C9ORF72*, including a loss of function resulting from failure of mRNA translation, toxic gain of function from the formation of RNA foci and RNA-binding protein sequestration, and repeat-associated non-ATG (RAN) translation generating dipeptide repeat proteins (Stepito et al., 2014). Although much work remains to be done, RNA-binding protein sequestration by RNA foci and RAN translation protein products appear to be of significance in the toxic mechanism of *C9ORF72* (Zu et al., 2013; Lee et al., 2013). Conversely, loss of function of *C9ORF72* protein seems to be less important in disease pathogenesis (Fratta et al., 2013).

1.4.4 **Ataxin-2**

Ataxin-2 is a protein that has been functionally linked to many aspects of mRNA processing, including polyadenylation and micro RNA (miRNA) synthesis (Blokhuys, Groen, Koppers, van den Berg, & Pasterkamp, 2013). Similar to the pathogenic expansion of GGGCC repeats in *C9ORF72*, the gene for ataxin-2, *ATXN2* contains pathogenic CAG nucleotide expansions, although to a less impressive extent (Elden et al., 2010; Liu et al., 2013). Although the exact mechanism by which the pathogenic expansion of CAG repeats in ataxin-2 induce neuronal pathology is unknown, it is known

that the number of repeats is a critical determinant of disease induction: CAG repeat length between 27 and 33 are linked to ALS (Elden et al., 2010) while longer repeats are associated with the disease spinocerebellar ataxia 2 (SCA2) (Hart & Gitler, 2012). SCA2 differs from ALS as it is a disorder of cerebellar function which is only rarely associated with motor neuron disease degeneration. The importance of ataxin-2 in mRNA processing implies that its dysfunction can lead to impairments in mRNA metabolism, further supporting the RNA hypothesis of ALS.

1.4.5 **TAR DNA-binding protein of 43 kDa**

TAR DNA-binding protein of 43 kDa was originally discovered in human immunodeficiency virus (HIV) as a DNA-binding protein that could repress *in vitro* transcription of *HIV-1*, a gene expressed by the human immunodeficiency virus (HIV) (Ou, Wu, Harrich, Garcia-Martinez, & Gaynor, 1995). TDP-43 was also found to have a role in splicing the cystic fibrosis transmembrane conductance regulator (CFTR) (Buratti et al., 2001). In 2006, two groups discovered that TDP-43 was also the major component of ubiquitinated aggregates observed in ALS motor neurons, thus implicating this protein in the disease pathology (Neumann et al., 2006; Arai et al., 2006). Shortly thereafter, our laboratory demonstrated that TDP-43 was a stability determinant for *NEFL* mRNA through a direct interaction with its 3' UTR (Strong et al., 2007).

TDP-43 is found ubiquitously in cells and normally appears in the nucleus where it participates at multiple levels in both DNA and RNA processing, including splicing, miRNA biogenesis, RNA transport, and stress granule formation (Ling, Polymenidou, & Cleveland, 2013). In response to cellular injury or stress, neuronal TDP-43 expression is massively up-regulated and the protein is translocated from the nucleus to the cytoplasm where it is postulated to be integral to the stabilization of mRNAs through its incorporation into both transport and stress granules, discussed further below (Moisse et al., 2009).

Interestingly, TDP-43 expression is predominantly cytoplasmic in the motor neurons in ALS where it also forms NCIs. Concomitant with this aggregate formation, there is a loss of nuclear expression, in part due to a loss of cytosolic-nuclear transport (Lee, Lee, &

Trojanowski, 2012). While the exact mechanism by which TDP-43 forms pathological NCIs is not clear, it does appear to be dependent on its C-terminal glycine region which is normally responsible for its protein-protein interactions (Igaz et al., 2009).

Mutations in the gene encoding TDP-43 (*TARDBP*) are observed in approximately 4% of all fALS cases, with all but one of the documented mutations being found within the C-terminal glycine region of TDP-43 (Sreedharan et al., 2008).

1.4.6 **Fused in sarcoma/translocated in liposarcoma**

Similar to TDP-43, Fused in Sarcoma/Translocated in Liposarcoma (FUS or FUS/TLS) is an RNA-binding protein that has been observed to form pathological NCIs in ALS motor neurons and is mutated in approximately 4% of all fALS cases (Renton et al., 2014).

Under physiological conditions, FUS is normally localized to the nucleus and has many similar functions to TDP-43 such as participation in RNA splicing and transcription, in addition to miRNA processing (Ling et al., 2013). Also like TDP-43, FUS can associate with RNA granules (Lagier-Tourenne et al., 2012). In ALS motor neurons, FUS becomes mostly cytoplasmic and forms protein aggregates. FUS has also been shown to be able to bind murine *NEFL* mRNA, further solidifying the linkage between known genetic linkages in ALS and the metabolism of *NEFL* mRNA (Kwiatkowski, Jr. et al., 2009).

1.4.7 **Ewing's sarcoma protein and TATA-binding protein associated factor 2N**

FUS protein belongs to a family of proteins called the FET proteins (FUS, EWS, TAF15) that also contains two other members: Ewing's sarcoma protein (EWS) encoded by the gene *EWSR1* and TATA-binding protein associated factor 2N (TAF15) encoded by the gene *TAF15*. Both *EWSR1* and *TAF15* have been shown to be mutated in cases of ALS. All three FET proteins are very similar in structure (Tan & Manley, 2009) and both EWS and TAF15 are also observed to be mislocated to the cytoplasm as punctate granules in ALS motor neurons (Couthouis et al., 2012; Couthouis et al., 2011). However, in spite of their close functional relationship, FUS NCIs in ALS do not colocalize with EWS or TAF15 NCIs (Neumann et al., 2011). Similar to TDP-43 and FUS, EWS and TAF15 normally function in regulating RNA processes such as transcriptional activation, splicing, miRNA processing, and RNA granule formation (Tan & Manley, 2009).

1.4.8 **Angiogenin**

Angiogenin is a protein that is induced by hypoxia to elicit angiogenesis and cell division. Specifically, it is a ribonucleolytic protein that functions in the nucleus to stimulate ribosomal RNA (rRNA) transcription through its binding to a promoter in the ribosomal DNA (Li & Hu, 2012). This function is intricately related to the function of another angiogenic protein called vascular endothelial growth factor (VEGF) (Kishimoto, Liu, Tsuji, Olson, & Hu, 2005). Angiogenin is also found within motor neurons and indeed the gene that encodes it, *ANG*, has been described as a susceptibility gene for ALS (Greenway et al., 2006). In fact, the mutations described have been associated with a loss of its functioning (Wu et al., 2007). Within motor neurons, angiogenin has been described to have neuroprotective functions, and so the loss of its function in ALS-related *ANG* mutations may provide a causative link for angiogenin's role in ALS (Subramanian, Crabtree, & Acharya, 2008; Kieran et al., 2008). In addition, its connection to the function of VEGF provides further evidence of angiogenin's role in ALS pathology as transgenic mouse models with VEGF deletions exhibit motor neuron cell death (Oosthuyse et al., 2001).

1.4.9 **Heterogeneous nuclear ribonucleoprotein A1**

Heterogeneous nuclear ribonucleoprotein A1 (hnRNP A1) is an RNA-binding protein with a diverse roles in the nucleus. Similar to TDP-43 and the FET family of proteins, hnRNP A1 has been shown to process mRNAs through splicing, to shuttle mature mRNA through the nuclear pore complex, and to interact with the Drosha complex in miRNA biogenesis (Bekenstein & Soreq, 2013). *HNRNPA1*, the gene encoding hnRNP A1, is rarely mutated in ALS (Kim et al., 2013; Calini et al., 2013). Interaction between hnRNP A1 and TDP-43 has also been observed, implying that dysfunction in one protein could lead to dysfunction in the other.

1.4.10 **Senataxin**

Senataxin is a protein predicted to be an RNA helicase that has been implicated in the disease process of ALS. Mutations in its gene, *SETX*, are associated with an autosomal dominant form of juvenile ALS known as ALS4 (Chen et al., 2004). However, its role in

causing pathology remains unknown. Normally, RNA helicases appear to function to rearrange RNA-protein interactions through an unwinding of short, double stranded RNA sequences (Tanner & Linder, 2001). By extension, RNA helicases have been related to mRNA splicing and mRNA translational initiation and termination (Gustafson & Wessel, 2010). Therefore, like TDP-43, the FET family proteins and hnRNP A1, senataxin may be contributing to ALS pathology via a disruption in RNA metabolism (Strong, 2010).

1.5 RNA granules

A commonality of the proteins described above is that they can all be linked to aberrant RNA metabolism in ALS, including *C9ORF72* which does not directly bind RNA but appears to have a toxic RNA gain of function through its sequestration of RNA binding proteins or its induction of RNA translation (Strong, 2010; Strong et al., 2007; Ge et al., 2005; Stepto et al., 2014; Kim et al., 2013; Chen et al., 2004; Couthouis et al., 2012; Couthouis et al., 2011). Because of the many RNA processing duties of RNA-binding proteins like TDP-43 and the FET family of proteins, there are many areas in which RNA metabolism may go wrong in ALS. Nuclear splicing, miRNA processing, and intron stabilization may all be affected by the disease process.

Our laboratory has been particularly interested in the role of these various RNA interacting proteins in the formation and function of RNA granules (or ribonucleoprotein particles, RNPs). RNA granules are macromolecular structures within the cell composed of RNA, RNA binding proteins and all of the regulatory proteins for controlling localized RNA translation, silencing or destruction (Strong, 2010). They thus represent a critical structure in RNA metabolism, and although controversial, have been postulated to be the precursor to NCIs in which RNA binding proteins have been incorporated (Wolozin, 2012; Ling et al., 2013). Within neurons, there are currently four known RNA granules: stress granules, transport granules, processing bodies, and nuclear paraspeckles (Table 2).

Table 2: Types of RNA granules found in neurons

Name	Marker	Function	References
Stress Granules	TIA1 protein	Forms in response to a stress (e.g. heat shock, oxidative stress, etc.) and appears to play an important role in deciding mRNA fate (storage or decay) during stress	Kedersha et al., 2000
Transport Granules	Staufen protein	Ubiquitous within the neuron and appears to shuttle mRNAs throughout the cell for localized translation of protein	Martin & Ephrussi, 2009
Processing Bodies	XRN1 protein	Ubiquitous within neurons, serving as a hub for storing and degrading mRNA and works closely with stress granules	Ingelfinger et al., 2002
Nuclear Paraspeckles	NEAT1 long non-coding RNA	Stores RNAs within nuclei and selectively releases them under stress conditions	Shelkovernikova et al., 2014

1.5.1 Stress granules

Stress granules (SG) are not present in the resting state, but are formed when cells are exposed to stressors such as heat shock, oxidative, or osmotic stressors (Kedersha, Gupta, Li, Miller, & Anderson, 1999; Sama et al., 2013). These granules contain mRNA in the presence of not only RNA-binding proteins that modulate the stability and translational activation of the mRNAs, but also a number of proteins that can be used in their characterization, for instance T-cell intracellular antigen 1 (TIA-1) and a Ras GAP SH3 binding protein (G3BP) (Kedersha et al., 1999; Tourriere et al., 2003). TIA-1 and G3BP are known to regulate stress granule assembly, which is both rapid to combat stress efficiently and transient in order to disassemble when the stressor has been removed (Anderson & Kedersha, 2009; Wolozin, 2012). In addition, TIA-1 protein has shown to rapidly shuttle in and out of SGs (Kedersha et al., 2000). SGs are dynamic structures that may act as foci of triage for RNA, deciding the fate of individual transcripts: whether to be stored safely in SGs or degraded in processing bodies (a type of RNA granule described below) (Anderson & Kedersha, 2008).

The formation of SGs also appears to be protective against a stress. When the formation of SG is inhibited, the survival of these cells significantly decreases compared to uninhibited cells in response to a stressor (Eisinger-Mathason et al., 2008). Also, apoptosis-promoting factors such as tumor necrosis factor α (TNF α) and receptor for activated C kinase (RACK1) have been observed to be sequestered in SGs, suggesting an anti-apoptotic function (Kim, Back, Kim, Ryu, & Jang, 2005; Arimoto, Fukuda, Imajoh-Ohmi, Saito, & Takekawa, 2008). Although some doubts remain regarding the conclusions of these studies, namely that blocking SG assembly with drugs such as cycloheximide may be affecting several other cellular processes, SGs seem to be intimately involved in cellular survival during a stress (Kedersha, Ivanov, & Anderson, 2013).

Recently, stress granule formation has become an interesting topic of discussion regarding the protein aggregates observed in ALS. This interest may be attributed to the role of ALS-related RNA-binding proteins in the formation of SGs. Indeed, TDP-43 and FUS have both been observed to colocalize with TIA-1 positive stress granules (Sama et

al., 2013; Liu-Yesucevitz et al., 2010). Taken together, a strong implication is made for the involvement of pathological stress granules in ALS. Indeed, stress granules can be observed in the ALS cortical tissues (Liu-Yesucevitz et al., 2010). The idea of irreversible SG formation leading to insoluble aggregates has been raised as a possible etiology for the aggregates seen ALS. This argument is strengthened by the fact that many SG associated RNA binding proteins, such as TIA-1, contain glycine-rich prion-like domains (Gilks et al., 2004). It has been hypothesized that these domains have the potential to become pathological and form irreversible amyloid aggregates, similar to prion protein itself (Arimoto et al., 2008; Wolozin, 2012). However, this hypothesis has yet to be proven.

1.5.2 **Transport granules**

Transport granules are responsible for transporting mRNA to specific sites for localized protein translation (Martin & Ephrussi, 2009). Unlike SG's, transport granules are necessary for normal cellular functioning and can be found throughout the cell under physiological conditions. Staufen is a key constituent of transport granules that can bind stem-loop structures within mRNA 3' UTRs and transport them to sites, such as neuronal dendrites, for localized protein translation (Ferrandon, Koch, Westhof, & Nusslein-Volhard, 1997; Kiebler et al., 1999).

Defects in RNA transport have been implicated in various neurodegenerative diseases including fragile X mental retardation syndrome and spinocerebellar ataxia 2 (Tosar et al., 2012). Motor neuron degeneration has been indirectly linked to aberrant RNA transport through the finding of a mutation in the motor protein dynactin in ALS (Puls et al., 2003). TDP-43 has also shown to associate with staufen-positive transport granules, with ALS-related mutations impairing the function of these transport granules, further suggesting the involvement of transport granules in ALS pathology (Alami et al., 2014; Volkening, Leystra-Lantz, Yang, Jaffee, & Strong, 2009).

1.5.3 **Processing bodies**

Processing bodies (PB) function to store mRNAs in a translationally quiescent form so that they can later be degraded or returned for translation (Bregues, Teixeira, & Parker,

2005; Parker & Sheth, 2007). Similar to SGs, PBs are upregulated during a stressor, though PBs are also observed in the absence of stress and therefore form independently from SGs (Li, King, Shorter, & Gitler, 2013; Kedersha et al., 2005). Interestingly, SG and PB share certain RNA binding proteins and this sharing may be related to the ability of SG and PB to interact with each other (Kedersha et al., 2005). However, the two granules differ in that PBs contain RNA degradation machinery such as Decapping enzyme 1 (DCP1A) and 5'-3' exoribonuclease 1 (XRN1) while SGs contain translation initiation machinery such as Poly(A)-binding protein 1 (PABP1) (Kedersha et al., 1999; Eulalio, Behm-Ansmant, & Izaurralde, 2007; Ingelfinger, Arndt-Jovin, Luhrmann, & Achsel, 2002). It is worth noting that the dynamic conditions of both PBs and SGs further SGs role as a site of RNA triage during stress, and that both granule types are necessary for this task (Anderson & Kedersha, 2008).

The relationship between PBs and ALS pathology has not been studied in detail. It is worthwhile to note that, like SGs, PBs colocalize with TDP43 and FUS (Volkening et al., 2009; Li et al., 2013). In addition, as PBs are similar to SGs they may also be implicated in the pathogenic conversion of granule to aggregate. This is because many of the RNA binding proteins associated with PBs, like SGs, contain prion-like domains which have the potential to form irreversible aggregates within the cytoplasm (Wolozin, 2012).

1.5.4 Nuclear paraspeckles

Nuclear paraspeckles are a type of RNA granule that, unlike the other three granules described, are restricted to the nucleus. Initially discovered in 2002 by Fox et al. (Fox et al., 2002), paraspeckles are formed from the long non-coding RNA (lncRNA) called nuclear-enriched abundant transcript 1 (NEAT1) and its constituent RNA-binding proteins (Nakagawa & Hirose, 2012). Protein components shuttle rapidly between other structures in the nucleus, whereas NEAT1 lncRNA is structurally vital to the formation of paraspeckles (Mao, Sunwoo, Zhang, & Spector, 2011). Paraspeckles appear to function by sequestering specific RNAs, preventing their release from the nucleus unless the cell encounters a stress such as transcriptional inhibition. Upon stress, the transcripts are released from the paraspeckles (Nakagawa & Hirose, 2012).

Paraspeckles have been recently implicated in the early stages of ALS pathology. ALS motor neurons show increased formation of paraspeckles compared to control motor neurons while both TDP-43 and FUS colocalize with paraspeckles (Nishimoto et al., 2013). It is currently unknown whether paraspeckles are pathological or protective in ALS motor neurons, though Shelkovernikova et al. found that the loss of FUS from the nucleus destabilizes paraspeckles and may leave cells vulnerable to stress (Shelkovernikova, Robinson, Troakes, Ninkina, & Buchman, 2014).

1.6 Rho guanine nucleotide exchange factor

Our laboratory recently discovered that Rho guanine nucleotide exchange factor (RGNEF) forms pathological NCIs in ALS spinal motor neurons (Keller et al., 2012). As its name suggests, RGNEF can bind and activate small GTPase RhoA using two domains: a Dbl-homology domain and a Pleckstrin-homology domain (Fig. 2) (Volkening et al., 2010). The Dbl-homology domain is responsible for the GDP/GTP exchange while the Pleckstrin-homology domain allows the protein to locate to the cell membrane to bind RhoA (Zheng, 2001). RGNEF is also an RNA binding protein and has been shown to bind and destabilize *NEFL* mRNA (Droppelmann et al., 2013; Volkening et al., 2010). To date it is the only known RNA binding protein that also participates in RhoA activation. In addition, *ARHGEF28*, the gene that encodes RGNEF, has been shown to be mutated in both sALS and fALS, although this observation is exceptionally rare (Ma et al., 2014; Droppelmann et al., 2013). This mutation involves a deletion of a single nucleotide leading to either a frameshift mutation or a splicing mutation within the gene. The result is a truncated RGNEF product predicted, respectively, to be either 319 or 259 amino acids long, which is a massive difference compared to the normal 1731 amino acid length of RGNEF (Droppelmann et al., 2013). Taken together, these characteristics of RGNEF strongly implicate the protein in ALS pathogenesis.

p190RhoGEF is the murine homologue of RGNEF. It was originally discovered as a guanine exchange factor protein that specifically activated the small GTP-ase RhoA (Gebbinck et al., 1997; van Horck, Ahmadian, Haeusler, Moolenaar, & Kranenburg, 2001). Mutations in p190RhoGEF that alter its interaction with murine *NEFL* mRNA

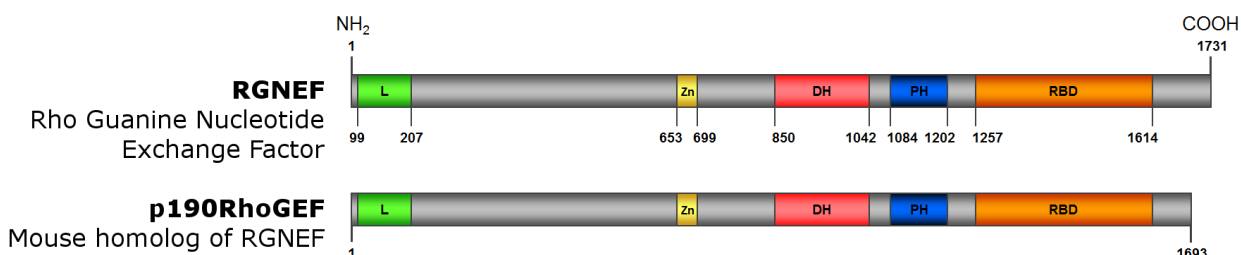


Figure 2: Comparing the protein structures of RGNEF and p190RhoGEF. RGNEF is longer than p190RhoGEF by 38 amino acids and this difference in length has also caused some differences in domain locations. Both proteins share similar domains based on previous studies and protein analysis by UniProt, however RGNEF destabilizes *NEFL* mRNA while p190RhoGEF stabilizes it. Both proteins utilize their DH/PH domains to activate the cell signaling small GTPase RhoA.

L = leucine rich domain; Zn = Zinc-binding domain; DH = Dbl homology domain; PH = Pleckstrin homology domain; RBD = RNA-binding domain.

give rise to a motor neuron degeneration in which NF immunoreactive NCIs are prominent (Lin, Zhai, & Schlaepfer, 2005). Though p190RhoGEF has been shown by northern blotting to be found in several tissues, including kidney and lung, its presence in the brain was of particular interest due to its ability to bind and stabilize *NEFL* mRNA (Gebbinck et al., 1997; Canete-Soler, Wu, Zhai, Shamim, & Schlaepfer, 2001). p190RhoGEF also forms aggregates that co-localize with NFL protein aggregates when *NEFL* mRNA and its 3' UTR are overexpressed in Neuro 2A cells, a mouse neuronal cell line (Lin et al., 2005).

It has been suggested that p190RhoGEF and NFL protein exist in a complex with each other where p190RhoGEF modulates levels of both *NEFL* mRNA and NFL oligomers to restrict the self-assembly of NFL *in vivo* (Lin et al., 2005). Because NF must assemble in stoichiometrically correct ratios, overexpressing NFL exclusively may cause issues in p190RhoGEF's function and lead to aggregation of these p190RhoGEF-NFL complexes (Wong et al., 2000). Moreover, p190RhoGEF is seen to form punctate aggregates alongside NF aggregates in transgenic mtSOD1 mouse expressing the human G93A mutation. This linkage of p190RhoGEF with the induction of NF pathology and a motor neuron degeneration was of particular interest.

In addition to its potential role in motor neuron degeneration, p190RhoGEF has also been shown to interact with focal adhesion kinase (FAK) and in this way modulate axonal branching and synapse formation in neurons (Zhai et al., 2003; Rico et al., 2004). This interaction may be a result of p190RhoGEF acting as a scaffold, where the pleckstrin homology domain of p190RhoGEF locates the protein to the cell membrane. At the membrane, p190RhoGEF interacts with FAK and brings other proteins together, such as Paxillin and integrin proteins, for signal transduction activity (Miller et al., 2013). Whether this function is preserved in human RGNEF is currently unknown.

Though RGNEF and p190RhoGEF are homologues of each other, they may still differ from one another. Indeed, the lengths of the two proteins differ slightly: RGNEF is 1731 amino acids long while p190RhoGEF is 1693 amino acids long (Droppelmann et al., 2013) (Fig. 2). When comparing amino acid similarities between the two proteins, 80%

homology is obtained. The guanine exchange factor domain, shown to specifically activate RhoA in both RGNEF and p190RhoGEF, is particularly similar between the two proteins, showing 92% identity (van Horck et al., 2001; Droppelmann et al., 2013). Although this degree of homology would suggest identical functions, we have shown that while both p190RhoGEF and RGNEF can interact directly with *NEFL* mRNA, p190RhoGEF stabilizes the transcript while RGNEF destabilizes it (Canete-Soler et al., 2001; Droppelmann et al., 2013). It is unclear how this difference between the two proteins affects their roles in ALS pathogenesis. However it does demonstrate that even with 80% identity, the two proteins are not the same and research performed in p190RhoGEF must be confirmed with experiments using RGNEF so that the results are more applicable in humans.

While many studies have been performed regarding p190RhoGEF and NFL related motor neuron degeneration, there remains much to be explored for RGNEF. For example, though illustrations of p190RhoGEF show the existence of a leucine-rich domain and a cysteine-rich zinc binding domain, not much research has been performed on these domains (van Horck et al., 2001; Droppelmann et al., 2013). In particular, the leucine-rich domain of RGNEF is predicted to be located between amino acids 99 and 207. Traditionally, leucine-rich domains (or leucine-rich repeats) have been shown to mediate protein-protein interactions and have been shown to be important in cellular processes such as apoptosis and neural development (Inohara et al., 1999; Mutai et al., 2000). Interestingly, leucine-rich domains have been implicated in Parkinson's disease. Specifically, mutations in Leucine-rich repeat kinase 2 (LRRK2) have been described as a major cause in both sporadic and familial cases of Parkinson's disease (Paisan-Ruiz et al., 2004; Zimprich et al., 2004). However, when looking at this domain in RGNEF it is clear that the domain does not resemble classical leucine-rich domains. The amino acid sequence in this region of RGNEF lacks the typical LxxLxLxxNxL pattern (Kobe & Kajava, 2001). Nevertheless, this region is enriched with leucine amino acid residues (about 26.6% of the amino acids in this region are leucines) and its role in the protein should not be overlooked.

The cysteine-rich zinc binding domain of RGNEF is predicted to be located between amino acids 654 and 699. RGNEF's domain here does resemble the typical zinc binding domain which is responsible for binding phospholipids such as diacylglycerol (DAG) or phorbol esters (Ono et al., 1989). Originally, this domain is utilized by protein kinase C (PKC) to locate itself to the cell membrane, bind DAG, and initiate signal cascades such as glycogen synthase kinase 3 β (GSK-3 β) inhibition (Alkon, Sun, & Nelson, 2007). Though this may imply a scaffolding role of RGNEF for targets of PKC, no studies have been performed to examine the domain's function.

In addition to protein domains, RGNEF is also predicted to have many sites available for post-translational modifications. Indeed, RGNEF can be phosphorylated and SUMOylated at a myriad of sites throughout its length indicating that cells may modulate RGNEF activity in a vast number of ways (Droppelmann et al., 2014). In summary, more studies need to be performed to better characterize RGNEF's physiological role so that its aggregation in ALS can be better understood.

1.7 RGNEF's potential role in stress response

As discussed earlier, there are numerous reasons for motor neurons in ALS to be under significant oxidative stress (Shibata et al., 2001; Ferrante et al., 1997). This oxidative stress may arise from several sources, including malfunctioning mitochondria, surrounding inflammatory responses from microglia, and excitotoxicity (Simpson, Yen, & Appel, 2003). Whether or not aggregates of protein such as TDP-43 or FUS are also adding to this stress or acting as an innocent bystander remains to be seen. However, it has been found that TDP-43 is important in the assembly of stress granules, and that removing TDP-43 by RNA interference (RNAi) from cells reduces survivability in cells exposed to stress (Higashi et al., 2013; Aulas, Stabile, & Vande Velde, 2012). Similarly, FUS has been shown to colocalize with TIA-1 positive stress granules, and when knocked down using RNAi, a decrease in cell survivability in response to stress is observed (Sama et al., 2013). These studies suggest that, physiologically, TDP-43 and FUS play a protective role that may be lost when the two proteins aggregate in ALS motor neurons.

p190RhoGEF can also provide protection against stress, albeit using a different mechanism from SG formation. Wu and colleagues identified two domains on the C-terminal region of p190RhoGEF shown to interact with either c-Jun N-terminal kinase (JNK) Interacting Protein 1 (JIP-1) or 14-3-3 proteins (Wu et al., 2003). When overexpressing either of these domains in a mouse neuronal cell line and then exposing these cells to chemical and heat shock stressors, cells overexpressing the domains experienced significantly less apoptosis compared to controls. This implies that, through an interaction with either JIP-1 or 14-3-3, p190RhoGEF can protect cells against stress.

Taken together, the above would suggest that RGNEF can play a role in the cellular stress response. Like TDP-43 and FUS/TLS, RGNEF is an RNA binding protein whose expression is upregulated following axonal injury (Strong lab, unpublished observation); therefore RGNEF might be expected to participate in the stress response through the formation of SGs. Alternatively, because it is the human homologue of p190RhoGEF, RGNEF may also participate in the stress response through a JIP-1/14-3-3 mediated mechanism. In spite of the differences between RGNEF and p190RhoGEF in terms of destabilizing or stabilizing *NEFL* mRNA, respectively, both proteins nevertheless show 80% homology and are demonstrated (Strong lab, unpublished observation) to be upregulated in response to sciatic nerve injury. Therefore, I would predict that RGNEF could have an equivalent function to p190RhoGEF in regards to its participation in the stress response. Furthermore, the RhoA activation ability of RGNEF could indicate another mechanism involved in the cellular stress response. Indeed, the RhoA signaling pathway, through Akt activation, has been described to protect against cellular stress (Del Re, Miyamoto, & Brown, 2008). The purpose of my studies was to characterize RGNEF as a protein involved in the cellular stress response.

1.8 Hypothesis

My hypothesis is that RGNEF participates in the cellular stress response. This participation includes providing protection to cells stressed with oxidative, osmotic, or heat shock stress and this protection may occur through its guanine nucleotide exchange domain or its RNA binding domain.

Chapter 2

2 Specific aims

My first aim was to determine whether RGNEF expression in cells is protective against oxidative, osmotic, or heat shock stressors. To accomplish this, I used the human embryonic kidney 293 cell line containing large T antigen (HEK 293T cells). These cells were either stably transfected or transiently transfected and expressed RGNEF under a cytomegalovirus promoter. Cells were then exposed to either oxidative, osmotic, or heat shock stress and their resultant survival was examined using an MTT cell viability assay. Stably transfected, RGNEF overexpressing HEK 293T cells were compared to non-transfected HEK 293T cells as a control. HEK 293T cells transfected with an empty vector plasmid were used as a control for all transiently transfected cells overexpressing an RGNEF construct.

My second aim was to determine which domain of RGNEF was required for its protective effect. To do this, HEK 293T cells were transiently transfected with plasmid constructs containing different deletions of the RGNEF in which key functional domains (e.g. DH/PH domain, RNA binding domain, etc.) were removed. Cells were then subjected to the stresses defined in aim 1 and the resultant survival compared against both control transfections and transfections expressing the full length RGNEF construct.

My third aim was to determine whether RGNEF is incorporated into RNA granules in response to cellular stress. To accomplish this, HEK 293T cells were either stably transfected or transiently transfected with full length RGNEF and then the cells subjected to stressors characterized in aim 1. Fluorescence immunocytochemistry was used to label proteins marking RNA granules and RGNEF. Then, using, confocal microscopy, I examined whether RGNEF colocalized with RNA granules under a stress.

2.1 Cell lines and transfections

All experiments used HEK 293T cells. This cell line was chosen because they are amenable to transfection and because they express *NEFL* mRNA (Shaw, Morse, Ararat, & Graham, 2002). Cells were maintained in Dulbecco's modified eagle's medium

(Gibco, Life Technologies Inc., Burlington, Ontario) supplemented with 10% fetal bovine serum (Gibco) and kept in a water-jacketed, 37°C 5% CO₂ incubator (Forma Scientific, Thermo Fisher Scientific, Ottawa, Ontario).

HEK 293T cells stably transfected with the human RGNEF gene were created in our lab by Dr. Cristian Droppelmann using a full length myc-tagged RGNEF gene via the Jump-in Fast Gateway Targeted Integration System (Invitrogen, Life Technologies Inc., Burlington, Ontario) (Droppelmann et al., 2013). These cells were convenient because they allowed us to observe RGNEF without needing to transiently transfect the cells beforehand. However, it may be possible that unforeseen variables would not be eliminated when comparing these stable-transfected cells against non-transfected cells. Thus, to better control for variables possibly introduced by a stable transfection, transient transfections in HEK 293T cells were also used to corroborate stable transfection results.

For transient transfection, plasmid constructs of RGNEF using the plasmid backbone: pcDNA 3.1(+)/myc-His A were purified by Miniprep (Invitrogen) from transformed, chemically competent DH5α *Escherichia coli* (*E. coli*, Invitrogen). Different plasmid constructs were generated by inserting the gene of interest (variations on the full length cDNA of RGNEF) using restriction enzyme digests; more details are provided in the RGNEF constructs section below. The Miniprep was performed according to the manufacturer's protocol. However the lysis time for the full length intact RGNEF construct (lysis buffer incubation step) was shortened to 3 minutes instead of the recommended 5 in order to reduce DNA fragmentation which we found to occur with the longer incubation period. DNA quality of the miniprep DNA was assessed by running gel electrophoresis on a 1% agarose gel to compare purified plasmids against a control plasmid. GeneRuler 1kb Plus DNA Ladder (Thermo Fisher Scientific – Canada, Ottawa, Ontario) was used to observe the sizes of plasmids in 1% agarose gel.

Transient transfections for this series of experiments were performed in 6-well plates using Lipofectamine 2000 (Invitrogen) according to the manufacturer's protocol. HEK 293T cells were be seeded at 200,000 cells per well in 6-well plates and allowed to grow 48 hours to obtain a confluency of 70% in each well just before transfection. Cells were

transfected using Lipofectamine 2000, and 3.5 µg of plasmid DNA, according to manufacturer's protocol. After overnight recovery, cells were seeded to a 96-well plate (12,000 cells per well), a 6-well plate (600,000 cells per well), or cover slips (600,000 cells per well in a 6-well plate) and allowed 24 hours for recovery before MTT analysis, protein lysis, or immunocytochemistry protocols respectively. Trypan blue exclusion assay, introduced as a second measure of cell death, also required cells seeded to 6-well plates (600,000 cells per well). Figure 3 shows a graphical representation of this procedure.

Note that while the cell seeding density for all MTT assay experiments were equal, the cell seeding density for trypan blue exclusion assays were slightly different. Seeding densities in 96-well plates for MTT assay were 50% confluent while seeding densities in 6-well plates for trypan blue exclusion were 70% confluent. This discrepancy means that the survival results from the two experiments could be differentially affected by their differences in cell contact signaling (greater confluence observed leads to increased cellular contact and greater signaling). This is a limitation to be considered when comparing the MTT assay and trypan blue exclusion assay results.

2.2 Western blot

To ensure successful transfection by lipofectamine and to compare levels of protein expression across the different transfected RGNEF constructs, western blots were performed on protein lysates of transfected cells.

Protein lysates from transfected HEK 293T cells were obtained by lysing cells on ice using a lysis buffer containing 1% Nonidet P-40 (NP-40), 2.5 mM phenylmethanesulfonyl fluoride (PMSF) in 90% ethanol, and “cOmplete protease inhibitor” (Hoffman-La Roche Ltd., Mississauga, Ontario) diluted in TBS. A cell scraper was used to mechanically scrape off remaining cells, and the resultant lysates were sonicated at output setting 40 to homogenize the lysate (Vibracell Sonicator; Sonics & Materials Inc., Newtown, Connecticut, USA). The homogenate was then centrifuged at 4°C, 10,000 g for 10 minutes to pellet cell debris.

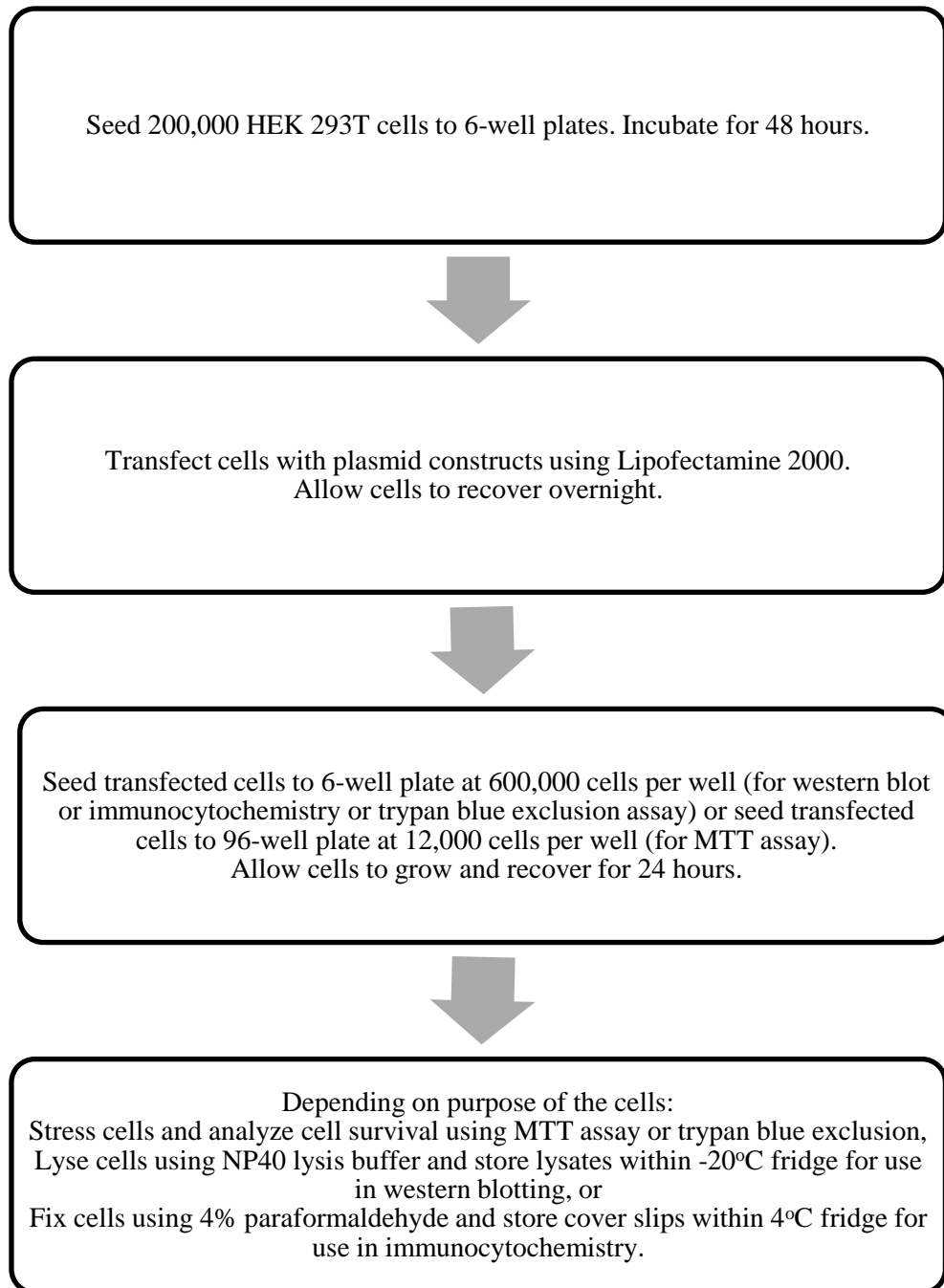


Figure 3: Flowchart describing process of transfecting and seeding cells for use in experiments.

The supernatant containing protein was extracted and frozen at -20°C for storage. To quantify the concentration of protein within lysates, the Bio-Rad Dc protein assay was used according to the manufacturer's protocol and colorimetric analysis was performed using a microplate reader (Microplate Reader Benchmark; Bio-Rad Laboratories Canada Ltd., Mississauga, Ontario) reading at 655 nm. Polyacrylamide gels were made at 10% to visualize RGNEF-myc constructs and an α -tubulin, or a GAPDH, protein loading control. All protein lysates were loaded at 40 μg per well based on protein concentrations determined from the Dc Assay. Lysates were also mixed with a protein loading buffer.

The loading buffer contained 62.5 mM Tris base (pH to 6.8 using HCl), 2% SDS, 10% glycerol, 0.006 % Bromophenol blue, and 50% β -mercaptoethanol diluted in water. After mixing with buffer, lysates were denatured on a heat block (95°C) for 1 minute. Gels were run at constant 100 V until the dye front from the loading buffer reached the edge of the polyacrylamide gel. The running buffer contained 50 mM Tris base, 200 mM glycine, and 2 mM SDS diluted in deionized water. Gels were electrophoretically transferred to a nitrocellulose membrane at a constant 300 mA for 90 minutes. All equipment used for running and transferring gels was manufactured by Bio-Rad. A temporary ponceau-S red stain (Bio-Rad) was used on nitrocellulose membranes after protein transfer to confirm that the transfer was successful. Nitrocellulose was kept at 4°C overnight submerged in washing solution and held within a container with parafilm on top to prevent dehydration. The washing solution of pH 7.4 was made using 50 mM Tris base, 100 mM NaCl, and 1% Tween20.

Nitrocellulose membranes were blocked using a 5% milk blocking solution for non-specific antibody binding, following which primary antibodies diluted in the 5% milk blocking solution were incubated with nitrocellulose film for 60 minutes at room temperature on an orbital shaker. Afterwards, the nitrocellulose membrane was washed 5 times using 5% milk blocking solution, then incubated using secondary antibodies diluted in 5% milk blocking solution at room temperature. Table 3 lists the antibodies used and their dilutions.

Table 3: Antibodies used for western blotting

Name	Species	Dilution	Manufacturer	Secondary Antibody
Myc (monoclonal)	Mouse	1:5000	Cedarlane (Burlington, Ontario)	Goat α -Mouse, linked to horseradish peroxidase (titre: 1:5000) (Bio-Rad)
α -tubulin (polyclonal)	Rabbit	1:2500	Abcam (Toronto, Ontario)	Swine α -Rabbit linked to horseradish peroxidase (titre: 1:2500) (DAKO)
GAPDH (polyclonal)	Rabbit	1:2500	Abcam (Toronto, Ontario)	Swine α -Rabbit linked to horseradish peroxidase (titre: 1:2500) (DAKO)

After secondary antibody incubation, the nitrocellulose membrane was washed 3 times using the washing buffer described previously. Western Lightning ECL reagent (PerkinElmer Woodbridge, Ontario), incubated on nitrocellulose for 2 minutes, was used to generate chemiluminescence signal from the washed nitrocellulose.

Afterwards, a medical-grade film (Fuji Medical X-Ray Film; Christie InnoMed Inc., Mississauga, Ontario) was exposed and developed by a HOPE MicroMax X-Ray Processor (Hope X-Ray Products Inc., Warminster, Philadelphia, USA) in a dark room to obtain protein signals. Densitometry of the bands on exposed film was performed using ImageJ (version 1.48v; National Institutes of Health, USA) software on scanned x-ray films using a computer scanner (HP Scanjet G4010; Hewlett-Packard Canada Co., Mississauga, Ontario).

2.3 RGNEF constructs

To accomplish aim 2 it was necessary to generate different deletion constructs of RGNEF so that they could be transfected and analyzed in stressed cells, providing answers about the regions of RGNEF that are important in cellular stress response. Thus, in addition to full length RGNEF (1-1731 amino acid length), other constructs of RGNEF were transiently transfected into HEK 293T cells. These constructs were made by deleting parts of the full length protein by using PCR, by Pfu DNA polymerase (Thermo Scientific) utilizing primers (Table 4) designed for specific regions within the full length RGNEF cDNA. All constructs, including full length RGNEF, contain a myc-tag at the C-terminal end of the protein so that transfected constructs can be easily detected using an anti-myc antibody. RGNEF constructs were inserted into the pcDNA 3.1(+)/myc-His A plasmid using restriction enzymes XhoI and KpnI (Invitrogen). Plasmids containing constructs were ligated at room temperature and transformed into chemically competent DH5 α *E. coli*, after which the transformation was plated onto an agar plate containing the selective antibiotic ampicillin and incubated at 37°C overnight. Colonies were picked from the agar plate and grown in LB media overnight, following which they were harvested the next day using a Miniprep kit to obtain DNA plasmids for use in subsequent transfections.

Table 4: Primers used in PCR to generate different RGNEF constructs.

Name	Forward or reverse primer	DNA sequence (5' to 3')
RGNEF- Δ DH Δ PH	Forward(1)	ATT <u>GGTACCAT</u> GGAGTTGAGCTGCAGCGAA
	Reverse(1)	TAAGGAGGTGTTTGATGACATCCTTCTCCTGC
	Forward(2)	TGTCATCAAACACCTCCTTATTAAACCTGACCCA
	Reverse(2)	AGACT <u>CGAGC</u> CACCTTGAGGTCTACTTGATGTT
RGNEF- Δ COOH	Forward	ATT <u>GGTACCAT</u> GGAGTTGAGCTGCAGCGAA
	Reverse	CAACT <u>GGAGGGG</u> CTCTAGATGGACGTCCTC
RGNEF- Δ DH Δ PH Δ COOH	Forward	ATT <u>GGTACCAT</u> GGAGTTGAGCTGCAGCGAA
	Reverse	TTT <u>CTCGAGT</u> TTTGATGACATCCTTCTCCTGCCTATTAC
RGNEF- Δ NH ₂	Forward	ATAG <u>GTACCAT</u> GAGACAGGATGTCATTTTTGAGCTA
	Reverse	AGACT <u>CGAGC</u> CACCTTGAGGTCTACTTGATGTT
RGNEF- Δ L Δ DH Δ PH Δ COOH	Forward	ATAG <u>GTACCAT</u> GATTCATCTCATCGGAAACGCT
	Reverse	TTT <u>CTCGAGT</u> TTTGATGACATCCTTCTCCTGCCTATTAC
RGNEF- Δ L	Forward	ATAG <u>GTACCAT</u> GATTCATCTCATCGGAAACGCT
	Reverse	AGACT <u>CGAGC</u> CACCTTGAGGTCTACTTGATGTT

*Restriction enzyme sequences are underlined. XhoI = CTCGAG; KpnI = GGTACC.

**RGNEF- Δ DH Δ PH is a fusion protein made by using two sets of primers, and where reverse(1) and forward(2) exhibit complementary sequence overlap.

RGNEF- Δ DH Δ PH (deletion of amino acids 850-1202 and amino acids 1614-1731, the latter deletion performed to account for differences in predicted RGNEF isoforms containing the RNA-binding domain; this construct would be predicted to be nonfunctional as a guanine exchange factor (GEF) given that the combination of the DH and PH domain constitutes the RhoA GEF domain (Zheng, 2001), thus making this construct devoid of RhoA activating capacity),

RGNEF- Δ COOH (deletion of amino acids 1257-1731; this construct would be predicted to be devoid of any RNA binding capacity but also microtubule binding capacity and FAK activity),

RGNEF- Δ DH Δ PH Δ COOH (deletion of amino acids 850-1731; this construct would be predicted to be devoid of both GEF activity and RNA binding capacity),

RGNEF- Δ NH₂ (deletion of amino acids 1-850 and amino acids 1614-1731, the latter deletion was performed for the same reasons as was described for RGNEF- Δ DH Δ PH; this construct would contain only GEF activity and RNA binding, but be devoid of both the leucine rich domain and the zinc binding domain),

RGNEF- Δ L Δ DH Δ PH Δ COOH (deletion of amino acids 1-242 and amino acids 850-1731; this construct is identical to the RGNEF- Δ DH Δ PH Δ COOH construct but lacks the leucine rich domain), and

RGNEF- Δ L (deletion of amino acids 1-242; this construct is the full length RGNEF construct without the leucine rich domain).

Note that both the RGNEF- Δ L Δ DH Δ PH Δ COOH and RGNEF- Δ L contain a deletion of greater size than the predicted putative leucine-rich domain in order to fully eliminate any leucine-rich domain functions. Figure 4 illustrates graphically the different constructs.

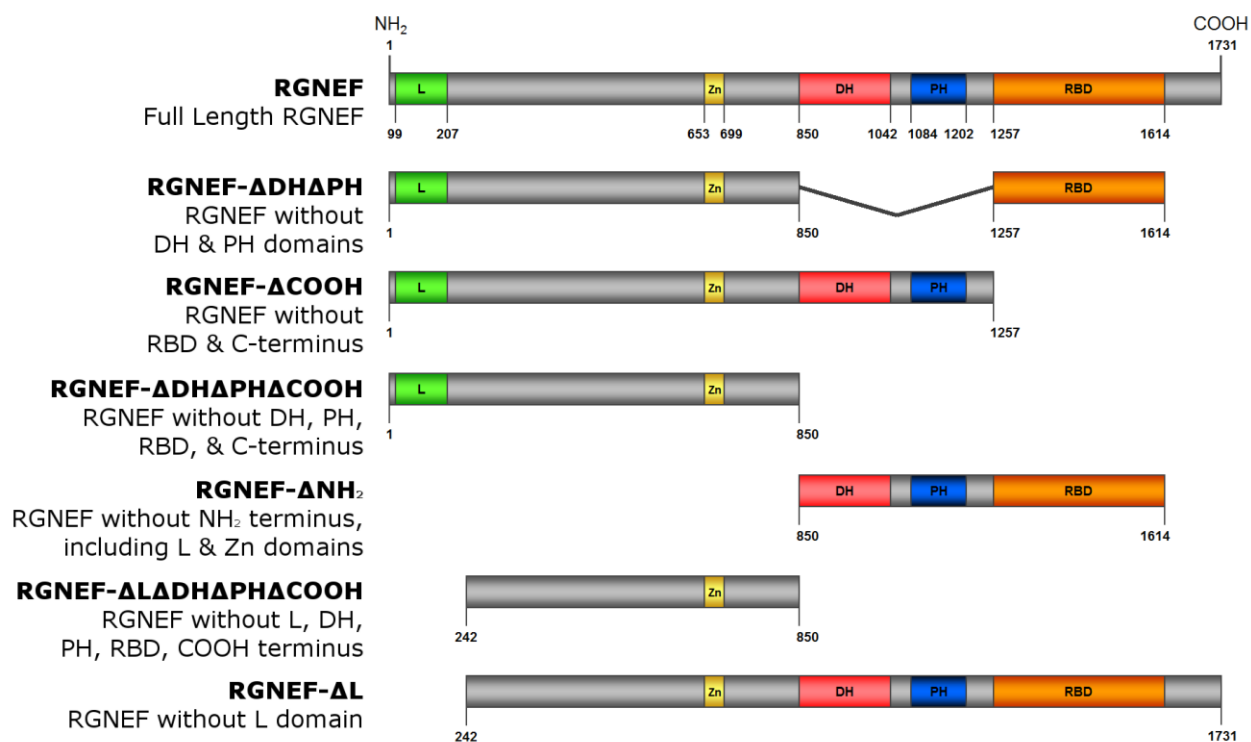


Figure 4: Comparison of the different deletion constructs of RGNEF. The cDNA of these constructs were placed into a pcDNA 3.1(+)/myc-His A plasmid and transfected to cells so that it could be determined which domain of the RGNEF protein was important in the cellular stress response.

L = Putative leucine-rich domain, Zn = Zinc-binding domain, DH = Dbl-homology domain, PH = Pleckstrin-homology domain, RBD = RNA-binding domain.

2.4 Stress conditions

Three types of stress were used with HEK 293T cells: oxidative stress, osmotic stress and heat shock. These stressors were chosen to provide a diverse panel of stressors with which to analyze cell survival and for their ability to induce stress granules as reported in the literature (Kedersha & Anderson, 2007). To induce oxidative and osmotic stress, sodium arsenite and sorbitol were used, respectively (Sigma-Aldrich, Oakville, Ontario). To determine the optimum conditions for the induction of cell injury, both time course and dose-response studies were conducted using MTT assays to assess the differences in cell viability. These optimization studies are further described in the results section.

The duration of exposure and the concentration of stressor were optimized using MTT experiments on either stable or transiently transfected HEK 293T cells. Based on these studies, performed in part to answer the first aim of this thesis, we induced oxidative stress with 0.5 mM sodium arsenite for 1 hour (in DMEM with 10% FBS; Gibco) and osmotic stress with 400 mM sorbitol for 4 hours (in DMEM with 10% FBS; Gibco). These optimized conditions for stress induction were maintained and utilized in aims 2 and 3. Note that for stress survival studies, all stressed cells were immediately analyzed by MTT assay and no recovery time was allotted after either oxidative or osmotic stressors.

Heat shock was performed by placing cells into a water-jacketed, 5% CO₂ cell incubator set to the temperature 42.5°C. Heat shock was induced by either shocking cells for 1, 2, or 3 hours and allowing 24 hours to recover, or by inducing sustained heat shock (24 hour exposure).

2.5 Immunofluorescence and confocal microscopy

In order to observe whether RGNEF associates, or colocalizes, with RNA granules under stress, immunofluorescence coupled with confocal microscopy was used to observe transfected HEK 293T cells after a stress.

Cells were seeded at 600,000 per well to a 22 x 22 mm cover slip within a 6-well plate and allowed to grow overnight. Stressors were applied afterwards (as described in the

previous section) and then cover slips were washed once with PBS and then fixed in a 4% paraformaldehyde, PBS solution for 15 minutes followed by 0.2% Triton X-100 in PBS solution for 10 minutes to permeabilize cells. Afterwards, 50 mM ammonium chloride solution was added for 30 minutes to quench aldehyde groups, reducing background. Non-specific antibody interactions were reduced by incubating cover slips for 60 minutes with an 8% bovine serum albumin (BSA; Fisher Scientific Company, Ottawa, Ontario) in PBS solution at room temperature. Each primary antibody was diluted into the 8% BSA solution, as indicated in Table 5, and incubated with coverslips for 90 minutes at room temperature. Specifically, antibodies against c-myc were used to identify RGNEF constructs, which were myc-tagged at the C-terminus. Antibodies against TIA-1 and Staufen were used to detect stress granules and transport granules respectively (Kedersha et al., 2000; Ferrandon et al., 1997). After this incubation, cover slips were washed twice with PBS and then incubated for 60 minutes at room temperature with secondary antibody diluted in BSA solution, as described in Table 5. Fluorescent AlexaFluor® antibodies (Life Technologies) were used to visualize fluorescence in cells. Afterwards, a 1 µg/mL Hoechst stain in PBS was applied for 10 minutes to visualize nuclei, and cover slips were then washed, first with PBS and then with deionized H₂O, and left to dry overnight. After drying, cover slips were mounted to frosted glass microscope slides using a fluorescent mounting media (Dako Canada Inc., Burlington, Ontario). All cover slips were examined using a multi-photon confocal microscope (LSM 510 META; Carl Zeiss Canada Ltd., Toronto, ON) and AIM software (version 4.2; Carl Zeiss Canada Ltd.).

2.6 Cell survival assays

The MTT assay (Thiazol Blue Tetrazolium Bromide; Sigma-Aldrich), utilizing 96-well plates and a microplate reader (Bio-Rad), was performed to determine cell viability after stress. Each plate was divided in half where one half of the plate (6 wells) was left untreated and another half (6 wells) was treated with a stressor. MTT (1 mg/ml) was incubated with cells for 1 hour during the stress treatment, after which all liquid was removed from the wells using a 200 µL multi-channel pipettor.

Table 5: Antibodies used in immunocytochemistry for confocal microscopy

Name	Species	Titre	Manufacturer	Secondary Antibody
c-Myc (monoclonal)	Mouse	1:250	Cedarlane (Burlington, Ontario)	Donkey or Goat α - Mouse, 488 nm absorbance, Life Technologies (titre: 1:800)
Staufen (polyclonal)	Rabbit	1:100	Millipore (Canada) Ltd (Etobicoke, Ontario)	Goat α -Rabbit, 555 nm absorbance, Life Technologies (titre: 1:800)
TIA-1 (polyclonal)	Goat	1:100	Biovision (Edmonton, Alberta)	Donkey α -Goat, 546 nm absorbance, Life Technologies (titre: 1:800)

To lyse cells and solubilize purple formazan crystals for detection by microplate reader, 200 μ L of 99% Dimethyl Sulfoxide (DMSO; VWR International, Mississauga, Ontario) was added to the empty wells in the 96-well plate. For each experimental condition, 6 duplicate wells of that condition were prepared on the same plate to make the colorimetric measurement of each condition more robust. Colorimetric analysis was performed by the microplate reader at 570 nm with background absorbance referenced at 655 nm.

We also used the trypan blue (Gibco) exclusion assay as a second measure of cell death. Where the MTT assay is a measure of mitochondrial function by assaying mitochondrial dehydrogenase activity, the trypan blue assay shows the loss of cell membrane integrity and as a result dying cells stain blue (Hoskins, Meynell, & Sanders, 1956; Slater, Sawyer, & Strauli, 1963). Cells were incubated for 1 minute with trypan blue (1/100, v/v), washed and then the ratio of live to total (live and dead) cells, or the “ratio of surviving cells” was determined by counting with a hemocytometer under a light microscope. This cell counting was performed by observing 4 squares (one square grid from each corner of the hemocytometer).

The ratio of surviving cells was calculated per square and these 4 values were combined to calculate a mean and standard error of the mean for the specific condition.

2.7 siRNA experiments

To corroborate survival data from stably transfected cells, RNA interference, in the form of siRNA transfections, was used to knockdown RGNEF. All siRNA experiments used stably transfected, RGNEF overexpressing HEK 293T cells (RGNEF⁺) as previously described (Droppelmann et al., 2013). RGNEF⁺ cells were transfected, using lipofectamine 2000 (Invitrogen), with either a control siRNA (SASI_HS02_00315236; Sigma-Aldrich) or a siRNA against RGNEF (SASI_HS01_00264015; Sigma-Aldrich). It was noted that the siRNA transfections did not completely eliminate the expression of RGNEF from the RGNEF⁺ cells. To further lower expression of RGNEF in the RGNEF⁺ cells, a sequential transfection of siRNA was performed using both control siRNA and the siRNA against RGNEF. This transfection was performed 3 times, allowing for 48

hours of recovery after ending each transfection. Transfections of siRNA were ended by seeding the transfected cells to a new plate and this seeding was required to ensure cells did not become overconfluent.

Western blot was used to determine the amounts of RGNEF knock down as a result of siRNA transfection. MTT assay was used to analyze the differences in survival between the two groups mentioned (control siRNA and siRNA against RGNEF) when those cells are stressed with either 0.5 mM arsenite for 1 hour or 400 mM sorbitol for 4 hours. Note that for the MTT assay experiments performed here, only one siRNA transfection was used to knock down RGNEF expression. This is because the additional sequential transfections of siRNA (either 2 or 3 sequential transfections) did not appear to lower RGNEF expression more than using just a single siRNA transfection. Also, this limited any additional stress that the siRNA transfection may have been causing. To examine whether the transfection of siRNA itself, in the absence of arsenite or sorbitol stress treatments, was leading to cell stress, a control transfection of lipofectamine 2000 without siRNA mixed into it was performed on RGNEF+ cells and compared to the stressed cells.

2.8 Statistical analysis

To interpret the results obtained from MTT survival assays, statistical analysis was required to analyze the raw data. The absorbance values obtained from the MTT assay in all experiments were transformed to represent a “Percent Survival” value using the following equation:

$$\text{Percent Survival} = \frac{\text{Stressed Cell Absorbance (570 nm)}}{\text{Untreated Cell Absorbance (570 nm)}} \times 100\%$$

“Stressed Cell Absorbance” is the mean absorbance value calculated for cells that have been exposed to a stress condition (e.g. arsenite). “Untreated Cell Absorbance” is the mean absorbance value for corresponding cells that have only had their media replaced. Both “Stressed Cell Absorbance” and “Untreated Cell Absorbance” represent the mean of 6 duplicate wells on the same 96-well plate. As mentioned previously, 6 replicated wells were used to make the colorimetric analysis more robust. Each “Percent Survival” that

was calculated represented one independent experimental value for its corresponding condition (e.g. a “Percent Survival” value for HEK 293T cells transiently transfected with full length RGNEF treated with 400 mM sorbitol for 4 hours). These resultant “Percent Survival” values were then compared amongst each other.

For example, a mean and standard error of the mean was calculated from five “Percent Survival” values obtained from five independent experiments performed for the condition: HEK 293T cells transiently transfected with full length RGNEF treated with 400 mM sorbitol for 4 hours. To search for outliers within the “Percent Survival” data of each construct, “R software” using the Grubb’s test for outliers, contained within the “outliers” package, was used according to an online statistics handbook maintained by the National Institute of Standards and Technology (Filliben & Heckert, 2014). Grubb’s test for outliers generates a p-value based on a given dataset and we chose to reject either the highest or lowest value in the dataset if $p < 0.05$.

All conditions were analyzed for significant differences between each other using either Student’s t-test when comparing two groups or one-way ANOVA when comparing more than two groups. When using one-way ANOVA, significance was defined as $p < 0.05$ as provided by the Fisher least significant difference (Fisher LSD) post-hoc test to reduce the occurrence of “Do Not Test” values generated by the statistical software. All statistical analyses, including line and bar graphs, were performed or generated using SigmaPlot 10.0 (Systat Software Inc., San Jose, California, USA) based on mean and standard error of the mean.

Chapter 3

3 Experimental results

3.1 Survival experiments in stably transfected cells

To examine the effects of RGNEF on the stress response, I first examined a stably transfected HEK 293T cell line that overexpressed myc-tagged RGNEF (RGNEF-myc). Cells were exposed to either of an oxidative, osmotic, and heat shock stress. The concentrations for the stressors were chosen based on their reported ability to induce the formation of stress granules and a range of concentrations around this accepted value was then tested (Kedersha & Anderson, 2007). The cells were exposed over the course of 24 hours following which cell survival was assayed using the MTT assay. The mean survival, with standard error of the mean, was plotted over time for stably transfected cells and for non-transfected HEK 293T cells (control). A survival curve was fitted using non-linear regression.

For all concentrations of arsenite and sorbitol, the stably transfected cells showed increased survival compared to non-transfected cells when comparing their respective curves (Fig. 5). When comparing different concentrations of stressors, 0.5 mM arsenite (Fig. 5B) showed the greatest difference between the curves suggesting that it would be easier to resolve the survival differences between control cells and cells overexpressing RGNEF. Though 200 mM sorbitol (Fig. 5D) showed the greatest difference between the curves, 400 mM sorbitol (Fig. 5E) was chosen to be the standard concentration used in the proceeding experiments. The two concentrations: 0.5 mM arsenite and 400 mM sorbitol, were chosen because of their smaller error bars in the data, the separation between the two curves (non-transfected cells and stably transfected cells), and because these concentrations have been used in previously published studies examining cellular stress (Sama et al., 2013; Higashi et al., 2013).

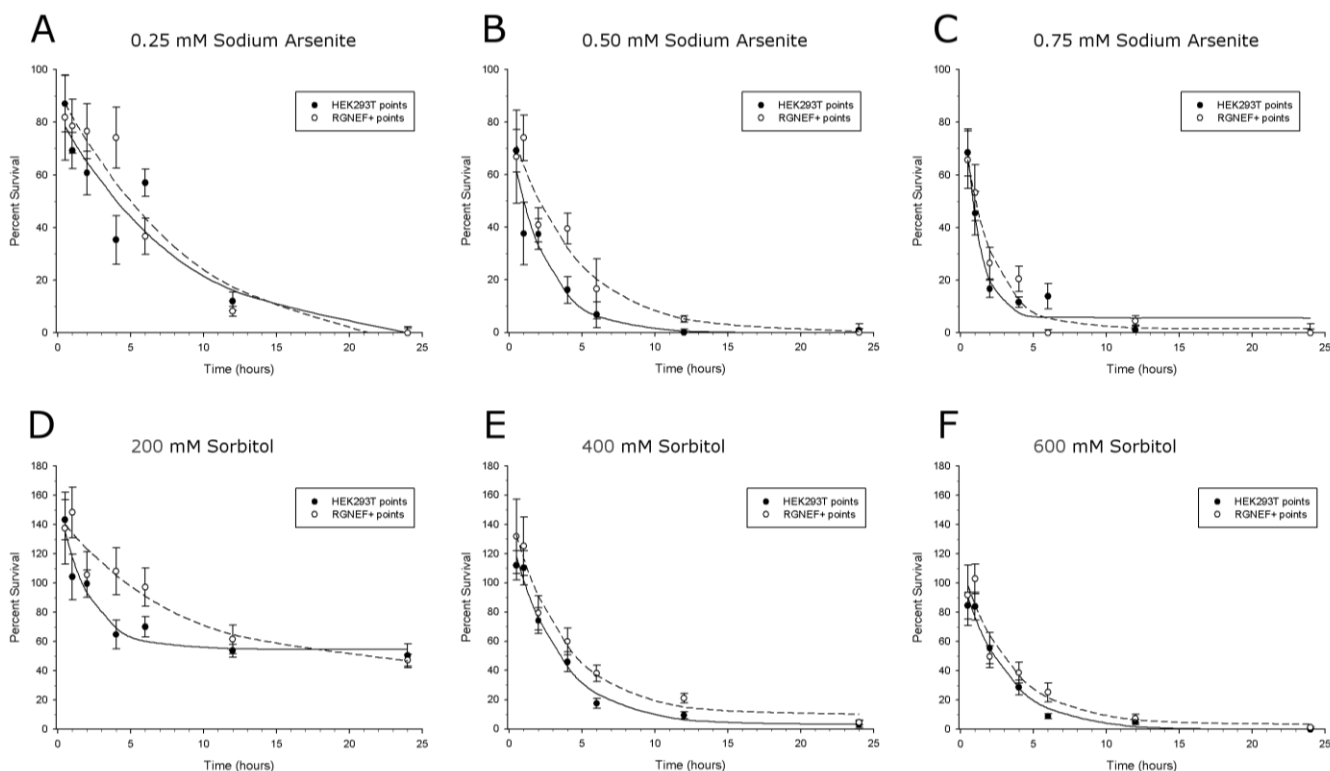


Figure 5: Survival over time of cells exposed to different oxidative and osmotic stress concentrations. (A-C) Graphs showing different concentrations of arsenite used to induce oxidative stress in cells. (D-F) Graphs showing different concentrations of sorbitol used to induce osmotic stress in cells. All graphs presented here had a curve generated by non-linear regression and fitted to data points plotted within the graph. In all graphs, the dotted line (representing cells overexpressing RGNEF) shows greater survival over the solid line (representing non-transfected HEK 293T cells).

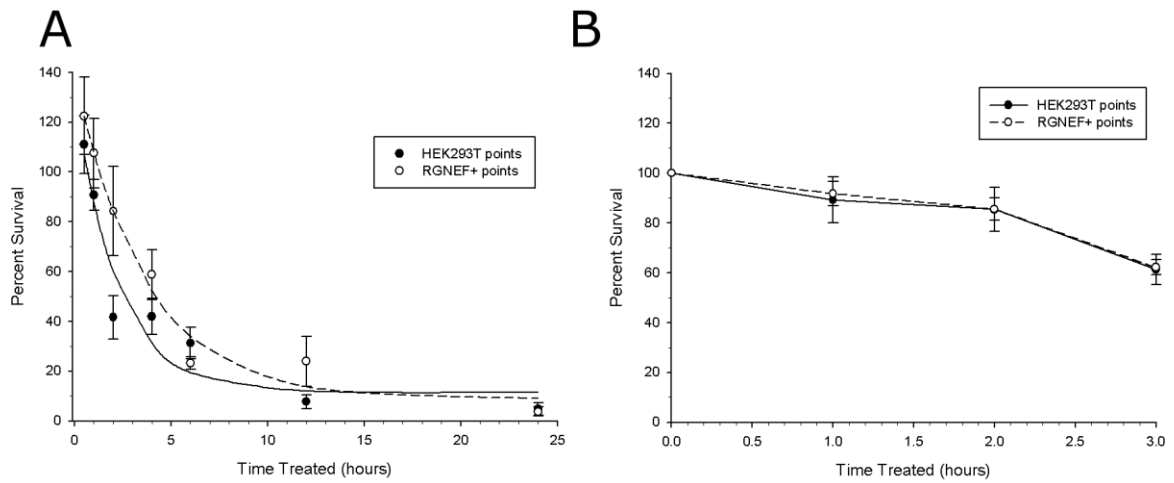


Figure 6: Survival over time of cells exposed to sustained or recovery heat shock protocols. (A) Graph showing the change in cell survival of cells exposed to a sustained level of heat shock of 42.5°C over time. (B) Graph showing the change in survival compared to an untreated condition of cells exposed to 1, 2 or 3 hours of heat shock at 42.5°C then allowed 24 hours recovery.

For the experiments examining the effect of heat shock, two experimental paradigms were used (Fig. 6). In the first, cells stably transfected with RGNEF or non-transfected cells were exposed to 42.5°C continuously over 24 hours. In the second, cells stably transfected with RGNEF or non-transfected cells were transiently exposed to heat shock at 42.5°C for intervals of 1, 2, or 3 hours of 42.5°C and then allowed to recover for 24 hours. At the 24 hour mark, cell survival was then assayed using the MTT assay.

There appeared to be a dichotomy between cells continuously exposed to heat shock over 24 hours and cells allowed to recover after their heat shock. In the continuously exposed condition (Fig. 6A), stably transfected cells showed greater survival than non-transfected cells when comparing the two curves. It should be noted that the data point at 2 hours of heat shock for non-transfected cells appears to strongly influence the non-transfected survival curve to show this difference. Conversely, in the recovery condition (Fig. 6B), stably transfected cells showed no difference in survival as the line graphs generated show overlapping curves. Because of these inconclusive results, the heat shock condition was not re-iterated in survival experiments involving transiently transfected cells.

3.2 Survival experiments in transiently transfected cells

To corroborate oxidative and osmotic stress results from the stably transfected cells, and in anticipation of using the various RGNEF constructs, transiently transfected cells were used in place of stably transfected and non-transfected cells. Transient transfection experiments were also used to better control for any hidden variables that may have been introduced by the stable transfection protocol as non-transfected cells are an imperfect control for stably transfected cells. Note that for the reasons described earlier, heat shock experiments were not performed on these cells.

Cells transfected with RGNEF-myc plasmid demonstrated a greater survival following either 0.5 mM arsenite or 400 mM sorbitol as illustrated in figure 7A and 7B. This is most evident at the exposure times of 1 hour for 0.5 mM arsenite ($p = 0.006$) and 4 hours for 400 mM sorbitol ($p = 0.043$; Student's t-test) and thus these stress conditions were chosen as the standard in later experiments. A western blot was performed to confirm expression of RGNEF-myc in transfected cells (Fig. 7C).

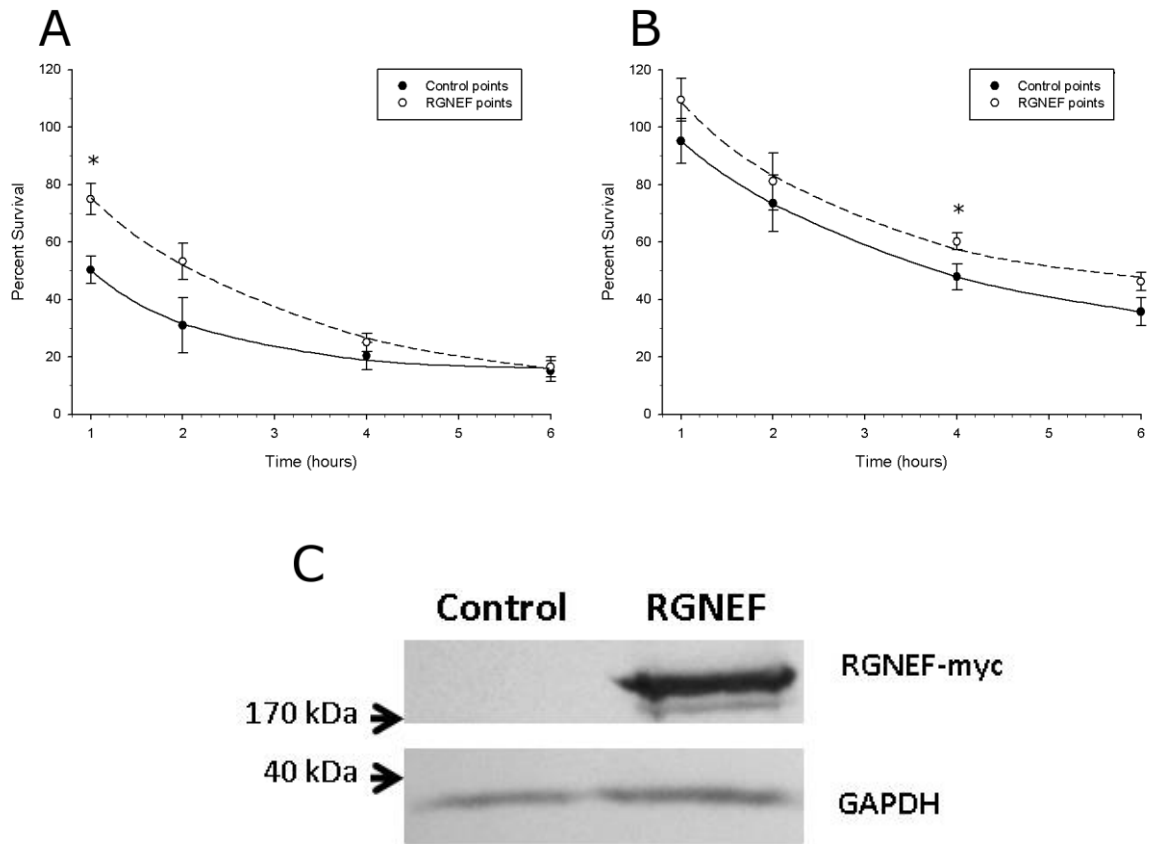


Figure 7: Survival over time of transiently transfected cells exposed to arsenite or sorbitol stress. (A) Graph showing the change in cell survival of cells exposed to 0.5 mM arsenite over time. (B) Graph showing the change in cell survival of cells exposed to 400 mM sorbitol over time. Note that for (A) and (B), the asterisk shows $p < 0.05$ by Student's t-test. (C) Western blot showing presence of RGNEF-myc in transfected cells.

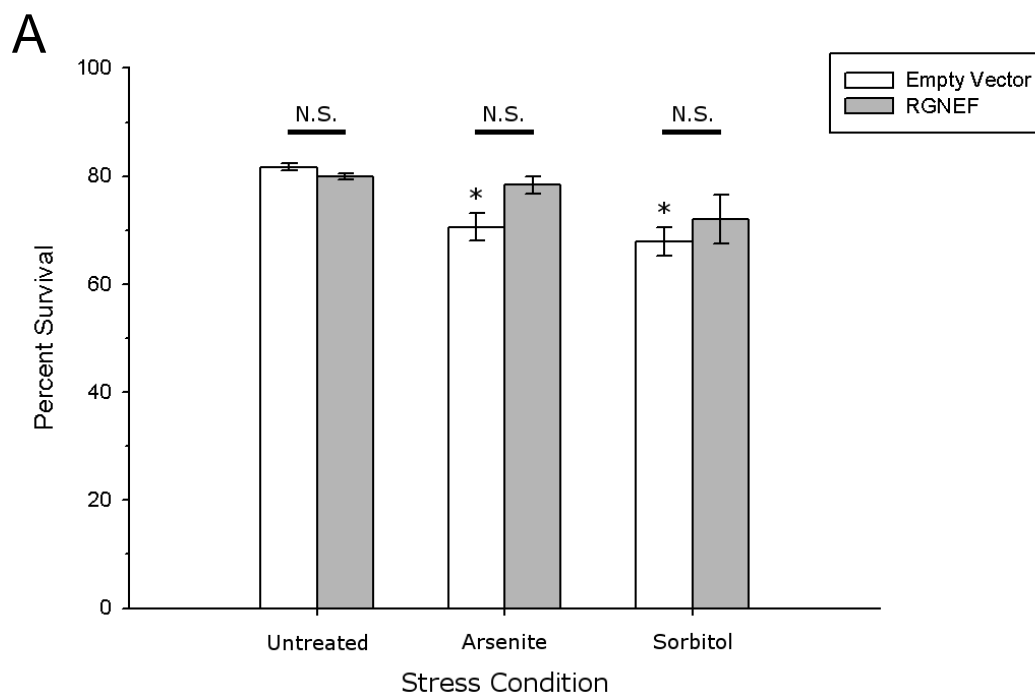
3.3 Trypan blue assay

The MTT assay relies on the reduction of 3-(4,5-dimethylthiazol-2-yl)-2,5-diphenyltetrazolium bromide within the cell to provide a measure of cell viability. Because this reaction is reliant on mitochondrial activity, it is possible that the MTT assay may be showing decreases in cellular metabolism as opposed to cellular death (Slater et al., 1963). For this reason, a trypan blue exclusion assay was performed as an alternate measure of cell death to confirm that data from MTT assay is describing changes in cell viability (Hoskins et al., 1956).

HEK 293T cells transiently transfected with either an empty vector or a plasmid containing RGNEF-myc were stressed by arsenite or sorbitol as previously described and trypan blue exclusion assay was performed immediately after. Cells that were transfected with an empty vector plasmid showed a significant reduction in survival between unstressed cells and cells stressed with 0.5 mM arsenite ($p = 0.008$) or with 400 mM sorbitol ($p = 0.003$). Conversely, cells that were transfected with RGNEF showed no significant differences in survival between unstressed and arsenite or sorbitol stressed cells (Fig. 8). Note that while there was no significant difference between the percent survival of empty vector cells and RGNEF transfected cells within their groups of stress conditions (untreated, arsenite, sorbitol), there was a significant difference in survival between stressed (arsenite or sorbitol) and untreated conditions for empty vector cells.. This result implies that RGNEF does provide protection against stress and agrees with the MTT assay results shown in Figure 7. Furthermore, it confirms that loss of cell viability observed with the MTT assay is reflective of cell death in response to either sorbitol or arsenite.

3.4 RNA silencing experiments

To further corroborate survival data from transient transfections of myc-tagged RGNEF, silencing RNA (siRNA) against RGNEF was transfected into stably transfected RGNEF-myc overexpressing cells and stressed with 0.5 mM arsenite or 400 mM sorbitol at 1 and 4 hours respectively.



Transfected plasmid	Stress condition	Mean percent survival	ANOVA p-value against control
Empty vector	0.5 mM arsenite, 1 hour	70.603	0.005
	400 mM sorbitol, 4 hours	67.795	0.001
RGNEF	0.5 mM arsenite, 1 hour	78.331	0.194
	400 mM sorbitol, 4 hours	72.102	0.194

Figure 8: Survival of transiently transfected cells exposed to 0.5 mM arsenite or 400 mM sorbitol stress measured using the trypan blue exclusion assay. (A) White bars show empty vector transfected cells, while grey bars show RGNEF-myc transfected cells. Stress was applied at 0.5 mM arsenite for 1 hour or 400 mM sorbitol for 4 hours. Using Student's t-test, bars within either untreated, arsenite or sorbitol groups were not significantly different (N.S.) from each other in the same group. Asterisks denote $p < 0.05$ when comparing untreated bars with arsenite or sorbitol bars within either empty vector or RGNEF groups. (B) Table showing mean percent survival and p-values for data shown in (A). Statistics were performed within empty vector or RGNEF-myc data groups and used one-way ANOVA with Fisher LSD post-hoc test.

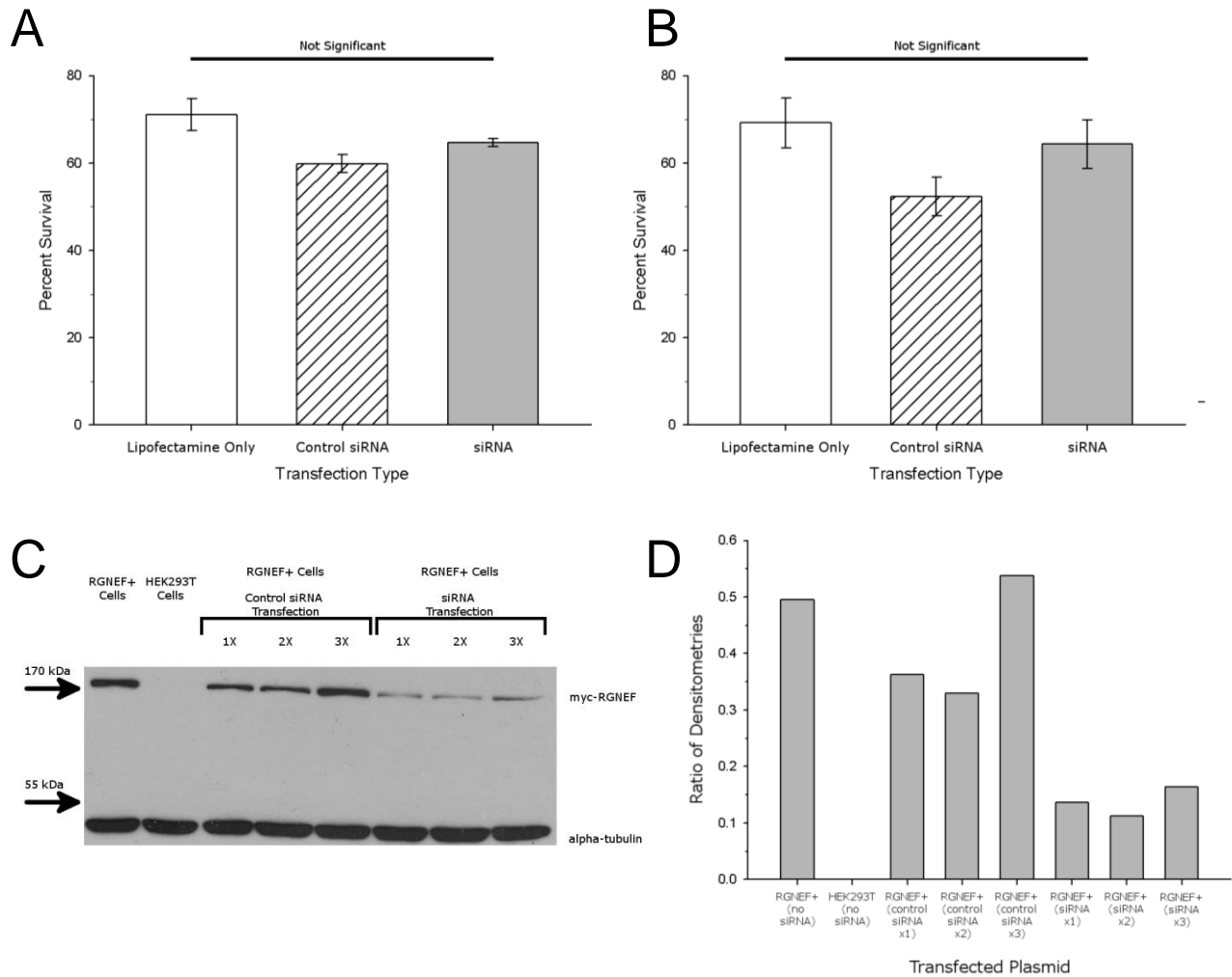


Figure 9: Survival of stably transfected RGNEF-myc cells transfected with siRNA against RGNEF and exposed to arsenite or sorbitol stress. (A) Graph showing percent survival of cells stressed using 0.5 mM arsenite for 1 hour. (B) Graph showing percent survival of cells stressed using 400 mM sorbitol for 4 hours. Statistics by one-way ANOVA found no significant differences between groups in (A) or (B). (C) Representative western blot showing knockdown of RGNEF-myc from stably transfected cells. 1x, 2x, 3x describe the number of siRNA transfections sequentially performed on the cells to further decrease protein levels by knockdown, or as a corresponding control to these transfections. RGNEF+ stands for stably transfected, RGNEF overexpressing HEK 293T cells. HEK293T stands for non-transfected, HEK 293T cells. (D) Densitometry graph showing the differences in intensity (as a ratio of corresponding alpha-tubulin intensity) of RGNEF bands shown in (C).

As a control, a silencing RNA shown not to affect RGNEF-myc protein levels was transfected to stably transfected RGNEF-myc cells (Fig. 9A). Note that while the knockdown of RGNEF-myc by siRNA was successful, some expression of RGNEF-myc remains in the stably transfected cells. Upon analysis, there was no significant difference between stably transfected cells that were exposed to lipofectamine 2000 only (no siRNA transfected; used to control for the stress of the siRNA transfection), stably transfected cells transfected with control siRNA, or stably transfected cells transfected with siRNA against RGNEF-myc in either arsenite ($p = 0.052$) or sorbitol ($p = 0.147$) stressed cells (Fig. 9B).

These results show that the siRNA transfection itself appears to have an impact on cell survival (cells that were only transfected with lipofectamine showed greater survival than either siRNA transfected cells), albeit an insignificant one. Also, the western blot and graph shown in Figure 9C and 9D respectively show that the sequential siRNA transfection do not appear to be able to abolish RGNEF-myc expression by the stably transfected cells. In fact, after 3 sequential transfections there appears to be an increase in RGNEF-myc expression (for both control siRNA and siRNA transfections). This could indicate that the sequential transfection presents a significant stress, leading to an upregulation of RGNEF within the cells (agreeing with unpublished data from our lab pertaining to the upregulation of RGNEF in transected sciatic nerves of rodents).

Interestingly, there appears to be a trend in the data where cells treated with siRNA against RGNEF-myc had increased survival under arsenite or sorbitol stress. This trend may indicate that siRNA against RGNEF is non-specific, potentially targeting other proteins endogenous to the cell and affecting cell signaling in a manner that is subtly beneficial under stress conditions. However, this possibility was not investigated and, as mentioned, the difference between the three groups shown in Figure 9A and B is not significant by one-way ANOVA. When analyzing the control siRNA and siRNA groups alone, the two were insignificant by Student's t-test (arsenite: $p = 0.103$; sorbitol: $p = 0.169$).

3.5 Survival experiments examining different constructs of RGNEF

In order to determine which domain of RGNEF was providing the stress protection in response to either arsenite or sorbitol, we constructed a number of RGNEF constructs using the pcDNA 3.1 myc His A plasmid such that every construct was myc-tagged at their C-terminus. Each deletion removed at least one domain of RGNEF as previously described. All experiments were performed using the protocol described previously for the transient transfections. The MTT assay was used to determine cell survival after exposure to either 0.5 mM arsenite (Fig. 10A) or 400 mM sorbitol (Fig. 10B) stress, for 1 and 4 hours, respectively. We used western blotting to confirm the expression of myc-tagged constructs in transfected cells.

In both arsenite ($p < 0.001$) and sorbitol ($p < 0.001$) stresses, full length RGNEF conferred a significant improvement in cell survival when compared to empty vector control. When the guanine exchange domain comprised of both Dbl homology and Pleckstrin homology domains of RGNEF was deleted (RGNEF- Δ DH Δ PH), a significant difference between cells overexpressing this construct and empty vector cells was still observed in arsenite ($p = 0.009$) and sorbitol ($p = 0.018$) stress. Similarly, cells overexpressing a construct of RGNEF where the RNA-binding domain was deleted (RGNEF- Δ COOH) exhibited greater survival compared to empty vector in both arsenite ($p = 0.006$) and sorbitol ($p = 0.034$) stresses.

When observing cells overexpressing RGNEF with its C-terminal half deleted (RGNEF- Δ DH Δ PH Δ COOH), there continued to be a greater survival compared to empty vector transfected cells following either arsenite ($p = 0.003$) or sorbitol ($p = 0.018$) exposure. Conversely, cells overexpressing RGNEF with its N-terminal half deleted (RGNEF- Δ NH₂) only showed significantly greater survival than empty vector cells in sorbitol stress ($p = 0.047$). When treated with arsenite, there was no significant difference ($p = 0.083$) between empty vector cells and RGNEF- Δ NH₂ cells.

These results were unexpected and suggested that neither the GEF domain nor RNA binding domain, alone or in combination, conferred the protective benefit of RGNEF

against either arsenite or sorbitol stress. Indeed, the results suggest that the N-terminal region of RGNEF is critical to conferring this protection.

To focus further on the N-terminal domain of RGNEF which contains both the leucine rich domain and the zinc binding domain, cells were transfected with a construct that contained only the N-terminal domain of RGNEF but in which the leucine rich domain was deleted (RGNEF- Δ L Δ DH Δ PH Δ COOH). Cells overexpressing this construct showed no significant difference in survival between empty vector in either arsenite ($p = 0.152$) or sorbitol ($p = 0.592$) stress. This is not entirely unexpected however as the construct now lacks virtually all of the domains that could confer any effect, and indeed, bears little resemblance to RGNEF. To overcome this, we designed a construct in which full length RGNEF was expressed but with the leucine rich domain deleted (RGNEF- Δ L). Using this construct, RGNEF- Δ L transfected cells again showed significantly greater survival compared to empty vector cells in arsenite ($p = 0.002$), but not sorbitol ($p = 0.301$) stress. This suggests that the leucine rich domain may be of importance in providing the cytoprotective effect of RGNEF, but not under all conditions of stress.

In order to ensure that the observed differences were not a reflection of differing levels of protein expression, we examined the level of protein expression for each construct using Western blotting (Fig. 11A). Three independent protein lysates were analyzed for each construct, and the resulting densitometry results plotted (Fig. 11B).

Densitometries for each construct were obtained by ImageJ software and calculated as a value relative to a corresponding α -tubulin loading control to control for any errors in loading of the polyacrylamide gel. Using a one-way ANOVA analysis, we found no significant differences in protein expression between any of the constructs ($p = 0.143$). Transfection efficiencies were also analyzed for transfected plasmids using immunofluorescence microscopy (Fig. 11C). The efficiency is expressed as a ratio of green cells, denoting a transfected cell, to blue cells, denoting a general cell nucleus (i.e. transfected cells : total cells).

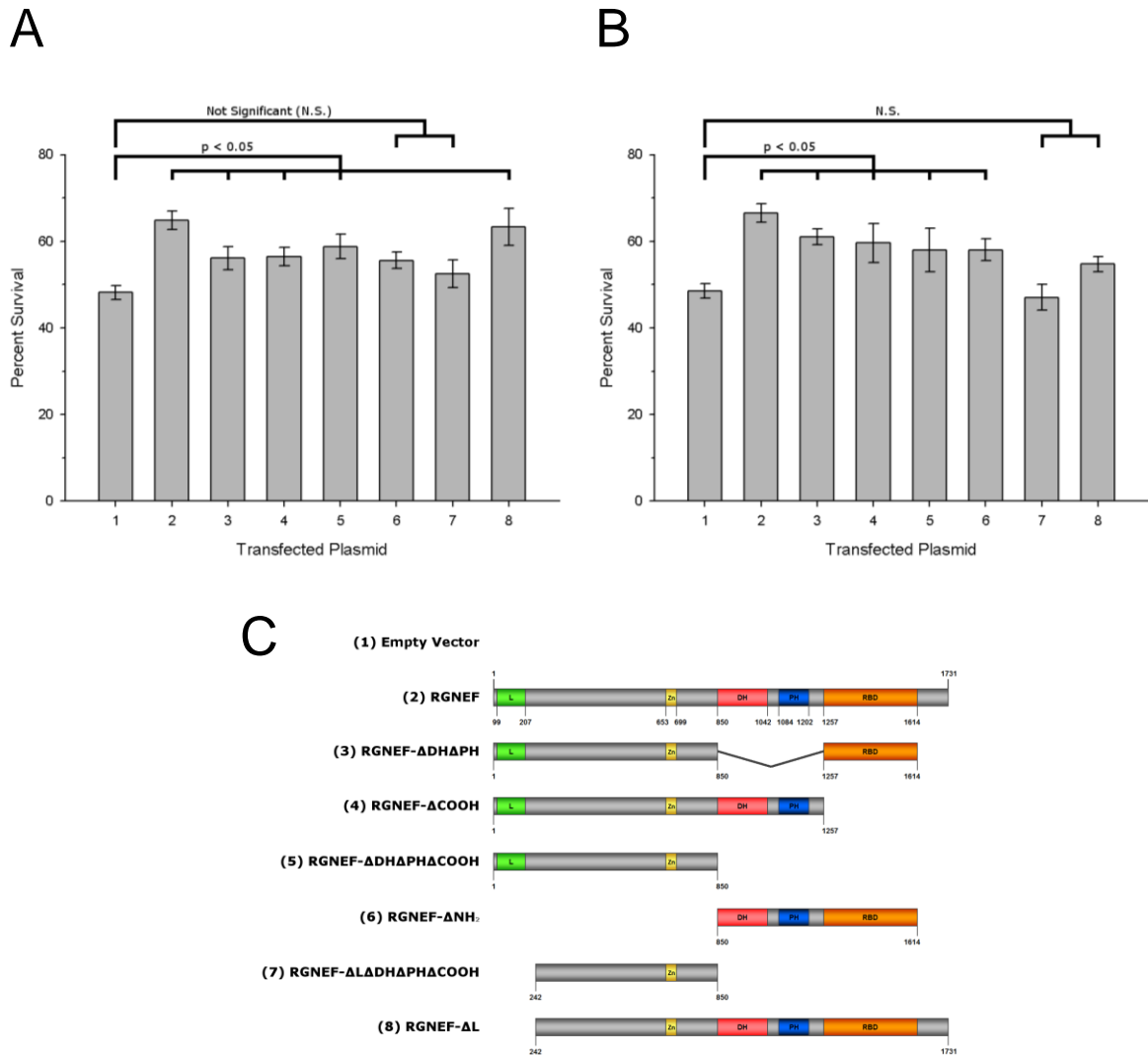


Figure 10: Survival over time of cells transiently transfected with different constructs of RGNEF and exposed to arsenite or sorbitol stress. (A) Graph showing the percent survival of cells exposed to 0.5 mM arsenite for 1 hour. (B) Graph showing the percent survival of cells exposed to 400 mM sorbitol for 4 hours. Significance was determined as $p < 0.05$ and calculated by one-way ANOVA with the Fisher LSD post-hoc test. (C) Legend of the different constructs shown, as bars, in graphs (A) and (B).

Upon statistical analysis by one-way ANOVA with the Fisher LSD post-hoc test, there was a significant difference found for only two constructs: RGNEF- Δ COOH and RGNEF- Δ DH Δ PH Δ COOH. The other 5 constructs did not differ significantly from each other.

RGNEF- Δ COOH had significantly lower transfection efficiencies compared to full length RGNEF ($p = 0.001$), RGNEF- Δ DH Δ PH ($p = 0.031$), RGNEF- Δ NH₂ ($p = 0.004$), RGNEF- Δ L Δ DH Δ PH Δ COOH ($p = 0.003$), and RGNEF- Δ L ($p = 0.047$). RGNEF- Δ DH Δ PH Δ COOH only had significantly lower transfection efficiencies compared to full length RGNEF ($p = 0.043$). It should be noted that survival benefit continues to be evident for both RGNEF- Δ COOH and RGNEF- Δ DH Δ PH Δ COOH in spite of their significantly lower transfection efficiency. Moreover, the transfection efficiency of constructs that do not show survival benefit, such as RGNEF- Δ L Δ DH Δ PH Δ COOH, shows similar efficiencies to constructs that do show survival benefit, such as RGNEF.

Referring back to the protocol used for transient transfections, a constant of 3.5 μ g of plasmid DNA was used in all transient transfection experiments. This means that the amount of plasmid DNA transfected was not normalized by molar concentration. Where constructs were larger and had a greater molar mass, less moles of the larger construct DNA would be transfected than constructs that were smaller and had a lower molar mass. This effect appears to be present in Figure 11B where the amount of protein expression observed for RGNEF- Δ L Δ DH Δ PH Δ COOH is much greater than the amount for RGNEF- Δ COOH. Consequently, this may have also affected the efficiency of transfection, though again the constructs that had significantly lower transfection efficiencies continued to demonstrate survival benefit. It may follow then that the amount of survival observed in Figure 10 is underestimated for the two constructs: RGNEF- Δ COOH and RGNEF- Δ DH Δ PH Δ COOH.

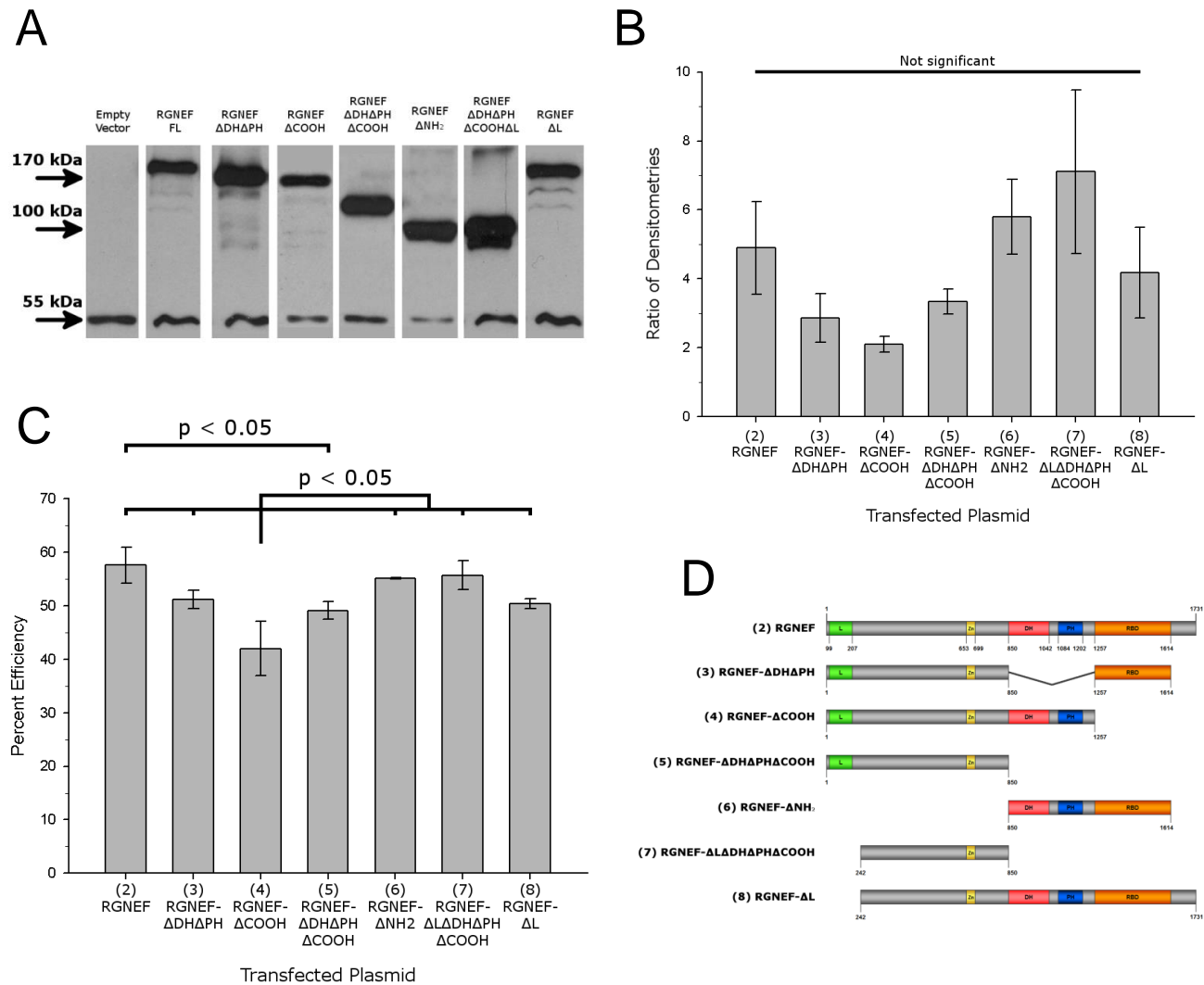


Figure 11: Confirming efficiencies of transfections of different RGNEF constructs by western blot and immunofluorescence microscopy. (A) A representative, composite western blot showing the protein signals for different, myc-tagged RGNEF constructs. (B) Comparison of densitometries of western blots for different RGNEF constructs. By one-way ANOVA there is no significant difference between these values ($p = 0.143$). (C) Transfection efficiencies as observed by immunofluorescence microscopy and represented as a percentage of transfected cells vs. total cells. Significant difference determined by one-way ANOVA and Fisher LSD post-hoc test. (D) Legend showing constructs described in (B) and (C)

In summary, this set of experiments suggests that RGNEF expression confers a survival benefit in the face of two different cellular stresses: 0.5 mM arsenite and 400 mM sorbitol. The studies further suggest that this effect, independent of either the GEF or RNA binding domains, differs somewhat based on the nature of the cellular stress. In the next section, given the importance of the N-terminus domain to the survival benefit and given the presence of both a leucine rich domain and Zn binding domain which would be predicted to confer both protein interaction capacity and stability, we examined whether the cytoprotective effect of RGNEF is mediated through its incorporation into stress granules.

3.6 RNA granules and RGNEF localization under stress

To determine whether integration into stress granules was the mechanism by which RGNEF was providing protection against stress, confocal microscopy was used to observe the subcellular localization of myc-tagged RGNEF and TIA-1 protein when exposed to 0.5 mM arsenite for 1 hour or 400 mM sorbitol for 4 hours. These experiments used stably transfected HEK 293T cells overexpressing RGNEF-myc. We observed that granular formations of RGNEF-myc did not colocalize with TIA-1 stress granules in either the arsenite or sorbitol stresses (Fig. 12). This makes stress granule formation an unlikely mechanism by which RGNEF was protecting against stress.

Transport granules were also examined in stressed, stably transfected RGNEF-myc overexpressing cells to observe the relationship between transport granule localization and RGNEF granule localization during stress. We observed that staufen-positive transport granules occasionally colocalized with RGNEF-myc granules under arsenite or sorbitol stresses (Fig. 13). This implies that the transport of RGNEF may be important under stress conditions. Figure 14 shows a close-up comparison between stress granules and transport granules forming in RGNEF overexpressing cells. Notice that the colocalizing transport granules are yellow (overlap of red immunolabeled Staufen and green immunolabeled RGNEF-myc) while the stress granules are red (immunolabeled TIA-1) and separate from the green (immunolabeled RGNEF-myc).

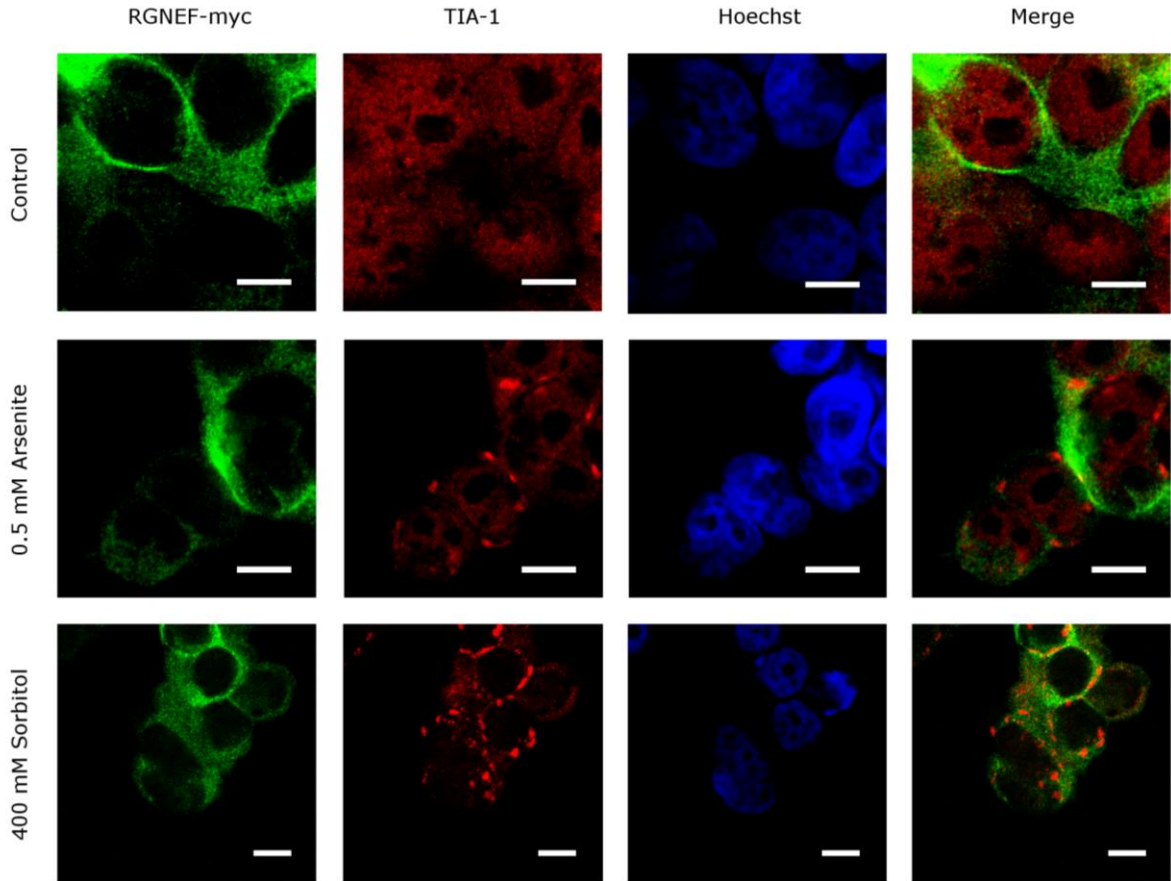


Figure 12: Localization of RGNEF-myc and TIA-1 stress granules formed when stably transfected RGNEF-myc cells are exposed to arsenite or sorbitol stress. The top row shows an unstressed control to compare the different localizations of RGNEF-myc and TIA-1 when exposed to arsenite or sorbitol stress. TIA-1 forms large granular structures in the cell in response to either arsenite or sorbitol. These granules do not colocalize with RGNEF-myc in either arsenite or sorbitol stress. Scale bars represent 10 μm .

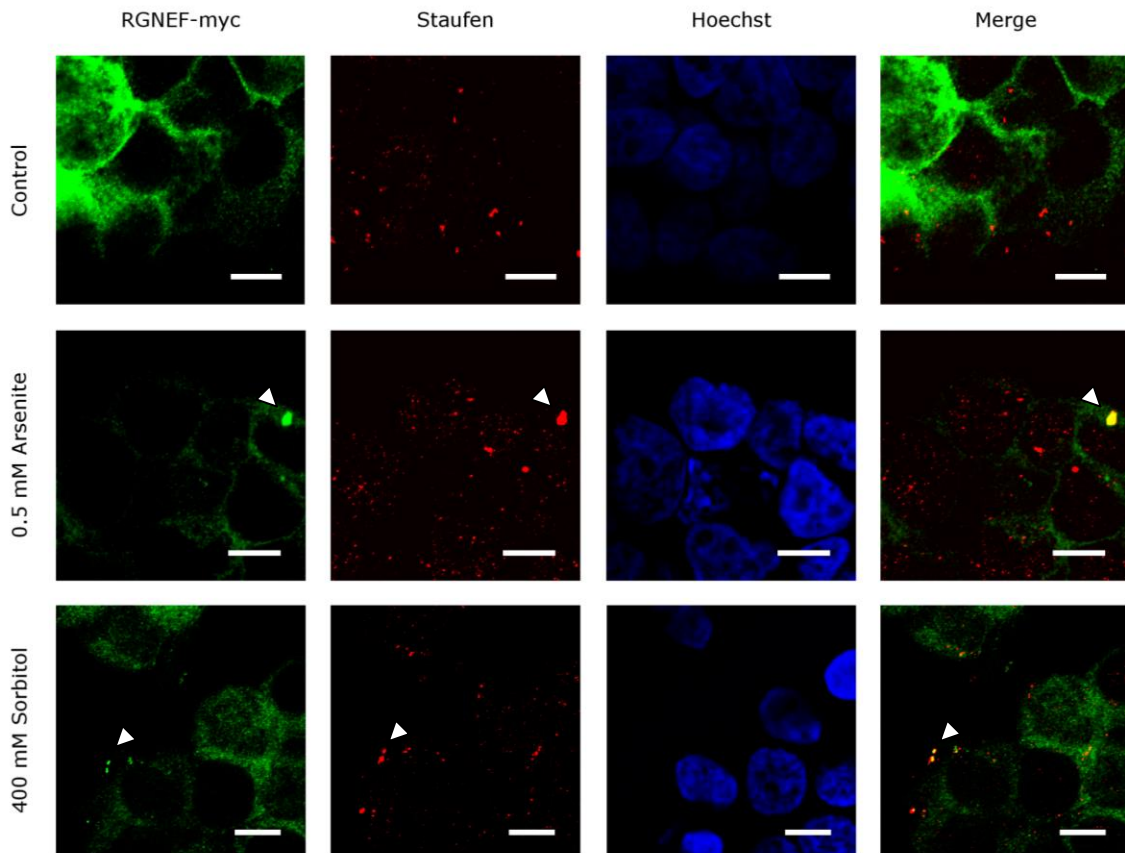


Figure 13: Localization of RGNEF-myc and staufen transport granules formed when stably transfected RGNEF-myc cells are exposed to arsenite or sorbitol stress. The top row shows an unstressed control to compare the localizations of RGNEF-myc and staufen when exposed to arsenite or sorbitol stress. Staufen forms granular structures whether or not the cells are stressed. These granules occasionally colocalize with RGNEF-myc in either arsenite or sorbitol stress and are shown with arrowheads. Arrows point to colocalizing granules. Scale bars represent 10 μm .

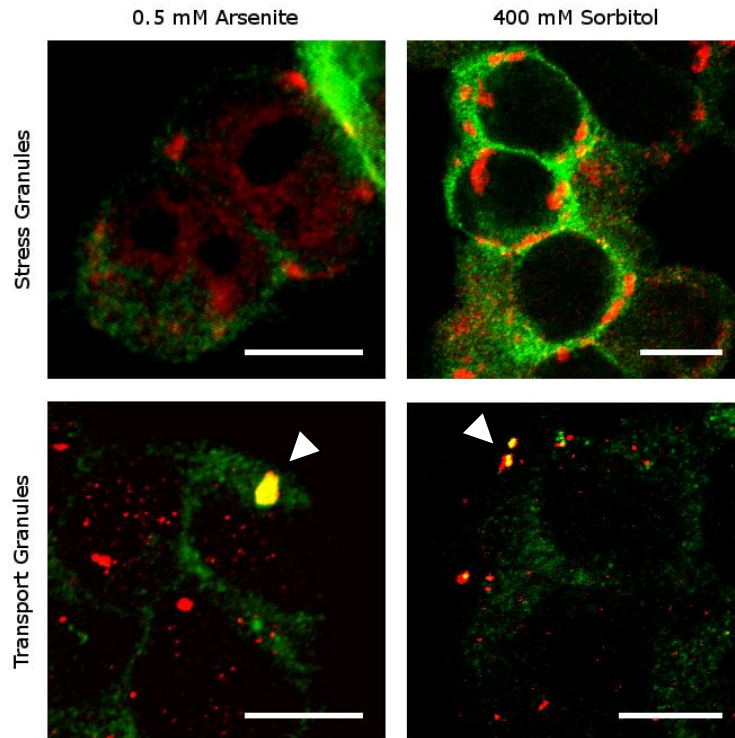


Figure 14: Comparison of stress granules and transport granules. The top two pictures represent stress granules and are immunolabeled red for TIA-1, green for RGNEF-myc. The bottom two pictures represent transport granules and are immunolabeled red for Staufen, green for RGNEF-myc. Scale bars represent 10 μm . Colocalization is indicated by the white arrowheads. Notice that the colocalized transport granules are yellow while the stress granules, which do not colocalize, are red.

Chapter 4

4 Discussion

4.1 RGNEF protects against stress

In both stably transfected and transiently transfected RGNEF overexpressing HEK 293T cells, we found that cells overexpressing RGNEF showed greater survival than the controls when exposed to 0.5 mM arsenite or 400 mM sorbitol stress. Overall, these results are consistent with the literature in that RNA-binding proteins that have been observed to form NCIs within spinal motor neurons of ALS are also described to be involved in the neuronal response to stress, including TDP-43, FUS, and angiogenin (Higashi et al., 2013; Sama et al., 2013; Subramanian et al., 2008). While it may be argued that the protection conferred by RGNEF is somewhat small (about 15% survival benefit in both 0.5 mM arsenite and 400 mM sorbitol stress), it is nevertheless significant in the context of ALS where several of these cytoprotective, RNA-binding proteins may be colocalized within the same NCIs within motor neurons (Keller et al., 2012). Thus, these small survival benefits that are lost may eventually act collectively to manifest as catastrophic failure of the motor neuron's stress response resulting in cell death.

It should be noted that in contrast to oxidative and osmotic stress, heat shock stress in stable transfection experiments produced mixed results. When applying a sustained heat shock of 42.5°C, stably transfected RGNEF cells (RGNEF+) showed a non-linear regression curve that was greater and separated from the non-transfected HEK 293T (293T) cell curve indicating that RGNEF has protective effects against heat shock. However, when performing heat shock recovery experiments, there were no differences between the survival of RGNEF+ cells and 293T cells exposed to 1, 2, or 3 hours of 42.5°C heat shock and allowed 24 hours recovery. This discrepancy in results is surprising, though the difference between the curves observed for sustained heat shock may be explained by the large decrease in 293T cell survival seen at 2 hours of heat shock pointing to a possible outlier in the data. These results differ from a previous study describing p190RhoGEF providing anti-apoptotic effects against heat shock stress in mouse neuroblastoma Neuro2A cells (Wu et al., 2003). However, we have shown that

RGNEF functions differently from p190RhoGEF despite extensive sequence homology (Droppelmann et al., 2013). My observations illustrate another example of the functional differences between RGNEF and p190RhoGEF. In addition, HEK293T cells exhibit a constitutive transcription of the heat shock protein 70 which may provide the cells with an intrinsic resistance to heat shock stress and mask the protection benefit provided by RGNEF (Kao & Nevins, 1983). Future experiments should utilize a different cell line such as HeLa cells to account for this.

When using siRNA transfection to attenuate the overexpression of RGNEF in stably transfected RGNEF+ cells, we observed no statistically significant difference in cell survival for either oxidative or osmotic stress. There is however a trend in favour of enhanced survival even in the presence of siRNA to RGNEF. Because the expression of RGNEF-myc is not completely eliminated (Fig. 9C), we cannot rule out the possibility that even in small amounts RGNEF can provide some degree of protection against the two stressors. In future studies, this issue could be addressed by using a cell line that shows endogenous expression of RGNEF and siRNA methodologies so that the overexpression of RGNEF itself is not affecting cellular behavior in an unforeseen manner. Indeed, when referring to previous stress protection studies involving TDP-43 and FUS, the proteins are endogenously expressed by the cell line being examined and the siRNA used to attenuate this endogenous expression leads to decreased survival of the stressed cells (Higashi et al., 2013; Sama et al., 2013).

4.2 N-terminal portion of RGNEF is important for its stress protection

In order to determine the portion of RGNEF that is most important for providing protection against oxidative and osmotic stress (0.5 mM arsenite and 400 mM sorbitol respectively), different deletions of the protein were performed and expressed in stressed cells (Fig. 15). We first examined the significance of the RNA-binding domain by using a construct of RGNEF with its RNA-binding domain deleted: RGNEF- Δ COOH. After removing the RNA-binding domain from RGNEF, cells continued to exhibit significantly greater levels of survival when compared to empty vector control (0.5 mM arsenite, $p = 0.006$; 400 mM sorbitol, $p = 0.026$). These results show that the protective effects of

RGNEF could be retained in the absence of its RNA-binding domain for oxidative or osmotic stress protection. Moreover, these results suggest that stress granule formation is not the mechanism by which full length RGNEF provides stress protection. Thus we looked at the RhoA activating domain of RGNEF next, which is composed of the Dbl homology (DH) and Pleckstrin homology (PH) domains.

Our construct RGNEF- Δ DH Δ PH was examined in stressed cells and, similar to RGNEF- Δ COOH, showed significantly greater survival compared to empty vector control (oxidative, $p = 0.009$; osmotic, $p = 0.013$). These results show that the DH and PH domains are not critical for the protection provided by full length RGNEF and suggest that RhoA activation is not the mechanism by which full length RGNEF protects cells from stress. Regarding RhoA's role in protection, there is literature supporting both an apoptotic role (Al-Gayyar et al., 2013) and a protective role (Abe et al., 2014) of RhoA. This dichotomy appears to be related to the duration of RhoA activation and the subsequent pathway this activation leads to. One study has shown that less chronic activation of RhoA in rat cardiomyocytes activates a pathway involving focal adhesion kinase and culminating in cytoskeletal reorganization of the cell along with anti-apoptotic effects mediated by Akt (Del Re et al., 2008). Though this pathway may be linked to RGNEF's protective function, especially due to RGNEF's implied and p190RhoGEF's proven involvement in the RhoA-FAK pathway, it is difficult to determine whether it is the mechanism by which the protein's stress protection occurs (Miller et al., 2013). Indeed the protection observed in the absence of the DH and PH domains suggests that this RhoA-FAK pathway is not involved in cytoprotection. Nevertheless, future experiments should determine whether RGNEF's effects on RhoA and FAK are retained in the absence of these domains.

As the deletion of the RNA-binding domain (RGNEF- Δ COOH) and the deletion of the DH-PH domains (RGNEF- Δ DH Δ PH) continued to demonstrate a protective effect against stress compared to empty vector controls, we decided to divide the RGNEF protein into two parts: an N-terminal half (RGNEF- Δ DH Δ PH Δ COOH) and a C-terminal half (RGNEF- Δ NH₂).

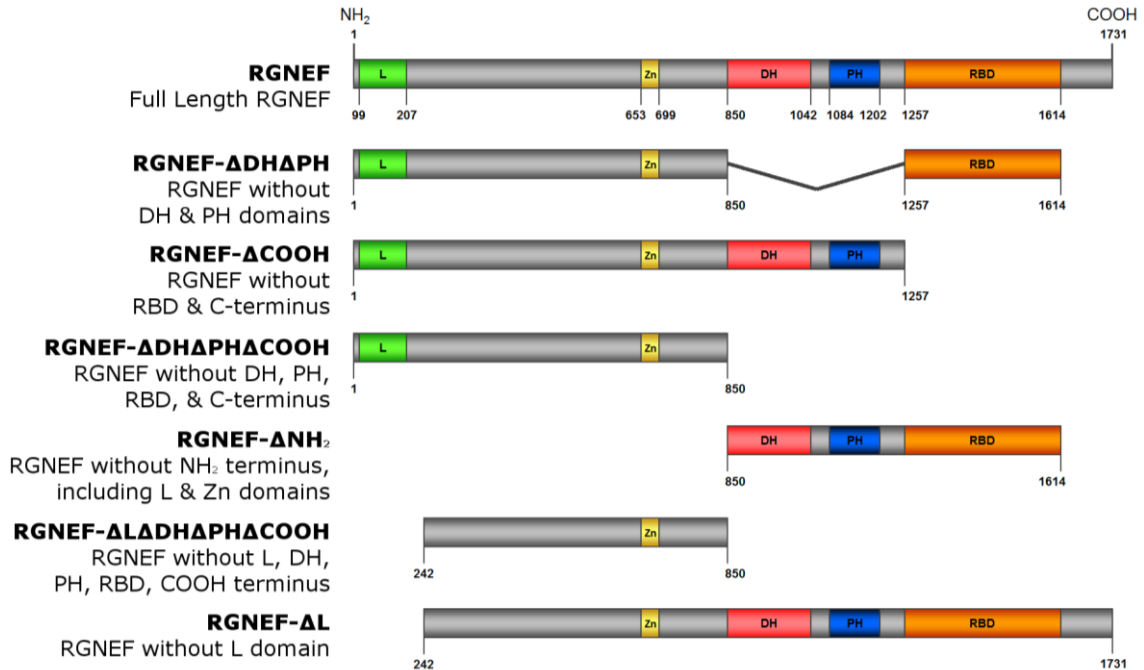


Figure 15: Review of deletion constructs of RGNEF used in experiments.

L = Putative leucine-rich domain, Zn = Zinc-binding domain, DH = Dbl-homology domain, PH = Pleckstrin-homology domain, RBD = RNA-binding domain.

The N-terminal RGNEF- Δ DH Δ PH Δ COOH contained neither the RNA-binding domain nor the GEF domain and was created to determine the combined importance of those two functional domains in stress protection. Conversely, the C-terminal RGNEF- Δ NH₂ contained only the RNA-binding domain and the GEF domain and was created to determine the importance of the largely unexplored N-terminal region of RGNEF in stress protection. The N-terminal protein RGNEF- Δ DH Δ PH Δ COOH demonstrated significant increase in survival over empty vector controls in both oxidative ($p = 0.002$) and osmotic ($p = 0.012$) stress, whereas the C-terminal protein RGNEF- Δ NH₂ only showed significant increase over empty vector controls in osmotic stress ($p = 0.036$). These results suggest that the N-terminal region of the RGNEF protein is more diverse in its protective function than the C-terminal RNA-binding domain and DH-PH domains. However, because both N-terminal RGNEF- Δ DH Δ PH Δ COOH and C-terminal RGNEF- Δ NH₂ show significantly greater survival under osmotic stress it appears that there are regions within both portions of the RGNEF protein that can provide protection.

After establishing that the N-terminal region of the RGNEF protein is important in both oxidative and osmotic stress, we decided to further explore the domains located in the N-terminal region, specifically the putative leucine-rich domain. We began by deleting the putative leucine-rich domain from the N-terminal region, creating an RGNEF- Δ L Δ DH Δ PH Δ COOH protein. The resulting protein showed no significant differences in survival when compared to an empty vector control under oxidative ($p = 0.149$) or osmotic ($p = 0.655$) stress. However, as this protein with its many deletions differed greatly in comparison to the full length RGNEF, we decided to make a deletion of the putative leucine-rich domain from the full length RGNEF, creating an RGNEF- Δ L protein. RGNEF- Δ L showed significantly greater survival under oxidative stress ($p = 0.002$), but not under osmotic stress ($p = 0.265$) when compared to an empty vector control.

This loss of protection against an osmotic stress following deletion of the leucine rich domain greatly was unexpected given our prior observation that cytoprotection had been maintained for both osmotic and oxidative stress using either of the N-terminal RGNEF- Δ DH Δ PH Δ COOH or C-terminal RGNEF- Δ NH₂ proteins. This could mean that

separation of the protein into an N-terminal and C-terminal half had unforeseen consequences on RGNEF's cellular activity leading to the activation of signaling pathways distinct from those that the full length RGNEF normally participates in. Further study focused on characterizing both the protein binding partners of full length RGNEF and those of the different RGNEF constructs will be of assistance in answering this question. Also, because the leucine-rich domain of RGNEF is dissimilar compared to previously published articles describing leucine-rich domains, it is difficult to predict the domain's function at this time. It is reasonable to assume that the domain is important in facilitating a protein-protein interaction, not only because conventional leucine-rich domains do so, but also because an ankyrin-repeat domain is embedded within this putative leucine rich domain (locus: NP_001073948; as described by NIH's Protein database). These protein-protein interactions may then facilitate a cell signaling pathway that prevents apoptosis leading to stress protection in cells. Indeed, some proteins containing leucine-rich domains have been shown to be protective against apoptosis, such as LRRK2 (Chuang, Lu, Wang, & Chang, 2014).

Taking the results from these deletion constructs as a whole, an interesting observation arises between the C-terminal half of RGNEF, RGNEF- Δ NH₂, and the deletion of the leucine-rich region from the full length of RGNEF, RGNEF- Δ L. Where RGNEF- Δ NH₂ protects against sorbitol and not arsenite, RGNEF- Δ L instead protects against arsenite and not sorbitol. This is unexpected because RGNEF- Δ L possesses the same domains that RGNEF- Δ NH₂ contains and would naturally be predicted to similarly protect against sorbitol. As mentioned previously, both the N-terminal region and C-terminal region of RGNEF may contain domains that can protect against cellular stress. The C-terminal region contains the GEF domain and RNA-binding domain, which may provide protection through, respectively, RhoA activation or interactions with JIP-1 and 14-3-3 as observed in the mouse homologue p190RhoGEF (Del Re et al., 2008; Wu et al., 2003). The N-terminal region contains the leucine-rich domain which may facilitate protein-protein interactions leading to stress protection (Chuang et al., 2014). Whether or not these domains are active could depend upon protein folding of RGNEF, as shown in figure 16.

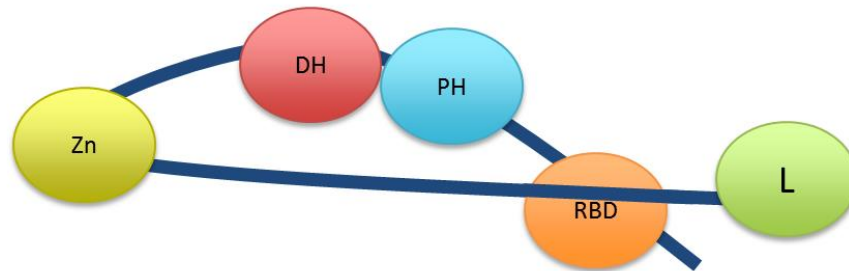


Figure 16: A proposed model for the folding of RGNEF. Notice that the leucine-rich domain of RGNEF partly obscures the C-terminal region and therefore may be regulating the behavior of those domains in the protein. Alternatively, the C-terminal region could also play a regulatory role on the leucine-rich domain, affecting what protein binding partners can interact with it. This figure is not to scale with the RGNEF protein.

In the observation mentioned previously between RGNEF- Δ NH₂ and RGNEF- Δ L, the protective effects may differ because of a potential regulatory role of the leucine-rich domain which inhibits the stress protection provided by the C-terminal region of RGNEF. Post-translational modifications to the protein, including phosphorylation and SUMOylation, could also be differentially regulated in these protein deletion constructs, leading to altered functionality of RGNEF protein. Indeed, more studies are needed to further explore the complex structure of RGNEF and the stress protective potential of its many domains.

4.3 RGNEF localizes to transport granules under stress

Previous studies have implicated RNA-binding proteins involved in ALS, specifically TDP-43 and FUS, as having stress protective properties through a mechanism of stress granule formation (Higashi et al., 2013; Sama et al., 2013). For example, TDP-43 is involved in the formation of stress granules and its knockdown by RNA interference decreases the survival of stressed cells (Aulas et al., 2012). Although RGNEF is similarly an RNA-binding protein with a role in the stress response, our results show that it does not colocalize with stress granules following either oxidative or osmotic stress. This result agrees with our observation that cells expressing RGNEF without its RNA-binding domain (RGNEF- Δ COOH) still exhibit protection against arsenite or sorbitol stress compared to controls. However, this contrasts with the previously described studies where TDP-43 and FUS have been shown to colocalize with stress granules. Instead, our results suggest that RGNEF does not protect cells through a mechanism of stress granule formation. It should be noted, however, that our methodology involves fixation of the cells which may affect the protein dynamics within the cell. Also, because only one time point was examined by confocal microscopy, it is possible that RGNEF associates with stress granules at a time earlier or later than we expected. To solve these questions, future experiments should examine a greater number of time points. Also, the localization of endogenous TDP-43 or FUS under a stress should be examined and used as a positive experimental control to observe whether the stress protocol and the immunocytochemistry protocol are able to visualize the expected colocalization of TDP-43 or FUS in stress granules. Furthermore, experiments utilizing live cell imaging should

be performed so that the protein dynamics of RGNEF and stress granules may be observed.

Because RGNEF is an RNA-binding protein, and because it was not found to associate with stress granules, we examined whether RGNEF would colocalize with transport granules. Under either arsenite or sorbitol stress, we observed that RGNEF would occasionally colocalize with transport granules. This colocalization suggests that RGNEF's protective mechanism involves transporting mRNA, or perhaps being transported itself, to specific locations within a cell during a stress. Alternatively, RGNEF may not be participating in RNA transport at all and may instead be involved in a process called staufen-mediated mRNA decay (Kim, Furic, Desgroseillers, & Maquat, 2005). Interestingly, staufen-mediated mRNA decay appears to agree with previous studies showing that RGNEF can destabilize *NEFL* mRNAs in cells. In contrast to transport granules, the protective mechanism of RGNEF in this case may involve the degradation of transcripts selected through Staufen binding to specific mRNAs. RGNEF's colocalization with Staufen may also indicate a pre-pathological aggregation of the protein as a result of stress. Although this mechanism of aggregate formation has only been suggested in a stress granule pathway (Wolozin, 2012), it may be possible to achieve a similar pathology through a transport granule pathway. To determine between these three possibilities: transport granule, staufen-mediated decay, or pre-pathological aggregate, future experiments should utilize live-cell imaging so that the protein dynamics of RGNEF can be monitored, specifically its movement or aggregation within cells. In addition, MS2-tagged mRNA targets of Staufen, in combination with RGNEF knockdown, may reveal whether RGNEF affects the process of staufen-mediated decay (Kim et al., 2005).

4.4 Conclusion and future directions

My hypothesis was that RGNEF participates in the cellular stress response. By participating in this stress response, we considered that RGNEF would behave similar to other RNA-binding proteins involved in ALS, or that it would do so through its role in the RhoA signaling pathway. Based on our results, I have shown that RGNEF is protective against oxidative or osmotic stress induced through 0.5 mM arsenite or 400

mM sorbitol respectively. However, unlike other RNA-binding protein in ALS such as FUS or TDP-43, RGNEF does not do this by participating in stress granules. Moreover, the activation of the RhoA pathway via RGNEF's DH/PH domain does not appear critical for its protection against stress. Instead, RGNEF's effects seem to involve many regions of the protein in both the N-terminal and C-terminal halves. The leucine-rich domain of the N-terminal region appears especially important under sorbitol stress where its deletion from the full length protein leads to sorbitol susceptibility. Also, instead of stress granule formation, RGNEF occasionally colocalizes with staufen-positive transport granules under arsenite and sorbitol.

Based on my results that show RGNEF provides protection against oxidative and osmotic stress, we can therefore hypothesize that where RGNEF is sequestered into NCIs within ALS spinal motor neurons, the protein's protective functions are lost. Moreover, RGNEF NCIs often harbor other RNA-binding proteins involved in ALS (Keller et al., 2012). The cumulative loss of these proteins (e.g. TDP-43, FUS, RGNEF, etc.) may ultimately cause ALS motor neurons to be specifically susceptible to oxidative stress, leading to their observed death in the disease course. Thus, my work provides another piece of evidence supporting a hypothesis which could potentially explain the selective death of motor neurons in ALS pathogenesis.

Future experiments building on my work should focus on elucidating the domains and interactors of RGNEF that participate in RGNEF's pathway in stress protection. My results suggest that there are domains of importance within the N-terminal region of the protein that need to be further studied. Moreover, the leucine rich domain of RGNEF suggests protein-protein interactions that may be integral to its function against stress, and for this reason should be studied in greater detail. In addition, experiments to characterize the biochemical properties of the massively truncated RGNEF mutant protein should be performed to see how this mutation may affect RGNEF's protective properties (Droppelmann et al., 2013; Ma et al., 2014). Interestingly, this truncation preserves the leucine rich region of RGNEF, once again highlighting this domain's potential importance in cellular function.

It should be noted that because experiments were performed using the HEK 293T cell line, results obtained in my experiments may differ in humans due to the large difference in physiological complexity (homogeneous cell line versus a multicellular organism) between the two systems. Therefore, future experimental models should move progressively closer to a human model. The progression should move next to examine neuronal cell lines such as human cortical neurons or inducible pluripotent stem cells differentiated into motor neurons to confirm that our observations do not change within a neuronal environment. From there, animal models should be studied so that our observations of RGNEF's protective abilities can be confirmed in a complex physiological system. Murine models may prove more difficult to use however as the presence of p190RhoGEF within these models means that unexpected interactions may occur between the two proteins, especially because the two proteins function differently despite being homologues of each other (Droppelmann et al., 2013).

Bibliography

- Abe, H., Kamai, T., Hayashi, K., Anzai, N., Shirataki, H., Mizuno, T. et al. (2014). The Rho-kinase inhibitor HA-1077 suppresses proliferation/migration and induces apoptosis of urothelial cancer cells. *BMC.Cancer*, *14*, 412.
- Al-Chalabi, A. & Hardiman, O. (2013). The epidemiology of ALS: a conspiracy of genes, environment and time. *Nat.Rev.Neurol.*, *9*, 617-628.
- Al-Chalabi, A., Jones, A., Troakes, C., King, A., Al-Sarraj, S., & van den Berg, L. H. (2012). The genetics and neuropathology of amyotrophic lateral sclerosis. *Acta Neuropathol.*, *124*, 339-352.
- Al-Gayyar, M. M., Mysona, B. A., Matragoon, S., Abdelsaid, M. A., El-Azab, M. F., Shanab, A. Y. et al. (2013). Diabetes and overexpression of proNGF cause retinal neurodegeneration via activation of RhoA pathway. *PLoS.One.*, *8*, e54692.
- Alami, N. H., Smith, R. B., Carrasco, M. A., Williams, L. A., Winborn, C. S., Han, S. S. et al. (2014). Axonal transport of TDP-43 mRNA granules is impaired by ALS-causing mutations. *Neuron*, *81*, 536-543.
- Alkon, D. L., Sun, M. K., & Nelson, T. J. (2007). PKC signaling deficits: a mechanistic hypothesis for the origins of Alzheimer's disease. *Trends Pharmacol.Sci.*, *28*, 51-60.
- Anderson, P. & Kedersha, N. (2008). Stress granules: the Tao of RNA triage. *Trends Biochem.Sci.*, *33*, 141-150.

Anderson, P. & Kedersha, N. (2009). RNA granules: post-transcriptional and epigenetic modulators of gene expression. *Nat.Rev.Mol.Cell Biol.*, *10*, 430-436.

Arai, T., Hasegawa, M., Akiyama, H., Ikeda, K., Nonaka, T., Mori, H. et al. (2006). TDP-43 is a component of ubiquitin-positive tau-negative inclusions in frontotemporal lobar degeneration and amyotrophic lateral sclerosis. *Biochem.Biophys.Res.Comm.*, *351*, 602-611.

Arimoto, K., Fukuda, H., Imajoh-Ohmi, S., Saito, H., & Takekawa, M. (2008). Formation of stress granules inhibits apoptosis by suppressing stress-responsive MAPK pathways. *Nat.Cell Biol.*, *10*, 1324-1332.

Aulas, A., Stabile, S., & Vande Velde, C. (2012). Endogenous TDP-43, but not FUS, contributes to stress granule assembly via G3BP. *Mol.Neurodegener.*, *7*, 54.

Banati, R. B., Gehrmann, J., Schubert, P., & Kreutzberg, G. W. (1993). Cytotoxicity of microglia. *Glia*, *7*, 111-118.

Bekenstein, U. & Soreq, H. (2013). Heterogeneous nuclear ribonucleoprotein A1 in health and neurodegenerative disease: from structural insights to post-transcriptional regulatory roles. *Mol.Cell Neurosci.*, *56*, 436-446.

Bergeron, C., Beric-Maskarel, K., Muntasser, S., Weyer, L., Somerville, M. J., & Percy, M. E. (1994). Neurofilament light and polyadenylated mRNA levels are decreased in amyotrophic lateral sclerosis motor neurons. *J.Neuropathol.Exp.Neurol.*, *53*, 221-230.

Blokhuis, A. M., Groen, E. J., Koppers, M., van den Berg, L. H., & Pasterkamp, R. J. (2013). Protein aggregation in amyotrophic lateral sclerosis. *Acta Neuropathol.*, *125*, 777-794.

Bregues, M., Teixeira, D., & Parker, R. (2005). Movement of eukaryotic mRNAs between polysomes and cytoplasmic processing bodies. *Science*, *310*, 486-489.

Brooks, B. R. (1994). El Escorial World Federation of Neurology criteria for the diagnosis of amyotrophic lateral sclerosis. Subcommittee on Motor Neuron Diseases/Amyotrophic Lateral Sclerosis of the World Federation of Neurology Research Group on Neuromuscular Diseases and the El Escorial "Clinical limits of amyotrophic lateral sclerosis" workshop contributors. *J.Neurol.Sci.*, *124 Suppl*, 96-107.

Bruijn, L. I., Becher, M. W., Lee, M. K., Anderson, K. L., Jenkins, N. A., Copeland, N. G. et al. (1997). ALS-linked SOD1 mutant G85R mediates damage to astrocytes and promotes rapidly progressive disease with SOD1-containing inclusions. *Neuron*, *18*, 327-338.

Bruijn, L. I., Houseweart, M. K., Kato, S., Anderson, K. L., Anderson, S. D., Ohama, E. et al. (1998). Aggregation and motor neuron toxicity of an ALS-linked SOD1 mutant independent from wild-type SOD1. *Science*, *281*, 1851-1854.

Bruijn, L. I., Miller, T. M., & Cleveland, D. W. (2004). Unraveling the mechanisms involved in motor neuron degeneration in ALS. *Annu.Rev.Neurosci.*, *27*, 723-749.

Brunelle, J. K. & Letai, A. (2009). Control of mitochondrial apoptosis by the Bcl-2 family. *J.Cell Sci.*, 122, 437-441.

Buratti, E., Dork, T., Zuccato, E., Pagani, F., Romano, M., & Baralle, F. E. (2001). Nuclear factor TDP-43 and SR proteins promote in vitro and in vivo CFTR exon 9 skipping. *EMBO J.*, 20, 1774-1784.

Calini, D., Corrado, L., Del, B. R., Gagliardi, S., Pensato, V., Verde, F. et al. (2013). Analysis of hnRNPA1, A2/B1, and A3 genes in patients with amyotrophic lateral sclerosis. *Neurobiol.Aging*, 34, 2695-2.

Canete-Soler, R., Wu, J., Zhai, J., Shamim, M., & Schlaepfer, W. W. (2001). p190RhoGEF Binds to a destabilizing element in the 3' untranslated region of light neurofilament subunit mRNA and alters the stability of the transcript. *J.Biol.Chem.*, 276, 32046-32050.

Charcot, J. M. & Joffroy, A. (1869). Deux cas d'atrophie musculaire progressive avec lesions de la substance grise et des faisceaux antero-lateraux de la moelle epiniere. *Arch.Physiol.Neurol.Pathol.*, 2, 744.

Chaudhuri, K. R., Crump, S., Al-Sarraj, S., Anderson, V., Cavanagh, J., & Leigh, P. N. (1995). The validation of El Escorial criteria for the diagnosis of amyotrophic lateral sclerosis: a clinicopathological study. *J.Neurol.Sci.*, 129 Suppl, 11-12.

Chen, H., Qian, K., Du, Z., Cao, J., Petersen, A., Liu, H. et al. (2014). Modeling ALS with iPSCs reveals that mutant SOD1 misregulates neurofilament balance in motor neurons. *Cell Stem Cell*, 14, 796-809.

Chen, S., Zhang, X., Song, L., & Le, W. (2012). Autophagy dysregulation in amyotrophic lateral sclerosis. *Brain Pathol.*, *22*, 110-116.

Chen, Y. Z., Bennett, C. L., Huynh, H. M., Blair, I. P., Puls, I., Irobi, J. et al. (2004). DNA/RNA helicase gene mutations in a form of juvenile amyotrophic lateral sclerosis (ALS4). *Am.J.Hum.Genet.*, *74*, 1128-1135.

Chio, A., Logroscino, G., Traynor, B. J., Collins, J., Simeone, J. C., Goldstein, L. A. et al. (2013). Global epidemiology of amyotrophic lateral sclerosis: a systematic review of the published literature. *Neuroepidemiology*, *41*, 118-130.

Chio, A., Traynor, B. J., Lombardo, F., Fimognari, M., Calvo, A., Ghiglione, P. et al. (2008). Prevalence of SOD1 mutations in the Italian ALS population. *Neurology*, *70*, 533-537.

Chuang, C. L., Lu, Y. N., Wang, H. C., & Chang, H. Y. (2014). Genetic dissection reveals that Akt is the critical kinase downstream of LRRK2 to phosphorylate and inhibit FOXO1, and promotes neuron survival. *Hum.Mol.Genet.*

Collard, J. F., Cote, F., & Julien, J. P. (1995). Defective axonal transport in a transgenic mouse model of amyotrophic lateral sclerosis. *Nature*, *375*, 61-64.

Collins, M., Riascos, D., Kovalik, T., An, J., Krupa, K., Krupa, K. et al. (2012). The RNA-binding motif 45 (RBM45) protein accumulates in inclusion bodies in amyotrophic lateral sclerosis (ALS) and frontotemporal lobar degeneration with TDP-43 inclusions (FTLD-TDP) patients. *Acta Neuropathol.*, *124*, 717-732.

Corbo, M. & Hays, A. P. (1992). Peripherin and neurofilament protein coexist in spinal spheroids of motor neuron disease. *J.Neuropathol.Exp.Neurol.*, *51*, 531-537.

Costa, J., Swash, M., & de Carvalho, M. (2012). Awaji criteria for the diagnosis of amyotrophic lateral sclerosis: a systematic review. *Arch.Neurol.*, *69*, 1410-1416.

Cote, F., Collard, J. F., & Julien, J. P. (1993). Progressive neuronopathy in transgenic mice expressing the human neurofilament heavy gene: a mouse model of amyotrophic lateral sclerosis. *Cell*, *73*, 35-46.

Couthouis, J., Hart, M. P., Erion, R., King, O. D., Diaz, Z., Nakaya, T. et al. (2012). Evaluating the role of the FUS/TLS-related gene EWSR1 in amyotrophic lateral sclerosis. *Hum.Mol.Genet.*, *21*, 2899-2911.

Couthouis, J., Hart, M. P., Shorter, J., DeJesus-Hernandez, M., Erion, R., Oristano, R. et al. (2011). A yeast functional screen predicts new candidate ALS disease genes. *Proc.Natl.Acad.Sci.U.S.A*, *108*, 20881-20890.

Cox, P. A. & Sacks, O. W. (2002). Cycad neurotoxins, consumption of flying foxes, and ALS-PDC disease in Guam. *Neurology*, *58*, 956-959.

Cui, F., Liu, M., Chen, Y., Huang, X., Cui, L., Fan, D. et al. (2014). Epidemiological characteristics of motor neuron disease in Chinese patients. *Acta Neurol.Scand.*

DeJesus-Hernandez, M., Mackenzie, I. R., Boeve, B. F., Boxer, A. L., Baker, M., Rutherford, N. J. et al. (2011). Expanded GGGGCC hexanucleotide repeat in noncoding region of C9ORF72 causes chromosome 9p-linked FTD and ALS. *Neuron*, 72, 245-256.

Del Re, D. P., Miyamoto, S., & Brown, J. H. (2008). Focal adhesion kinase as a RhoA-activable signaling scaffold mediating Akt activation and cardiomyocyte protection. *J.Biol.Chem.*, 283, 35622-35629.

Deng, H. X., Chen, W., Hong, S. T., Boycott, K. M., Gorrie, G. H., Siddique, N. et al. (2011). Mutations in UBQLN2 cause dominant X-linked juvenile and adult-onset ALS and ALS/dementia. *Nature*, 477, 211-215.

Deng, H. X., Zhai, H., Bigio, E. H., Yan, J., Fecto, F., Ajroud, K. et al. (2010). FUS-immunoreactive inclusions are a common feature in sporadic and non-SOD1 familial amyotrophic lateral sclerosis. *Ann.Neurol.*, 67, 739-748.

Droppelmann, C. A., Campos-Melo, D., Ishtiaq, M., Volkening, K., & Strong, M. J. (2014). RNA metabolism in ALS: When normal processes become pathological. *Amyotroph.Lateral.Scler.Frontotemporal.Degener.*

Droppelmann, C. A., Keller, B. A., Campos-Melo, D., Volkening, K., & Strong, M. J. (2013). Rho guanine nucleotide exchange factor is an NFL mRNA destabilizing factor that forms cytoplasmic inclusions in amyotrophic lateral sclerosis. *Neurobiol.Aging*, 34, 248-262.

Droppelmann, C. A., Wang, J., Campos-Melo, D., Keller, B., Volkening, K., Hegele, R. A. et al. (2013). Detection of a novel frameshift mutation and regions with

homozygosis within ARHGEF28 gene in familial amyotrophic lateral sclerosis.

Amyotroph.Lateral.Scler.Frontotemporal.Degener., 14, 444-451.

Eisinger-Mathason, T. S., Andrade, J., Groehler, A. L., Clark, D. E., Muratore-Schroeder, T. L., Pasic, L. et al. (2008). Codependent functions of RSK2 and the apoptosis-promoting factor TIA-1 in stress granule assembly and cell survival. *Mol.Cell*, 31, 722-736.

Elden, A. C., Kim, H. J., Hart, M. P., Chen-Plotkin, A. S., Johnson, B. S., Fang, X. et al. (2010). Ataxin-2 intermediate-length polyglutamine expansions are associated with increased risk for ALS. *Nature*, 466, 1069-1075.

Eulalio, A., Behm-Ansmant, I., & Izaurralde, E. (2007). P bodies: at the crossroads of post-transcriptional pathways. *Nat.Rev.Mol.Cell Biol.*, 8, 9-22.

Ferrandon, D., Koch, I., Westhof, E., & Nusslein-Volhard, C. (1997). RNA-RNA interaction is required for the formation of specific bicoid mRNA 3' UTR-STAUFIN ribonucleoprotein particles. *EMBO J.*, 16, 1751-1758.

Ferrante, R. J., Browne, S. E., Shinobu, L. A., Bowling, A. C., Baik, M. J., MacGarvey, U. et al. (1997). Evidence of increased oxidative damage in both sporadic and familial amyotrophic lateral sclerosis. *J.Neurochem.*, 69, 2064-2074.

Figlewicz, D. A., Krizus, A., Martinoli, M. G., Meininger, V., Dib, M., Rouleau, G. A. et al. (1994). Variants of the heavy neurofilament subunit are associated with the development of amyotrophic lateral sclerosis. *Hum.Mol.Genet.*, 3, 1757-1761.

Filliben, J. J. & Heckert, A. (2014). Grubbs' Test for Outliers. In J.J.Filliben (Ed.), *Engineering Statistics Handbook* (National Institute of Standards and Technology.

Fox, A. H., Lam, Y. W., Leung, A. K., Lyon, C. E., Andersen, J., Mann, M. et al. (2002). Paraspeckles: a novel nuclear domain. *Curr.Biol.*, 12, 13-25.

Fratta, P., Poulter, M., Lashley, T., Rohrer, J. D., Polke, J. M., Beck, J. et al. (2013). Homozygosity for the C9orf72 GGGGCC repeat expansion in frontotemporal dementia. *Acta Neuropathol.*, 126, 401-409.

Gama Sosa, M. A., Friedrich, V. L., Jr., DeGasperi, R., Kelley, K., Wen, P. H., Senturk, E. et al. (2003). Human mid-sized neurofilament subunit induces motor neuron disease in transgenic mice. *Exp.Neurol.*, 184, 408-419.

Garruto, R. M. (2006). A commentary on neuronal degeneration and cell death in Guam ALS and PD: an evolutionary process of understanding. *Curr.Alzheimer Res.*, 3, 397-401.

Garruto, R. M., Yanagihara, R., & Gajdusek, D. C. (1985). Disappearance of high-incidence amyotrophic lateral sclerosis and parkinsonism-dementia on Guam. *Neurology*, 35, 193-198.

Ge, W. W., Wen, W., Strong, W., Leystra-Lantz, C., & Strong, M. J. (2005). Mutant copper-zinc superoxide dismutase binds to and destabilizes human low molecular weight neurofilament mRNA. *J.Biol.Chem.*, 280, 118-124.

Gebbink, M. F., Kranenburg, O., Poland, M., van Horck, F. P., Houssa, B., & Moolenaar, W. H. (1997). Identification of a novel, putative Rho-specific GDP/GTP exchange factor and a RhoA-binding protein: control of neuronal morphology. *J.Cell Biol.*, *137*, 1603-1613.

Gilks, N., Kedersha, N., Ayodele, M., Shen, L., Stoecklin, G., Dember, L. M. et al. (2004). Stress granule assembly is mediated by prion-like aggregation of TIA-1. *Mol.Biol.Cell*, *15*, 5383-5398.

Greenway, M. J., Andersen, P. M., Russ, C., Ennis, S., Cashman, S., Donaghy, C. et al. (2006). ANG mutations segregate with familial and 'sporadic' amyotrophic lateral sclerosis. *Nat.Genet.*, *38*, 411-413.

Gros-Louis, F., Gaspar, C., & Rouleau, G. A. (2006). Genetics of familial and sporadic amyotrophic lateral sclerosis. *Biochim.Biophys.Acta*, *1762*, 956-972.

Gros-Louis, F., Lariviere, R., Gowing, G., Laurent, S., Camu, W., Bouchard, J. P. et al. (2004). A frameshift deletion in peripherin gene associated with amyotrophic lateral sclerosis. *J.Biol.Chem.*, *279*, 45951-45956.

Gurney, M. E., Pu, H., Chiu, A. Y., Dal Canto, M. C., Polchow, C. Y., Alexander, D. D. et al. (1994). Motor neuron degeneration in mice that express a human Cu,Zn superoxide dismutase mutation. *Science*, *264*, 1772-1775.

Gustafson, E. A. & Wessel, G. M. (2010). DEAD-box helicases: posttranslational regulation and function. *Biochem.Biophys.Res.Comm.*, *395*, 1-6.

Hanby, M. F., Scott, K. M., Scotton, W., Wijesekera, L., Mole, T., Ellis, C. E. et al. (2011). The risk to relatives of patients with sporadic amyotrophic lateral sclerosis. *Brain*, *134*, 3454-3457.

Hart, M. P. & Gitler, A. D. (2012). ALS-associated ataxin 2 polyQ expansions enhance stress-induced caspase 3 activation and increase TDP-43 pathological modifications. *J.Neurosci.*, *32*, 9133-9142.

He, B. P., Wen, W., & Strong, M. J. (2002). Activated microglia (BV-2) facilitation of TNF-alpha-mediated motor neuron death in vitro. *J.Neuroimmunol.*, *128*, 31-38.

Heath, P. R. & Shaw, P. J. (2002). Update on the glutamatergic neurotransmitter system and the role of excitotoxicity in amyotrophic lateral sclerosis. *Muscle Nerve*, *26*, 438-458.

Higashi, S., Kabuta, T., Nagai, Y., Tsuchiya, Y., Akiyama, H., & Wada, K. (2013). TDP-43 associates with stalled ribosomes and contributes to cell survival during cellular stress. *J.Neurochem.*, *126*, 288-300.

Hirano, A., Donnenfeld, H., Sasaki, S., & Nakano, I. (1984). Fine structural observations of neurofilamentous changes in amyotrophic lateral sclerosis. *J.Neuropathol.Exp.Neurol.*, *43*, 461-470.

Hoskins, J. M., Meynell, G. G., & Sanders, F. K. (1956). A comparison of methods for estimating the viable count of a suspension of tumour cells. *Exp.Cell Res.*, *11*, 297-305.

Igaz, L. M., Kwong, L. K., Chen-Plotkin, A., Winton, M. J., Unger, T. L., Xu, Y. et al. (2009). Expression of TDP-43 C-terminal Fragments in Vitro Recapitulates Pathological Features of TDP-43 Proteinopathies. *J.Biol.Chem.*, 284, 8516-8524.

Ingelfinger, D., Arndt-Jovin, D. J., Luhrmann, R., & Achsel, T. (2002). The human LSm1-7 proteins colocalize with the mRNA-degrading enzymes Dcp1/2 and Xrnl in distinct cytoplasmic foci. *RNA.*, 8, 1489-1501.

Inohara, N., Koseki, T., del, P. L., Hu, Y., Yee, C., Chen, S. et al. (1999). Nod1, an Apaf-1-like activator of caspase-9 and nuclear factor-kappaB. *J.Biol.Chem.*, 274, 14560-14567.

Kabashi, E. & Durham, H. D. (2006). Failure of protein quality control in amyotrophic lateral sclerosis. *Biochim.Biophys.Acta*, 1762, 1038-1050.

Kalla, R., Liu, Z., Xu, S., Koppius, A., Imai, Y., Kloss, C. U. et al. (2001). Microglia and the early phase of immune surveillance in the axotomized facial motor nucleus: impaired microglial activation and lymphocyte recruitment but no effect on neuronal survival or axonal regeneration in macrophage-colony stimulating factor-deficient mice. *J.Comp Neurol.*, 436, 182-201.

Kao, H. T. & Nevins, J. R. (1983). Transcriptional activation and subsequent control of the human heat shock gene during adenovirus infection. *Mol.Cell Biol.*, 3, 2058-2065.

Kedersha, N. & Anderson, P. (2007). Mammalian stress granules and processing bodies. *Methods Enzymol.*, 431, 61-81.

Kedersha, N., Cho, M. R., Li, W., Yacono, P. W., Chen, S., Gilks, N. et al. (2000). Dynamic shuttling of TIA-1 accompanies the recruitment of mRNA to mammalian stress granules. *J.Cell Biol.*, 151, 1257-1268.

Kedersha, N., Ivanov, P., & Anderson, P. (2013). Stress granules and cell signaling: more than just a passing phase? *Trends Biochem.Sci.*, 38, 494-506.

Kedersha, N., Stoecklin, G., Ayodele, M., Yacono, P., Lykke-Andersen, J., Fritzler, M. J. et al. (2005). Stress granules and processing bodies are dynamically linked sites of mRNP remodeling. *J.Cell Biol.*, 169, 871-884.

Kedersha, N. L., Gupta, M., Li, W., Miller, I., & Anderson, P. (1999). RNA-binding proteins TIA-1 and TIAR link the phosphorylation of eIF-2 alpha to the assembly of mammalian stress granules. *J.Cell Biol.*, 147, 1431-1442.

Keller, B. A., Volkening, K., Droppelmann, C. A., Ang, L. C., Rademakers, R., & Strong, M. J. (2012). Co-aggregation of RNA binding proteins in ALS spinal motor neurons: evidence of a common pathogenic mechanism. *Acta Neuropathol.*, 124, 733-747.

Kiebler, M. A., Hemraj, I., Verkade, P., Kohrmann, M., Fortes, P., Marion, R. M. et al. (1999). The mammalian stau protein localizes to the somatodendritic domain of cultured hippocampal neurons: implications for its involvement in mRNA transport. *J.Neurosci.*, 19, 288-297.

Kieran, D., Sebastia, J., Greenway, M. J., King, M. A., Connaughton, D., Concannon, C. G. et al. (2008). Control of motoneuron survival by angiogenin. *J.Neurosci.*, 28, 14056-14061.

Kiernan, M. C., Vucic, S., Cheah, B. C., Turner, M. R., Eisen, A., Hardiman, O. et al. (2011). Amyotrophic lateral sclerosis. *Lancet*, 377, 942-955.

Kim, H. J., Kim, N. C., Wang, Y. D., Scarborough, E. A., Moore, J., Diaz, Z. et al. (2013). Mutations in prion-like domains in hnRNPA2B1 and hnRNPA1 cause multisystem proteinopathy and ALS. *Nature*, 495, 467-473.

Kim, P. K., Hailey, D. W., Mullen, R. T., & Lippincott-Schwartz, J. (2008). Ubiquitin signals autophagic degradation of cytosolic proteins and peroxisomes. *Proc.Natl.Acad.Sci.U.S.A*, 105, 20567-20574.

Kim, W. J., Back, S. H., Kim, V., Ryu, I., & Jang, S. K. (2005). Sequestration of TRAF2 into stress granules interrupts tumor necrosis factor signaling under stress conditions. *Mol.Cell Biol.*, 25, 2450-2462.

Kim, Y. K., Furic, L., Desgroseillers, L., & Maquat, L. E. (2005). Mammalian Staufen1 recruits Upf1 to specific mRNA 3'UTRs so as to elicit mRNA decay. *Cell*, 120, 195-208.

King, A. E., Blizzard, C. A., Southam, K. A., Vickers, J. C., & Dickson, T. C. (2012). Degeneration of axons in spinal white matter in G93A mSOD1 mouse characterized by NFL and alpha-internexin immunoreactivity. *Brain Res.*, 1465, 90-100.

Kishimoto, K., Liu, S., Tsuji, T., Olson, K. A., & Hu, G. F. (2005). Endogenous angiogenin in endothelial cells is a general requirement for cell proliferation and angiogenesis. *Oncogene*, *24*, 445-456.

Kobe, B. & Kajava, A. V. (2001). The leucine-rich repeat as a protein recognition motif. *Curr.Opin.Struct.Biol.*, *11*, 725-732.

Kreutzberg, G. W. (1996). Microglia: a sensor for pathological events in the CNS. *Trends Neurosci.*, *19*, 312-318.

Kwiatkowski, T. J., Jr., Bosco, D. A., Leclerc, A. L., Tamrazian, E., Vanderburg, C. R., Russ, C. et al. (2009). Mutations in the FUS/TLS gene on chromosome 16 cause familial amyotrophic lateral sclerosis. *Science*, *323*, 1205-1208.

Lagier-Tourenne, C., Polymenidou, M., Hutt, K. R., Vu, A. Q., Baughn, M., Huelga, S. C. et al. (2012). Divergent roles of ALS-linked proteins FUS/TLS and TDP-43 intersect in processing long pre-mRNAs. *Nat.Neurosci.*, *15*, 1488-1497.

Lee, E. B., Lee, V. M., & Trojanowski, J. Q. (2012). Gains or losses: molecular mechanisms of TDP43-mediated neurodegeneration. *Nat.Rev.Neurosci.*, *13*, 38-50.

Lee, M. K. & Cleveland, D. W. (1996). Neuronal intermediate filaments. *Annu.Rev.Neurosci.*, *19*, 187-217.

Lee, M. K., Xu, Z., Wong, P. C., & Cleveland, D. W. (1993). Neurofilaments are obligate heteropolymers in vivo. *J.Cell Biol.*, *122*, 1337-1350.

Lee, Y. B., Chen, H. J., Peres, J. N., Gomez-Deza, J., Attig, J., Stalekar, M. et al. (2013). Hexanucleotide repeats in ALS/FTD form length-dependent RNA foci, sequester RNA binding proteins, and are neurotoxic. *Cell Rep.*, *5*, 1178-1186.

Leigh, P. N., Whitwell, H., Garofalo, O., Buller, J., Swash, M., Martin, J. E. et al. (1991). Ubiquitin-immunoreactive intraneuronal inclusions in amyotrophic lateral sclerosis. Morphology, distribution, and specificity. *Brain*, *114* (Pt 2), 775-788.

Levine, J. B., Kong, J., Nadler, M., & Xu, Z. (1999). Astrocytes interact intimately with degenerating motor neurons in mouse amyotrophic lateral sclerosis (ALS). *Glia*, *28*, 215-224.

Levine, T. P., Daniels, R. D., Gatta, A. T., Wong, L. H., & Hayes, M. J. (2013). The product of C9orf72, a gene strongly implicated in neurodegeneration, is structurally related to DENN Rab-GEFs. *Bioinformatics.*, *29*, 499-503.

Li, S. & Hu, G. F. (2012). Emerging role of angiogenin in stress response and cell survival under adverse conditions. *J.Cell Physiol*, *227*, 2822-2826.

Li, Y. R., King, O. D., Shorter, J., & Gitler, A. D. (2013). Stress granules as crucibles of ALS pathogenesis. *J.Cell Biol.*, *201*, 361-372.

Lin, H., Zhai, J., & Schlaepfer, W. W. (2005). RNA-binding protein is involved in aggregation of light neurofilament protein and is implicated in the pathogenesis of motor neuron degeneration. *Hum.Mol.Genet.*, *14*, 3643-3659.

Ling, S. C., Polymenidou, M., & Cleveland, D. W. (2013). Converging mechanisms in ALS and FTD: disrupted RNA and protein homeostasis. *Neuron*, *79*, 416-438.

Liu, X., Lu, M., Tang, L., Zhang, N., Chui, D., & Fan, D. (2013). ATXN2 CAG repeat expansions increase the risk for Chinese patients with amyotrophic lateral sclerosis. *Neurobiol.Aging*, *34*, 2236-2238.

Liu-Yesucevitz, L., Bilgutay, A., Zhang, Y. J., Vanderweyde, T., Citro, A., Mehta, T. et al. (2010). Tar DNA binding protein-43 (TDP-43) associates with stress granules: analysis of cultured cells and pathological brain tissue. *PLoS.One.*, *5*, e13250.

Ludolph, A. C., Bendotti, C., Blaugrund, E., Hengerer, B., Loffler, J. P., Martin, J. et al. (2007). Guidelines for the preclinical in vivo evaluation of pharmacological active drugs for ALS/MND: report on the 142nd ENMC international workshop. *Amyotroph.Lateral.Scler.*, *8*, 217-223.

Ma, Y., Tang, L., Chen, L., Zhang, B., Deng, P., Wang, J. et al. (2014). ARHGEF28 gene exon 6/intron 6 junction mutations in Chinese amyotrophic lateral sclerosis cohort. *Amyotroph.Lateral.Scler.Frontotemporal.Degener.*, *15*, 309-311.

Mao, Y. S., Sunwoo, H., Zhang, B., & Spector, D. L. (2011). Direct visualization of the co-transcriptional assembly of a nuclear body by noncoding RNAs. *Nat.Cell Biol.*, *13*, 95-101.

Martin, K. C. & Ephrussi, A. (2009). mRNA localization: gene expression in the spatial dimension. *Cell*, *136*, 719-730.

Maruyama, H., Morino, H., Ito, H., Izumi, Y., Kato, H., Watanabe, Y. et al. (2010). Mutations of optineurin in amyotrophic lateral sclerosis. *Nature*, *465*, 223-226.

Menzies, F. M., Grierson, A. J., Cookson, M. R., Heath, P. R., Tomkins, J., Figlewicz, D. A. et al. (2002). Selective loss of neurofilament expression in Cu/Zn superoxide dismutase (SOD1) linked amyotrophic lateral sclerosis. *J.Neurochem.*, *82*, 1118-1128.

Millecamps, S., Robertson, J., Lariviere, R., Mallet, J., & Julien, J. P. (2006). Defective axonal transport of neurofilament proteins in neurons overexpressing peripherin. *J.Neurochem.*, *98*, 926-938.

Miller, N. L., Lawson, C., Kleinschmidt, E. G., Tancioni, I., Uryu, S., & Schlaepfer, D. D. (2013). A non-canonical role for Rgnef in promoting integrin-stimulated focal adhesion kinase activation. *J.Cell Sci.*, *126*, 5074-5085.

Miller, R. G., Mitchell, J. D., & Moore, D. H. (2012). Riluzole for amyotrophic lateral sclerosis (ALS)/motor neuron disease (MND). *Cochrane.Database.Syst.Rev.*, *3*, CD001447.

Moisse, K. & Strong, M. J. (2006). Innate immunity in amyotrophic lateral sclerosis. *Biochim.Biophys.Acta*, *1762*, 1083-1093.

Moisse, K., Volkening, K., Leystra-Lantz, C., Welch, I., Hill, T., & Strong, M. J. (2009). Divergent patterns of cytosolic TDP-43 and neuronal progranulin expression following axotomy: implications for TDP-43 in the physiological response to neuronal injury. *Brain Res.*, *1249*, 202-211.

Mutai, H., Toyoshima, Y., Sun, W., Hattori, N., Tanaka, S., & Shiota, K. (2000). PAL31, a novel nuclear protein, expressed in the developing brain.

Biochem.Biophys.Res.Commun., 274, 427-433.

Nakagawa, S. & Hirose, T. (2012). Paraspeckle nuclear bodies--useful uselessness? *Cell Mol.Life Sci.*, 69, 3027-3036.

Neumann, M., Bentmann, E., Dormann, D., Jawaid, A., DeJesus-Hernandez, M., Ansorge, O. et al. (2011). FET proteins TAF15 and EWS are selective markers that distinguish FTLD with FUS pathology from amyotrophic lateral sclerosis with FUS mutations. *Brain*, 134, 2595-2609.

Neumann, M., Sampathu, D. M., Kwong, L. K., Truax, A. C., Micsenyi, M. C., Chou, T. T. et al. (2006). Ubiquitinated TDP-43 in frontotemporal lobar degeneration and amyotrophic lateral sclerosis. *Science*, 314, 130-133.

Nguyen, M. D., Lariviere, R. C., & Julien, J. P. (2001). Deregulation of Cdk5 in a mouse model of ALS: toxicity alleviated by perikaryal neurofilament inclusions. *Neuron*, 30, 135-147.

Nishimoto, Y., Nakagawa, S., Hirose, T., Okano, H. J., Takao, M., Shibata, S. et al. (2013). The long non-coding RNA nuclear-enriched abundant transcript 1_2 induces paraspeckle formation in the motor neuron during the early phase of amyotrophic lateral sclerosis. *Mol.Brain*, 6, 31.

Nodera, H., Izumi, Y., & Kaji, R. (2007). [New diagnostic criteria of ALS (Awaji criteria)]. *Brain Nerve*, 59, 1023-1029.

Okamoto, K., Hirai, S., Amari, M., Watanabe, M., & Sakurai, A. (1993). Bunina bodies in amyotrophic lateral sclerosis immunostained with rabbit anti-cystatin C serum. *Neurosci.Lett.*, *162*, 125-128.

Ono, Y., Fujii, T., Igarashi, K., Kuno, T., Tanaka, C., Kikkawa, U. et al. (1989). Phorbol ester binding to protein kinase C requires a cysteine-rich zinc-finger-like sequence. *Proc.Natl.Acad.Sci.U.S.A*, *86*, 4868-4871.

Oosthuysen, B., Moons, L., Storkebaum, E., Beck, H., Nuyens, D., Brusselmans, K. et al. (2001). Deletion of the hypoxia-response element in the vascular endothelial growth factor promoter causes motor neuron degeneration. *Nat.Genet.*, *28*, 131-138.

Ou, S. H., Wu, F., Harrich, D., Garcia-Martinez, L. F., & Gaynor, R. B. (1995). Cloning and characterization of a novel cellular protein, TDP-43, that binds to human immunodeficiency virus type 1 TAR DNA sequence motifs. *J.Virol.*, *69*, 3584-3596.

Paisan-Ruiz, C., Jain, S., Evans, E. W., Gilks, W. P., Simon, J., van der Brug, M. et al. (2004). Cloning of the gene containing mutations that cause PARK8-linked Parkinson's disease. *Neuron*, *44*, 595-600.

Pankiv, S., Clausen, T. H., Lamark, T., Brech, A., Bruun, J. A., Outzen, H. et al. (2007). p62/SQSTM1 binds directly to Atg8/LC3 to facilitate degradation of ubiquitinated protein aggregates by autophagy. *J.Biol.Chem.*, *282*, 24131-24145.

Parker, R. & Sheth, U. (2007). P bodies and the control of mRNA translation and degradation. *Mol.Cell*, *25*, 635-646.

Pasinelli, P., Belford, M. E., Lennon, N., Bacskai, B. J., Hyman, B. T., Trotti, D. et al. (2004). Amyotrophic lateral sclerosis-associated SOD1 mutant proteins bind and aggregate with Bcl-2 in spinal cord mitochondria. *Neuron*, *43*, 19-30.

Piao, Y. S., Wakabayashi, K., Kakita, A., Yamada, M., Hayashi, S., Morita, T. et al. (2003). Neuropathology with clinical correlations of sporadic amyotrophic lateral sclerosis: 102 autopsy cases examined between 1962 and 2000. *Brain Pathol.*, *13*, 10-22.

Plato, C. C., Garruto, R. M., Galasko, D., Craig, U. K., Plato, M., Gamst, A. et al. (2003). Amyotrophic lateral sclerosis and parkinsonism-dementia complex of Guam: changing incidence rates during the past 60 years. *Am.J.Epidemiol.*, *157*, 149-157.

Puls, I., Jonnakuty, C., LaMonte, B. H., Holzbaur, E. L., Tokito, M., Mann, E. et al. (2003). Mutant dynactin in motor neuron disease. *Nat.Genet.*, *33*, 455-456.

Purves, D., Augustine, G. J., Fitzpatrick, D., Katz, L. C., LaMantia, A., McNamara, J. O. et al. (2001). Neuroscience. Sunderland (MA): Sinauer Associates.

Raivich, G. (2005). Like cops on the beat: the active role of resting microglia. *Trends Neurosci.*, *28*, 571-573.

Raoul, C., Estevez, A. G., Nishimune, H., Cleveland, D. W., deLapeyriere, O., Henderson, C. E. et al. (2002). Motoneuron death triggered by a specific pathway downstream of Fas. potentiation by ALS-linked SOD1 mutations. *Neuron*, *35*, 1067-1083.

Renton, A. E., Chio, A., & Traynor, B. J. (2014). State of play in amyotrophic lateral sclerosis genetics. *Nat.Neurosci.*, *17*, 17-23.

Renton, A. E., Majounie, E., Waite, A., Simon-Sanchez, J., Rollinson, S., Gibbs, J. R. et al. (2011). A hexanucleotide repeat expansion in C9ORF72 is the cause of chromosome 9p21-linked ALS-FTD. *Neuron*, *72*, 257-268.

Rico, B., Beggs, H. E., Schahin-Reed, D., Kimes, N., Schmidt, A., & Reichardt, L. F. (2004). Control of axonal branching and synapse formation by focal adhesion kinase. *Nat.Neurosci.*, *7*, 1059-1069.

Rosen, D. R., Siddique, T., Patterson, D., Figlewicz, D. A., Sapp, P., Hentati, A. et al. (1993). Mutations in Cu/Zn superoxide dismutase gene are associated with familial amyotrophic lateral sclerosis. *Nature*, *362*, 59-62.

Rothstein, J. D., Martin, L. J., & Kuncl, R. W. (1992). Decreased glutamate transport by the brain and spinal cord in amyotrophic lateral sclerosis. *N.Engl.J.Med.*, *326*, 1464-1468.

Rothstein, J. D., van Kammen, M., Levey, A. I., Martin, L. J., & Kuncl, R. W. (1995). Selective loss of glial glutamate transporter GLT-1 in amyotrophic lateral sclerosis. *Ann.Neurol.*, *38*, 73-84.

Roussel, B. D., Kruppa, A. J., Miranda, E., Crowther, D. C., Lomas, D. A., & Marciniak, S. J. (2013). Endoplasmic reticulum dysfunction in neurological disease. *Lancet Neurol.*, *12*, 105-118.

- Rowland, L. P. & Shneider, N. A. (2001). Amyotrophic lateral sclerosis. *N.Engl.J.Med.*, 344, 1688-1700.
- Sama, R. R., Ward, C. L., Kaushansky, L. J., Lemay, N., Ishigaki, S., Urano, F. et al. (2013). FUS/TLS assembles into stress granules and is a prosurvival factor during hyperosmolar stress. *J.Cell Physiol*, 228, 2222-2231.
- Sanelli, T. & Strong, M. J. (2007). Loss of nitric oxide-mediated down-regulation of NMDA receptors in neurofilament aggregate-bearing motor neurons in vitro: implications for motor neuron disease. *Free Radic.Biol.Med.*, 42, 143-151.
- Sanelli, T. R., Sopper, M. M., & Strong, M. J. (2004). Sequestration of nNOS in neurofilamentous aggregate bearing neurons in vitro leads to enhanced NMDA-mediated calcium influx. *Brain Res.*, 1004, 8-17.
- Sasaki, S. & Maruyama, S. (1992). Increase in diameter of the axonal initial segment is an early change in amyotrophic lateral sclerosis. *J.Neurol.Sci.*, 110, 114-120.
- Scotton, W. J., Scott, K. M., Moore, D. H., Almedom, L., Wijesekera, L. C., Janssen, A. et al. (2012). Prognostic categories for amyotrophic lateral sclerosis. *Amyotroph.Lateral.Scler.*, 13, 502-508.
- Shaw, G., Morse, S., Ararat, M., & Graham, F. L. (2002). Preferential transformation of human neuronal cells by human adenoviruses and the origin of HEK 293 cells. *FASEB J.*, 16, 869-871.

Shelkovanikova, T. A., Robinson, H. K., Troakes, C., Ninkina, N., & Buchman, V. L. (2014). Compromised paraspeckle formation as a pathogenic factor in FUSopathies. *Hum.Mol.Genet.*, *23*, 2298-2312.

Shibata, N., Nagai, R., Uchida, K., Horiuchi, S., Yamada, S., Hirano, A. et al. (2001). Morphological evidence for lipid peroxidation and protein glycooxidation in spinal cords from sporadic amyotrophic lateral sclerosis patients. *Brain Res.*, *917*, 97-104.

Simpson, E. P., Yen, A. A., & Appel, S. H. (2003). Oxidative Stress: a common denominator in the pathogenesis of amyotrophic lateral sclerosis. *Curr.Opin.Rheumatol.*, *15*, 730-736.

Slater, T. F., Sawyer, B., & Straeuli, U. (1963). Studies on succinate-tetrazolium reductase systems. III. Points of coupling of four different tetrazolium salts. *Biochim.Biophys.Acta*, *77*, 383-393.

Sreedharan, J., Blair, I. P., Tripathi, V. B., Hu, X., Vance, C., Rogelj, B. et al. (2008). TDP-43 mutations in familial and sporadic amyotrophic lateral sclerosis. *Science*, *319*, 1668-1672.

Steele, J. C. & McGeer, P. L. (2008). The ALS/PDC syndrome of Guam and the cycad hypothesis. *Neurology*, *70*, 1984-1990.

Stenmark, H. (2009). Rab GTPases as coordinators of vesicle traffic. *Nat.Rev.Mol.Cell Biol.*, *10*, 513-525.

Stepito, A., Gallo, J. M., Shaw, C. E., & Hirth, F. (2014). Modelling C9ORF72 hexanucleotide repeat expansion in amyotrophic lateral sclerosis and frontotemporal dementia. *Acta Neuropathol.*, 127, 377-389.

Strong, M. J. (2001). Progress in clinical neurosciences: the evidence for ALS as a multisystems disorder of limited phenotypic expression. *Can.J.Neurol.Sci.*, 28, 283-298.

Strong, M. J. (2010). The evidence for altered RNA metabolism in amyotrophic lateral sclerosis (ALS). *J.Neurol.Sci.*, 288, 1-12.

Strong, M. J., Kesavapany, S., & Pant, H. C. (2005). The pathobiology of amyotrophic lateral sclerosis: a proteinopathy? *J.Neuropathol.Exp.Neurol.*, 64, 649-664.

Strong, M. J., Volkening, K., Hammond, R., Yang, W., Strong, W., Leystra-Lantz, C. et al. (2007). TDP43 is a human low molecular weight neurofilament (hNFL) mRNA-binding protein. *Mol.Cell Neurosci.*, 35, 320-327.

Subramanian, V., Crabtree, B., & Acharya, K. R. (2008). Human angiogenin is a neuroprotective factor and amyotrophic lateral sclerosis associated angiogenin variants affect neurite extension/pathfinding and survival of motor neurons. *Hum.Mol.Genet.*, 17, 130-149.

Szaro, B. G. & Strong, M. J. (2010). Post-transcriptional control of neurofilaments: New roles in development, regeneration and neurodegenerative disease. *Trends Neurosci.*, 33, 27-37.

- Tacconi, M. T. (1998). Neuronal death: is there a role for astrocytes? *Neurochem.Res.*, *23*, 759-765.
- Tan, A. Y. & Manley, J. L. (2009). The TET family of proteins: functions and roles in disease. *J.Mol.Cell Biol.*, *1*, 82-92.
- Tanner, N. K. & Linder, P. (2001). DExD/H box RNA helicases: from generic motors to specific dissociation functions. *Mol.Cell*, *8*, 251-262.
- Tosar, L. J., Thomas, M. G., Baez, M. V., Ibanez, I., Chernomoretz, A., & Boccaccio, G. L. (2012). Staufen: from embryo polarity to cellular stress and neurodegeneration. *Front Biosci.(Schol.Ed)*, *4*, 432-452.
- Tourriere, H., Chebli, K., Zekri, L., Courselaud, B., Blanchard, J. M., Bertrand, E. et al. (2003). The RasGAP-associated endoribonuclease G3BP assembles stress granules. *J.Cell Biol.*, *160*, 823-831.
- Troost, D., van den Oord, J. J., & Vianney de Jong, J. M. (1990). Immunohistochemical characterization of the inflammatory infiltrate in amyotrophic lateral sclerosis. *Neuropathol.Appl.Neurobiol.*, *16*, 401-410.
- van Damme, P., Bogaert, E., Dewil, M., Hersmus, N., Kiraly, D., Scheveneels, W. et al. (2007). Astrocytes regulate GluR2 expression in motor neurons and their vulnerability to excitotoxicity. *Proc.Natl.Acad.Sci.U.S.A*, *104*, 14825-14830.
- van Horck, F. P., Ahmadian, M. R., Haeusler, L. C., Moolenaar, W. H., & Kranenburg, O. (2001). Characterization of p190RhoGEF, a RhoA-specific guanine

nucleotide exchange factor that interacts with microtubules. *J.Biol.Chem.*, 276, 4948-4956.

Volkening, K., Leystra-Lantz, C., & Strong, M. J. (2010). Human low molecular weight neurofilament (NFL) mRNA interacts with a predicted p190RhoGEF homologue (RGNEF) in humans. *Amyotroph.Lateral.Scler.*, 11, 97-103.

Volkening, K., Leystra-Lantz, C., Yang, W., Jaffee, H., & Strong, M. J. (2009). Tar DNA binding protein of 43 kDa (TDP-43), 14-3-3 proteins and copper/zinc superoxide dismutase (SOD1) interact to modulate NFL mRNA stability. Implications for altered RNA processing in amyotrophic lateral sclerosis (ALS). *Brain Res.*, 1305, 168-182.

Williamson, T. L. & Cleveland, D. W. (1999). Slowing of axonal transport is a very early event in the toxicity of ALS-linked SOD1 mutants to motor neurons. *Nat.Neurosci.*, 2, 50-56.

Wolozin, B. (2012). Regulated protein aggregation: stress granules and neurodegeneration. *Mol.Neurodegener.*, 7, 56.

Wong, N. K., He, B. P., & Strong, M. J. (2000). Characterization of neuronal intermediate filament protein expression in cervical spinal motor neurons in sporadic amyotrophic lateral sclerosis (ALS). *J.Neuropathol.Exp.Neurol.*, 59, 972-982.

Wu, D., Yu, W., Kishikawa, H., Folkerth, R. D., Iafrate, A. J., Shen, Y. et al. (2007). Angiogenin loss-of-function mutations in amyotrophic lateral sclerosis. *Ann.Neurol.*, 62, 609-617.

Wu, J., Zhai, J., Lin, H., Nie, Z., Ge, W. W., Garcia-Bermejo, L. et al. (2003). Cytoplasmic retention sites in p190RhoGEF confer anti-apoptotic activity to an EGFP-tagged protein. *Brain Res.Mol.Brain Res.*, *117*, 27-38.

Xiao, S., McLean, J., & Robertson, J. (2006). Neuronal intermediate filaments and ALS: a new look at an old question. *Biochim.Biophys.Acta*, *1762*, 1001-1012.

Yuan, A., Rao, M. V., Sasaki, T., Chen, Y., Kumar, A., Veeranna et al. (2006). Alpha-internexin is structurally and functionally associated with the neurofilament triplet proteins in the mature CNS. *J.Neurosci.*, *26*, 10006-10019.

Zhai, J., Lin, H., Nie, Z., Wu, J., Canete-Soler, R., Schlaepfer, W. W. et al. (2003). Direct interaction of focal adhesion kinase with p190RhoGEF. *J.Biol.Chem.*, *278*, 24865-24873.

Zheng, Y. (2001). Dbl family guanine nucleotide exchange factors. *Trends Biochem.Sci.*, *26*, 724-732.

Zimprich, A., Biskup, S., Leitner, P., Lichtner, P., Farrer, M., Lincoln, S. et al. (2004). Mutations in LRRK2 cause autosomal-dominant parkinsonism with pleomorphic pathology. *Neuron*, *44*, 601-607.

Zu, T., Liu, Y., Banez-Coronel, M., Reid, T., Pletnikova, O., Lewis, J. et al. (2013). RAN proteins and RNA foci from antisense transcripts in C9ORF72 ALS and frontotemporal dementia. *Proc.Natl.Acad.Sci.U.S.A*, *110*, E4968-E4977.

Curriculum Vitae

Kevin Cheung

UNIVERSITY EDUCATION BACKGROUND

- 2012-2014 **Master of Science Candidate, Pathology**
 University of Western Ontario, London, Ontario
 Title: “The Role Of The RNA-Binding Protein Rho Guanine Nucleotide Exchange Factor In The Cellular Stress Response”
 Supervisor: Dr. Michael J. Strong
- 2008-2012 **Honours Bachelor of Medical Sciences, Pathology and Toxicology**
 University of Western Ontario, London, Ontario

HONORS, SCHOLARSHIPS AND AWARDS DURING UNIVERSITY

- 2012-2014 **Western Graduate Research Scholarship**
- Awarded through a nomination by the full-time student’s graduate program
- 2013 **Second Place Poster Award**, Fourth International Research Workshop on Frontotemporal Dementia in ALS
- Awarded to the poster presentation of “Rho Guanine Nucleotide Exchange Factor (RGNEF) Affects the Survival of HEK293T Cells Exposed to a Variety of Stressors” based on the decision of a panel of judges
- 2009-2012 **Dean’s Honour List**
- For outstanding academic achievement while maintaining a full course load
- 2009 **Western In-course Scholarship**
- Awarded through faculty nomination to a student based on their academic merit
- 2008 **Western Scholarship of Excellence**
- For achieving an average grade of over 90% in the final year of secondary school

RESEARCH EXPERIENCE

- 2012-present **Research-based Master's Thesis**, Department of Pathology, Western University
 Supervisor: Dr. Michael J. Strong
- Characterized the protective effect of RGNEF protein (implicated in amyotrophic lateral sclerosis) on the survival of stressed cells
 - Cultured and transfected several different cell types: HEK293T, Swiss 3T3, Neuro2A
 - Western blot and densitometry to analyze changes in protein levels
 - Fluorescence immunocytochemistry and confocal microscopy to visualize protein localizations and interactions within cells
 - MTT viability assay to examine the protective effect of RGNEF for cells
 - Molecular biology techniques including cloning and PCR to generate different gene constructs of RGNEF for study in eukaryotic cells
 - Presented results on a regular basis in formal and informal settings
- 2012 **Summer Research Student**, Ivey Eye Institute, St. Joseph's Hospital, London, Ontario
 Supervisor: Dr. Cindy Hutnik
- Investigated the effects of glaucoma medications on ocular surface disease and the potential therapeutic effects of amniotic membrane extract on the ocular surface
 - Imaged cell cultures using brightfield microscopy
 - Obtained clinical data and ocular surface samples from patients
 - Cryostat frozen sectioning used to obtain slides for analysis by fluorescence immunocytochemistry under confocal microscopy
 - Performed statistical analysis of data
 - Presented and discussed findings with colleagues in weekly lab meetings
- 2011-2012 **Fourth-Year Undergraduate Honours Thesis Project**, Department of Pathology, Western University
 Supervisor: Dr. Stephen Karlik
- Investigated the angiogenic factors involved in the pathogenesis of demyelinated spinal cord lesions in multiple sclerosis
 - Cut formalin-fixed, paraffin-embedded tissue samples and analyzed tissue using hematoxylin & eosin and immunohistochemistry methods
 - Scored slides based on appearance of staining as observed through light microscopy
 - Performed statistical analysis of data
 - Wrote and presented proposals to peers within the department
 - Presented findings in a graded podium presentation to departmental peers

PUBLICATIONS, PRESENTATIONS AND ABSTRACTS

- 2014 **Poster and Podium Presentation**, Robarts Research Retreat 2014, Western University, London, Ontario
- TITLE: The role of Rho Guanine Nucleotide Exchange Factor, an aggregate forming RNA-binding protein in amyotrophic lateral sclerosis, in the cellular stress response
 - AUTHORS: Kevin Cheung, Cristian Droppelmann, Kathryn Volkening, Michael J. Strong
- 2014 **Poster Presentation**, 2014 Annual Meeting of the Southern Ontario Neuroscience Association, Society for Neuroscience, London, Ontario
- TITLE: The role of Rho Guanine Nucleotide Exchange Factor, a novel RNA-binding protein discovered in amyotrophic lateral sclerosis, in the cellular stress response
 - AUTHORS: Kevin Cheung, Cristian Droppelmann, Kathryn Volkening, Michael J. Strong
- 2014 **Poster Presentation**, 2014 Annual Pathology Research Day, Schulich School of Medicine and Dentistry, Western University, London, Ontario
- TITLE: The role of Rho Guanine Nucleotide Exchange Factor, an RNA-binding protein discovered in amyotrophic lateral sclerosis, in stress response
 - AUTHORS: Kevin Cheung, Cristian Droppelmann, Kathryn Volkening, Michael J. Strong
- 2014 **Poster Presentation**, London Health Research Day 2014, London, Ontario
- TITLE: The role of Rho Guanine Nucleotide Exchange Factor, a novel RNA-binding protein discovered in amyotrophic lateral sclerosis, in the cellular stress response
 - AUTHORS: Kevin Cheung, Cristian Droppelmann, Kathryn Volkening, Michael J. Strong
- 2013 **Poster Presentation (abstract publication)**, 43rd Annual Meeting of the Society for Neuroscience, San Diego, California
- TITLE: Cytoprotective effect of Rho guanine nucleotide exchange factor (RGNEF)
 - AUTHORS: Kevin Cheung, Cristian Droppelmann, Kathryn Volkening, Ian Cameron, Stephen H. Pasternak, Michael J. Strong
- 2013 **Poster Presentation (abstract publication)**, ARVO Annual Meeting 2013, Orlando, Florida
- TITLE: The Effects of Amniotic Membrane Extract on Primary Human Corneal Epithelial Cells

- **AUTHORS:** David V.Dudok, Kevin Cheung, Hong Liu, Luca Vedovelli, Emiliano Ghinelli, Ken Kenyon, Sunil Parapuram, Cindy M. Hutnik
- 2013 **Poster Presentation**, 2013 Annual Pathology Research Day, Schulich School of Medicine and Dentistry, Western University, London, Ontario
- **TITLE:** RGNEF does not co-localize with stress granules, but may increase cell survival under various conditions of cellular stress
 - **AUTHORS:** Kevin Cheung, Cristian Droppelmann, Kathryn Volkening, Michael J. Strong
- 2013 **Poster and Podium Presentation**, Fourth International Research Workshop on Frontotemporal Dementia in ALS, London, Ontario
- **TITLE:** Rho guanine nucleotide exchange factor (RGNEF) affects the survival of HEK293T cells exposed to a variety of stressors
 - **AUTHORS:** Kevin Cheung, Cristian Droppelmann, Kathryn Volkening, Michael J. Strong
- 2013 **Poster Presentation**, ALS Canada Research Forum 2013, Toronto, Ontario
- **TITLE:** Rho guanine nucleotide exchange factor (RGNEF) affects the survival of HEK293T cells exposed to a variety of stressors
 - **AUTHORS:** Kevin Cheung, Cristian Droppelmann, Kathryn Volkening, Michael J. Strong
- 2013 **Poster Presentation**, London Health Research Day 2013, London, Ontario
- **TITLE:** RGNEF does not co-localize to stress granules in amyotrophic lateral sclerosis, but may increase cell survival under stress
 - **AUTHORS:** Kevin Cheung, Cristian Droppelmann, Kathryn Volkening, Michael J. Strong
- 2012 **Podium Presentation**, Western Undergraduate Research Journal's Research Forum, Western University
- **TITLE:** Immunohistochemical analysis of protein markers in mice with experimental allergic encephalomyelitis induced by MOG(35-55) peptide and in humans with multiple sclerosis
 - **AUTHORS:** Kevin Cheung, Wendy Roscoe, Robin Smith, Stephen Karlik
- 2012 **Poster Presentation**, Annual Pathology and Toxicology Research Day, Western University
- **TITLE:** Comparison of various protein factors in mice with Experimental Allergic Encephalomyelitis and in humans with Multiple Sclerosis

- **AUTHORS:** Kevin Cheung, Wendy Roscoe, Robin Smith, Stephen Karlik

TEACHING EXPERIENCE DURING UNIVERSITY

2014 Jan-Apr **Graduate Teaching Assistant**, Department of Pathology, Western University

Course Taught: Environmental Pathology (PATH 4400B)

- Grading assignments and tests according to rubric outlined by instructor
- Answering student questions about both course material and grading
- Proctoring course midterms and exams
- Providing professor with feedback about student performance on tests and assignments, and discussing rubrics prior to grading assignments